MASTER

Scheduling in next-generation wireless networks

Pijnappel, T.R.

Award date:
2019

Scheduling in Next-Generation Wireless Networks

Author:
T.R. Pijnappel, ID 0860018

Supervisors:
Prof.dr.ir. S.C. Borst   Prof. P.A. Whiting

April 12, 2019

Abstract

Next-generation wireless networks should efficiently support multiple types of traffic. Two main types of traffic are enhanced mobile broadband (eMBB) which have large demands and can tolerate some delay, and ultra-reliable low-latency communication (URLLC) which demand to transmit small packets. However, the demands of URLLC users are subject to extremely tight latency and high reliability constraints. Since it is unknown when a URLLC demand arrives, we will consider a scheduler that assigns resources (time-frequency blocks) to the eMBB users, but overwrites ongoing eMBB transmissions to satisfy the tight latency constraints of the URLLC demands.

For our scheduling policy we will show that the limiting behaviour of the sample paths of the throughputs converges to the solution of an ordinary differential equation (ODE), and that this ODE has a unique equilibrium. Furthermore we will verify these results using simulations for scenarios with independent exponential rates, but also with rates that are based on a Rayleigh fading model.

To investigate the performance of hijacking policies, we will compare its performance to the optimal scheduling in an offline setting. This comparison shows that our scheduler produces near-optimal results when there is a small probability of URLLC demands.

Preface

During the last phase of my master Industrial and Applied Mathematics at the TU/e, I got the opportunity to spend six weeks on a project at Macquarie University in Sydney, Australia. The subject of this project was ‘scheduling in next-generation wireless networks’. Sem Borst, Phil Whiting and I recognised that six weeks would not be enough to cover the project in full. Hence it became my master thesis.

I would like to thank Phil Whiting and his team at Macquarie for inviting me, and giving me an unforgettable experience in Australia. I also thank them for their help, support and guidance in dealing with the issues I encountered in this project.

I also thank Sem Borst for his encouragement and mentorship in the last phase of my mathematics study. The discussions we had together with Phil Whiting, scattered over two or sometimes even three continents where invaluable for this thesis.

Finally I would like to thank my family and friends for supporting me during my studies.

Without all of you I could not have done it!

Contents

Chapter 1

Introduction

Current wireless networks cannot support users (devices or applications) that are extremely delay-sensitive (delays must be less than a millisecond). For example, an application that would require these short delays autonomous driving and tele-surgery [1]-[3]. Therefore, next-generation wireless networks should be able to efficiently support these delay-sensitive users, but at the same time also support throughput-oriented users. The throughput-oriented users typically require large amounts of data, but can tolerate some delay. In contrast, delay-sensitive users may not require large amounts of data, but require extremely short delays with very high reliability. As we only need to satisfy instantaneous demands for the delay-sensitive users, these users are satisfied when the tight latency constraints are met with high reliability. So there is no point in optimizing throughputs of the delay-sensitive users.

As the scheduler assigns resources (time-frequency blocks) to the users, we need a way to satisfy the delay-sensitive demands while trying to maximize the throughput of throughput-oriented users subject to this constraint. As it is unknown when delay-sensitive demands arrive and these demands should have extremely short delays, there is very little time to determine a good scheduling assignment for these demands. Calculating an optimal assignment will take too much time, therefore the goal is to determine a (good) scheduling policy that has close to optimal performance in some suitable sense.

1.1 Problem description

In this report we consider a system with two types of traffic. The first type is the so called enhanced mobile broadband (eMBB or throughput-oriented) traffic. Let $\mathcal{E}$ denote the set of eMBB users, which are assumed to have infinite amounts of data to be served. Even though this assumption is common in the literature, it might seem a bit strange since an equivalent queuing model has infinite queues. However, this model allows us to investigate the throughput (the amount of data a user can transmit during a time period) of the users. Knowing the throughput of a user, we can estimate the amount of time it needs to transmit a file.

The second type of traffic is called 'ultra-reliable low-latency communication' (URLLC or delay-sensitive) traffic. Let $\mathcal{U}$ denote the set of URLLC users. The demands of these users should be satisfied in less than a millisecond with a reliability of 99.999% [4],[5]. For example, consider the case of autonomous driving. Then we would like two self driving cars to maintain a safety distance that is not extremely large, but at the same time we would like them to maintain a speed close to the speed limit. In this case, a longer delay means that either the cars should drive more slowly or maintain a larger safety distance. So if we reduce the delay, cars can drive faster with equal or smaller safety distance, without compromising safety. Since URLLC users should be satisfied with high reliability, we will seen them as having higher priority than eMBB users.

To serve all users, time is divided into small intervals of fixed length (1-2 milliseconds) called slots. During each of these slots the system can assign resources to the users to transmit data. The question is how the system should assign these resources to the users. To make it even more complicated, we do not know when the URLLC users need service, but when they do we can not postpone the demand until the next slot. Therefore we assume that we can assign all resources to eMBB users at slot level. To reduce access delay for the URLLC users and to restrict the impact on eMBB users, we divide each slot into M smaller time intervals called mini-slots. To satisfy the URLLC demands, we assume that the URLLC users can over-ride ongoing eMBB transmissions. This implies that the URLLC user 'hijacks' one or more resources (frequencies) from the eMBB users during a mini-slot. Figure 1.1 shows a scenario with only one frequency, where each slot is divided into M mini-slots. In this figure, the yellow, blue and green blocks (corresponding to resources of the frequency) are assigned to eMBB users 'yellow', 'blue' and 'green' during slots $t-1$, t and $t+1$ respectively, while the red block (resource of the frequency during mini-slot m) is hijacked from 'blue' to satisfy the URLLC demand of URLLC user 'red'.

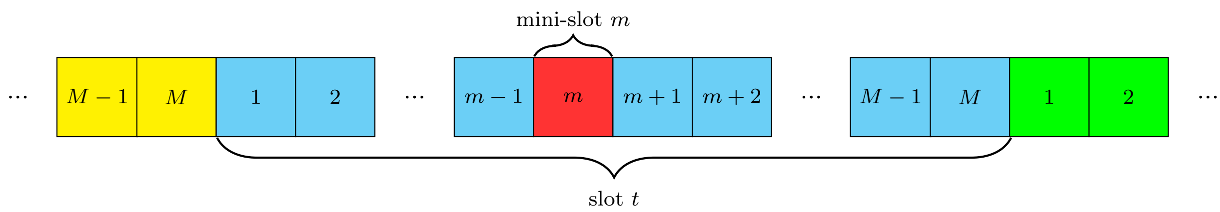

Figure 1.1: Hijacking of resources during a mini-slot

Our goal is to optimize the average throughputs of the eMBB users to maximize some utility function. However, as the URLLC users have a higher priority, the demands of these users influence the achievable average throughputs.

Assuming that there exists some stationary long-term average throughput vector $\theta = \left(\theta_1, \ldots, \theta_{|\mathcal{E}|}\right)$, we seek to find an online scheduling algorithm that attains long-term average throughputs close to the throughputs that optimize

$$\max \quad \sum_{i \in \mathcal{E}} U_i(\theta_i) \tag{1.1}$$

$$\text{subject to} \quad \theta \in \Theta, \tag{1.2}$$

where $U_i(\theta_i)$ are strictly concave smooth utility functions, and Θ the set of feasible long-term average throughputs of the eMBB users of this system. Where we notice that the URLLC demands are already incorporated in the set Θ.

1.2 Literature

Kushner and Whiting [6] consider a model with only one type of users, the eMBB users. In this work Kushner and Whiting assume that all eMBB users have saturated buffers, meaning that all users have an infinite amount of data to transmit. Furthermore, Kushner and Whiting consider a system with a single transmission frequency (e.g. Time Division Multiple Access (TDMA) operation). In their work Kushner and Whiting use a proportional fair scheduler which assigns the available resource to the user with the highest rate relative to its received average throughput. In this setting, Kushner and Whiting show that the limiting behaviour of the sample paths of the throughputs converges to the solution of an ordinary differential equation (ODE), and that this ODE has a unique (fixed) equilibrium point. In their work Kushner and Whiting indicate how their model could be extended to a scenario with multiple frequencies. However, they do not elaborate on what this means for system performance.

A somewhat similar model is considered by Stolyar [7]. Similar to Kushner and Whiting, Stolyar also considers saturated buffers, i.e. all users have an infinite amount of data to transmit. Furthermore, the algorithms of both [6] and [7] aim to optimize average service rates to maximize a concave utility function. However, as opposed to the model by Kushner and Whiting, in Stolyar's model multiple users can be served at the same time. Another difference between the models is that the rate vectors in Stolyar's work depend on the state of the system which is considered to take one of M possible states with certain probabilities, while in the work of Kushner and Whiting the rate vectors are generated by some stochastic process. Despite the differences in the models, both [6] and [7] show asymptotic optimality of the chosen algorithm.

Anand, De Veciana and Shakkottai [4] consider a system that supports two types of traffic, eMBB and URLLC traffic. In this paper the puncturing/superposition (hijacking) of time-frequency slots assigned to eMBB users is considered. For the loss in rate of the eMBB users due to this hijacking, the authors consider three models, namely a linear, a convex and a threshold loss model. For each of these models, the authors develop a scheduling algorithm (that takes URLLC users into account), and give theoretical guarantees for these scheduling algorithms. However, in [4] it is assumed that a user can achieve the same rate on all frequencies. This implies that the choice to hijack a frequency only depends on the user to which it was assigned. In reality the rates a user can achieve using different frequencies will typically differ, and should therefore be considered when choosing a frequency to hijack.

Pedersen et al. [5] present a punctured scheduling scheme for efficient transmission of URLLC traffic. In this work the authors consider three policies to puncture (over-ride) an ongoing transmission to satisfy the delay-sensitive demand. The results in this paper show that the tight latency and high reliability constraints of delay-sensitive demands can be satisfied by puncturing ongoing eMBB transmissions. As the puncturing of ongoing eMBB transmissions affects the throughput of the eMBB users in a negative way, the authors present simulation results indicating that the median throughput of all eMBB users decreases as the offered URLLC load increases. However, it is not quantified how much this puncturing scheme affects individual users.

In this report we will extend the model of Kushner and Whiting [6] to spread the signal across multiple frequencies within the frequency band it operates in (e.g. Orthogonal Frequency-Division Multiple Access (OFDMA) air interface), and to take two types (eMBB and URLLC) of traffic in to account.

1.3 Summary of results

The aim of our work is to extend the model of Kushner and Whiting [6] to work with any number of frequencies. Therefore we consider a scheduling algorithm that assigns a recourse to the user with the highest rate (corresponding to this resource) relative to its received average throughput. Furthermore we will extend this multi-frequency model to have two types of users (eMBB and URLLC) as assumed by Anand, De Veciana and Shakkottai [4]. To satisfy the URLLC demands we consider three different policies to determine which resources should be hijacked by the URLLC users. For this extended model we will show that that the sample paths of the throughputs converge to an ordinary differential equation, and that this solution is unique. To confirm this convergence we will consider some numerical examples in settings where rates are determined by independent exponential random variables or by a Rayleigh fading model. Similar to [8]-[10], but in the context of a different problem, we compare the performance of our online algorithm with hijacking policies to the optimal performance in an offline setting (where the channel rates and URLLC demands are known in advance) for a finite time horizon. Results of our comparison show that our scheduling algorithm and hijacking policies have near-optimal performance when the probability of having a non-zero URLLC demand during a mini-slot is small.

1.4 Notation

In this report we work with many indices denoting users, frequencies, slots and mini-slots. Next to these four indices we have the same variables (e.g. rates) for both types of users. To indicate the type of users we add a superscript e for eMBB users, and u for URLLC users. Furthermore, we consider a discrete-time process and its continuous-time interpolation for which we use similar notation. This might be confusing in some cases. However, to keep it as clear as possible, we will reserve some indices only for specific usages. A list of these indices and their usage is given in Table 1.1. The difference between the discrete-time process and its continuous-time counter part is that the continuous-time process is written as a function of time e.g. $\theta(t)$, while the discrete-time process has an index, e.g. θ_t.

Index	**Usage**
i	to indicate an eMBB user
j	to indicate an URLLC user
f	to indicate a frequency
t, n, τ	to indicate a time slot
m	to indicate a mini-slot

Table 1.1: Indices and their usage

1.5 Outline

We will start in Chapter 2 by describing the model and the algorithm without any hijacking that we will be using. In Chapter 3 we will formulate generalizations of the theorems in [6]. In Chapter 4 we will define three hijacking policies. In this chapter we will analyse these policies and a scenario without hijacking in a fairly simple setting where the rates are determined by independent exponential random variables. However, we notice that these hijacking policies can also be used in settings where the rates are not determined by independent exponential random variables. First we will analyse the case without hijacking in Section 4.1 and derive some theoretical results for this. In Section 4.2 we will analyse a hijacking policy that randomly hijacks frequencies to satisfy the URLLC demands. In Section 4.3 we formulate a hijacking policy that tries to hijack frequencies such that the loss in utility is minimized, but at the same time can be used in real time. The optimal score based (OSB) policy that we will describe in Section 4.4 determines which frequencies need to be hijacked by solving an integer program. In Chapter 5 we will show results of the algorithm when using one of the hijacking policies from Sections 4.2-4.4, and compare these to each other and the scenario without hijacking. In Chapter 6 we will consider a setting with Rayleigh fading, which is more realistic than the independent exponential setting. For this we discuss the fading model in Section 6.1. In Section 6.2 we will first discuss the fading simulator that we need to determine the rates. After this we will show and discuss some results for this setting with Rayleigh fading. To determine how well our hijacking policies actually perform, we will compare them to an offline setting (where the channel rates and URLLC demands is known in advance) in Chapter 7. We finish this report with conclusions and topics for further research in Chapter 8.

Chapter 2

Model

Consider a wireless network with fixed sets of eMBB and URLLC users denoted by $\mathcal{E}$ and $\mathcal{U}$ respectively. To transmit data we will assume that there is a fixed set of frequencies denoted by $\mathcal{F}$ that can be used at the same time. To determine when a user can transmit data, we will divide time into small scheduling intervals, which we will refer to as slots.

Even though the size of the eMBB data transfers are finite, we assume that the time needed to complete such a transfer is relatively long compared to a slot duration. Therefore, it is likely that the system attains some sort of equilibrium state after a relatively short period of time compared to the time needed for the data transfer. So for the purpose of slot-by-slot resource allocation it is reasonable to assume a time scale separation and pretend that eMBB transfers are of infinite size.

So in our model we will assume that the eMBB users have saturated buffers, which means that they want to transmit data at all times. As URLLC users have tight latency constraints, demands of these users are considered to have higher priority than eMBB demands. Furthermore we will assume that (at the end of slot $t-1$) we know the rates $r^e_{i,f,t}$ and $r^u_{j,f,t}$ (bits/slot) at which eMBB user $i \in \mathcal{E}$ and URLLC user $j \in \mathcal{U}$ can transmit data over frequency $f \in \mathcal{F}$ during slot t respectively.

In a stationary regime, we want to maximize the throughput of the eMBB users, but at the same time 1) share the resources fairly among the eMBB users and 2) satisfy demands of URLLC users. To do this we will consider the utility function

$$U(\theta) = \sum_{i \in \mathcal{E}} \log(\theta_i). \tag{2.1}$$

Here $\theta = \left(\theta_1, \ldots, \theta_{|\mathcal{E}|}\right)$ are the long-term average throughputs of the eMBB users, i.e. the amount of bits a user can transmit on average during a long period of time. As (2.1) is a strictly concave function, the marginal utility is higher when θ_i is low. Therefore increasing the throughput of users with low throughputs is more beneficial than increasing throughput of users with high throughputs. However, if users with lower throughputs also have lower data rates, it could still be more beneficial to increase the throughput of users that already have a higher throughput. Therefore maximizing (2.1) optimizes the throughputs of all users in some fair way.

As URLLC demands cannot be postponed for an entire slot, we divide each slot into M equally sized mini-slots, and number these as 1 up to M. Suppose that a demand arrives during mini-slot m, then it should be fulfilled during mini-slot $m+1$ or during mini-slot 1 of the next slot if $m = M$. Now we can superpose the URLLC transmissions on top of an ongoing eMBB transmission during a mini-slot, which we will refer to as hijacking of frequencies. As a result of hijacking frequencies during a mini-slot, the eMBB user transmitting on the hijacked frequencies loses the mini-slot for the hijacked frequencies. Therefore, we assume that the hijacking of a frequency initiates a hybrid automatic repeat request (HARQ) retransmission [5] to ensure that the overwritten (hijacked) data is received by the eMBB user.

Now the challenge is to determine good scheduling decisions on a slot-by-slot basis to maximize utility function (2.1), but at the same time satisfy URLLC demands. We introduce decision variables $I^{\varepsilon}_{i,f,t}$ which equal 1 if eMBB user i is scheduled to transmit on frequency f during slot t (if frequency f is not hijacked by a URLLC user), and zero otherwise. For hijacking we introduce decision variables $J^{\varepsilon}_{j,f,t,m}$ which equal 1 if URLLC user j hijacks frequency f during mini-slot m of slot t. Now define the discounted throughput (which for large t approximates the long-term average throughput θ_i) of user i up to time t as

$$\theta^{\varepsilon}_{i,t} = (1-\varepsilon)^t \theta^{\varepsilon}_{i,0} + \varepsilon \sum_{\tau=1}^{t} \sum_{f\in\mathcal{F}} (1-\varepsilon)^{t-\tau} r^e_{i,f,\tau} I^{\varepsilon}_{i,f,\tau} \left(1 - \frac{1}{M} \sum_{m=1}^{M} \sum_{j\in\mathcal{U}} J^{\varepsilon}_{j,f,\tau,m}\right), \tag{2.2}$$

where $\theta^{\varepsilon}_{i,0}$ is some initial value, and ε is the discount factor (or smoothing parameter). In Equation (2.2) we have that $\sum_{f\in\mathcal{F}} r_{i,f,\tau} I_{i,f,\tau}$ denotes the total throughput that eMBB user i has during slot τ, when no frequencies get hijacked. However, if some frequencies get hijacked, we correct for this by multiplying with $1 - \sum_{m=1}^{M} \sum_{j\in\mathcal{U}} J_{j,f,\tau,m}/M$ which is the fraction of mini-slots that are not hijacked (so if a mini-slot is hijacked, the eMBB user loses the entire mini-slot even if it was only partially needed to satisfy a URLLC demand). Notice that a smaller value of ε indicates that the most resent slots are less important. For example, take $\varepsilon = 1$, this implies that all terms where $\tau \neq t$ equal zero, and thus the throughput $\theta^{\varepsilon}_{i,t}$ does only depend on slot t. While setting $\varepsilon = 0$ implies that we do not update the throughput, which means that $\theta^{\varepsilon}_{i,t} = \theta^{\varepsilon}_{i,0}$ for all t.

Now define

$$Y^{\varepsilon}_{i,t} = \sum_{f\in\mathcal{F}} r^e_{i,f,t+1} I^{\varepsilon}_{i,f,t+1} \left(1 - \frac{1}{M} \sum_{m=1}^{M} \sum_{j\in\mathcal{U}} J^{\varepsilon}_{j,f,t+1,m}\right) - \theta^{\varepsilon}_{i,t}, \tag{2.3}$$

then we can write (2.2) in recursive form as

$$\theta^{\varepsilon}_{i,t+1} = \theta^{\varepsilon}_{i,t} + \varepsilon \left(\sum_{f\in\mathcal{F}} r^e_{i,f,t+1} I^{\varepsilon}_{i,f,t+1} \left(1 - \frac{1}{M} \sum_{m=1}^{M} \sum_{j\in\mathcal{U}} J^{\varepsilon}_{j,f,t+1,m}\right) - \theta^{\varepsilon}_{i,t} \right) = \theta^{\varepsilon}_{i,t} + \varepsilon Y^{\varepsilon}_{i,t}, \tag{2.4}$$

where $Y^{\varepsilon}_{i,t}$ denotes the update of the throughputs after slot t. To determine which user should transmit on each of the frequencies, we want to maximize the gain (minimize the loss) in utility during each slot, i.e. we want to maximize $U(\theta_t) - U(\theta_{t-1})$. Using a first-order Taylor expansion we get

$$\begin{aligned} U(\theta_t) - U(\theta_{t-1}) &= U(\theta_{t-1}) + \varepsilon \sum_{i\in\mathcal{E}} \frac{Y^{\varepsilon}_{i,t-1}}{\theta^{\varepsilon}_{i,t-1}} + \mathcal{O}(\varepsilon^2) - U(\theta_{t-1}) \\ &= \varepsilon \sum_{i\in\mathcal{E}} \frac{Y^{\varepsilon}_{i,t-1}}{\theta^{\varepsilon}_{i,t-1}} + \mathcal{O}(\varepsilon^2). \end{aligned} \tag{2.5}$$

So to maximize (2.5), we need to maximize $Y^{\varepsilon}_{i,t-1}/\theta^{\varepsilon}_{i,t-1}$, but at the same time satisfy all URLLC demands during slot t. This implies that the optimal assignment for slot t is given by the following optimization problem

$$\max \quad \sum_{i\in\mathcal{E}}\sum_{f\in\mathcal{F}} \frac{r^e_{i,f,t} I^\varepsilon_{i,f,t}\left(1-\frac{1}{M}\sum_{m=1}^{M}\sum_{j\in\mathcal{U}} J^\varepsilon_{j,f,t,m}\right)}{\theta^\varepsilon_{i,t-1}} \tag{2.6}$$

$$\text{subject to} \quad I^\varepsilon_{i,f,t} \in \{0,1\} \quad \forall_{i\in\mathcal{E}}\ \forall_{f\in\mathcal{F}}, \tag{2.7}$$

$$J^\varepsilon_{j,f,t,m} \in \{0,1\} \quad \forall_{j\in\mathcal{U}}\ \forall_{f\in\mathcal{F}}\ \forall_{m\in\{1,\dots,M\}}, \tag{2.8}$$

$$\sum_{i\in\mathcal{E}} I^\varepsilon_{i,f,t} \le 1 \quad \forall_{f\in\mathcal{F}}, \tag{2.9}$$

$$\sum_{j\in\mathcal{U}} J^\varepsilon_{j,f,t,m} \le 1 \quad \forall_{f\in\mathcal{F}}\ \forall_{m\in\{1,\dots,M\}}, \tag{2.10}$$

$$\sum_{f\in\mathcal{F}} \frac{r^u_{j,f,t}}{M} J^\varepsilon_{j,f,t,m} \ge D_{j,t,m}\mathbb{1}_{\left\{\sum\limits_{k\in\mathcal{U}}\sum\limits_{f\in\mathcal{F}} J^\varepsilon_{k,f,t,m}<|\mathcal{U}|\right\}} \quad \forall_{j\in\mathcal{U}}\ \forall_{m\in\{1,\dots,M\}}, \tag{2.11}$$

here $D_{j,t,m}$ denotes the random demand (in bits) of user $j \in \mathcal{U}$ during mini-slot m of slot t. As we assumed that an arriving demand should be fulfilled during the next mini-slot, the time of arrival determines the mini-slot m during which the demand $D_{j,t,m}$ must be fulfilled. In this optimization (2.6) maximizes $Y^\varepsilon_{i,t-1}/\theta^\varepsilon_{i,t-1}$ as we wanted. Constraints (2.7) and (2.8) ensure the decision variables $I^\varepsilon_{i,f,t}$ and $J^\varepsilon_{j,f,t,m}$ are indeed binary. Constraints (2.9) and (2.10) ensure that at most one eMBB or URLLC user can transmit on a frequency during a slot and mini-slot respectively. Note that scenarios where URLLC users hijack the frequency from eMBB users are already incorporated in the objective function. To make sure that all URLLC demands are met, we have Constraint (2.11), the factor $1/M$ is because $r^u_{j,f,t}$ is in bits/slot instead of bits/mini-slot. The indicator function in Constraint (2.11) makes sure that all frequencies are assigned to URLLC users when we can not satisfy all URLLC demands, and therefore ensures that the problem is feasible. In scenarios where not all URLLC demands can be met, we assume that unsatisfied URLLC demands are lost, meaning that we do not backlog this unsatisfied demand for later mini-slots. However, as URLLC demands should be satisfied with high reliability, we assume that there is an admission control mechanism that ensures this reliability constraint.

As the demands of URLLC users are only known at most a mini-slot in advance, we do not know the random demands $D_{j,t,m}$ in Constraint (2.11) at the time a scheduling decision has to be made. So we cannot make any scheduling decisions based on the problem given by (2.6)-(2.11) since we can not solve this problem. Therefore we schedule the eMBB users as if there are no URLLC demands, i.e. $D_{j,t,m} = 0$ for all $j \in \mathcal{U}$ and $m \in \{1,\dots,M\}$. When a URLLC demand arrives, we will hijack frequencies based on some hijacking rule (we will consider different rules in Sections 4.2.1, 4.2.2, 4.3 and 4.4).

So to determine a scheduling for the eMBB users when no URLLC demands are present, we can reduce problem (2.6)-(2.11) by setting $J^\varepsilon_{j,f,t,m} = 0$ for all $j \in \mathcal{U}$, $f \in \mathcal{F}$, $m \in \{1,\dots,M\}$, as each $J^\varepsilon_{j,f,t,m}$ that equals 1 would decrease the objective value. So the problem reduces to

$$\max \quad \sum_{i\in\mathcal{E}}\sum_{f\in\mathcal{F}} \frac{r^e_{i,f,t}}{\theta^\varepsilon_{i,t-1}} I^\varepsilon_{i,f,t} \tag{2.12}$$

$$\text{subject to} \quad I^\varepsilon_{i,f,t} \in \{0,1\} \quad \forall_{i\in\mathcal{E}}\ \forall_{f\in\mathcal{F}}, \tag{2.13}$$

$$\sum_{i\in\mathcal{E}} I^\varepsilon_{i,f,t} \le 1 \quad \forall_{f\in\mathcal{F}}. \tag{2.14}$$

Now Equation (2.13) and (2.14) imply that only user can be selected for each frequency. So to maximize Equation (2.12), we should select the user with highest $r^e_{i,f,t}/\theta^\varepsilon_{i,t-1}$ for each frequency. So an optimal assignment is given by

$$I^\varepsilon_{i,f,t} = \begin{cases} 1 & \text{if } i \in \arg\max\limits_{i\in\mathcal{E}} \frac{r^e_{i,f,t}}{\theta^\varepsilon_{i,t-1}}, \\ 0 & \text{otherwise,} \end{cases} \tag{2.15}$$

ties being broken arbitrarily. In a scenario with one frequency, this method for deciding which user can transmit on a frequency is known as the Proportional Fair scheduling rule [5],[6] since it assigns the frequency to the user that has the best rate relative to the received throughput. A possible reason why it is called the Proportional Fair scheduling rule is that the throughputs are proportional to the physical data rates of the various users, and the resource shares are approximately equal for all users.

Chapter 3

Extensions of the Kushner Whiting results

In [6] Kushner and Whiting already indicated that their model could be extended to work with multiple frequencies, and also stated that similar theorems should hold. The most significant difference between the results in this chapter and [6], is that our theorems incorporate scenarios with multiple frequencies where hijacking takes place while [6] only considers a single frequency without hijacking.

In this chapter we will first define the algorithm (recursive relation) that we will be considering. Furthermore we will introduce some notation to state the theorems and their assumptions in a compact way. In Section 3.2 we will state the assumptions. In Section 3.3 we will state the theorems for our scenario with multiple frequencies and hijacking.

3.1 Notation

Consider an algorithm of the form

$$\theta^\varepsilon_{t+1} = \theta^\varepsilon_t + \varepsilon\left(Z^\varepsilon_t - \theta^\varepsilon_t\right), \tag{3.1}$$

where θ^ε_n and Z^ε_n denote respectively the vectors $(\theta^\varepsilon_{1,n}, \ldots, \theta^\varepsilon_{|\mathcal{E}|,n})$ and $(Z^\varepsilon_{1,n}, \ldots, Z^\varepsilon_{|\mathcal{E}|,n})$, with the first subscript defining the eMBB user. Here we define

$$Z^\varepsilon_{i,t} := \sum_{f\in\mathcal{F}} r^e_{i,f,t+1} I^\varepsilon_{i,f,t+1}\left(1 - \frac{1}{M}\sum_{m=1}^{M}\sum_{j\in\mathcal{U}} J^\varepsilon_{j,f,t+1,m}\right) = Y^\varepsilon_{i,t} + \theta^\varepsilon_{i,t}, \tag{3.2}$$

where $Y^\varepsilon_{i,t}$ is defined in Equation (2.3).

As the rates might be dependent over time, the rates during previous slots carry some information about the rate during the next slot. Therefore we denote the set of all previous rates and demands by ξ^ε_t, i.e.

$$\xi^\varepsilon_t = \left\{\left(r^e_{i,f,n}, r^e_{j,f,n}, D_{j,\tau,m}\right) \in \mathbb{R}^{|\mathcal{E}|\times|\mathcal{F}|\times t} \times \mathbb{R}^{|\mathcal{U}|\times|\mathcal{F}|\times t} \times \mathbb{R}^{|\mathcal{U}|\times t\times M} \;\middle|\; i\in\mathcal{E}, j\in\mathcal{U}, f\in\mathcal{F}, n\le t, \tau<t, m\in\{1,\ldots,M\}\right\}. \tag{3.3}$$

Assuming that the demand distributions of the URLLC users does not change over time, we define $\mathcal{D}$ as the set of these demand distributions.

Now let $g_t^\varepsilon(\theta_t^\varepsilon, \xi_t^\varepsilon)$ denote the expected throughput during slot t, i.e. $g_t^\varepsilon(\theta_t^\varepsilon, \xi_t^\varepsilon) = \mathbb{E}\left[Z_t^\varepsilon \mid \mathcal{D}, \theta_\tau^\varepsilon, Z_{\tau-1}^\varepsilon, \xi_\tau^\varepsilon, \tau \leq t\right]$.

Lastly let $\theta^\varepsilon(t) = \theta_n^\varepsilon$ for $t \in [n\varepsilon, n\varepsilon + \varepsilon)$ be the continuous-time interpolation of the process θ_n^ε.

3.2 Assumptions

As we need some technical assumptions, we will state these now.

Assumption 1.
The rates $\{r_{i,f,n} : i \in \mathcal{U} \cup \mathcal{E}, f \in \mathcal{F}\}$ *are bounded.*

Assumption 2.
$g_t^\varepsilon(\theta_t^\varepsilon, \xi_t^\varepsilon)$ *is continuous in* θ *uniformly in* t, ε *and* ξ_t^ε.

Assumption 3.
ξ_t^ε *is defined on a compact sequence space.*

Assumption 4.
There is a continuous function $\bar{g}(\cdot)$ *such that*

$$\lim_{k,n,\varepsilon} \frac{1}{k} \sum_{t=n}^{n+k+1} \mathbb{E}\left[g_t^\varepsilon(\theta, \xi_t^\varepsilon) - \bar{g}(\theta) \mid \mathcal{D}, \theta_\tau^\varepsilon, Z_{\tau-1}^\varepsilon, \xi_\tau^\varepsilon, \tau \leq n\right] = 0 \tag{3.4}$$

in probability, where $\lim_{k,n,\varepsilon}$ *means that the limit is taken as* $k \to \infty$, $n \to \infty$ *and* $\varepsilon \downarrow 0$ *simultaneously in any way at all.*

3.3 Theorems

Theorem 1. *(This is part of [11, Theorems 2.1 and 2.2, Chapter 8])*
Under Assumptions 1-4, and algorithm (3.1), we have that for each subsequence of processes $\{\theta^{\varepsilon_{n_k}}(t), k = 1, 2, \ldots\}$, *there exists a further subsequence* $\varepsilon_{n_{k_l}}$ *such that* $\theta^{\varepsilon_{n_{k_l}}}(t)$ *converges weakly to*

$$\theta(t) = \theta(0) + \int_0^t \bar{g}(\theta(s)) - \theta(s)\, ds \tag{3.5}$$

as $\varepsilon_{n_{k_l}} \to 0$.

Theorem 2. *(This is part of [11, Theorems 2.1 and 2.2, Chapter 8])*
Under Assumptions 1-4, and algorithm (3.1), then for any $\delta > 0$, *the fraction of time* $\theta^\varepsilon(\cdot)$ *spends in a neighbourhood* $N_\delta(L)$ *on* $[0, T]$ *goes to one (in probability) as* $\varepsilon \downarrow 0$ *and* $T \to \infty$, *where* L *is the set of limit points of* $\theta(t)$.

To show that our assumptions are indeed sufficient for Theorems 1 and 2, we will show that all conditions of [11, Theorems 2.1 and 2.2, Chapter 8] are met. We will denote the assumptions in [11] by A1.x, these can be found in the reference, but we also added them in Appendix A. Assumption 1 covers A1.1, A1.8 and A1.10. The quantity β_n^ε in the reference equals zero, therefore Assumption 2 ensures that A1.2, A1.5 and A1.6 are met, but it also implies that A1.4 is met. Assumption 3 implies that A1.7 is met. Assumption 4 implies A1.3 and A1.9.

To be able to state and prove our next theorems, we define for $x, y \in \mathbb{R}^n$ that $x \geq y$ if $x_i \geq y_i$ for all i. When $x_i > y_i$ for all i we write $x \gg y$.

Definition 1. *(Kamke or K-condition)*
A function $f(\cdot)$ satisfies the Kamke or K-condition if for any $x, y \in \mathbb{R}^n$ and i, satisfying $x \geq y$ and $x_i = y_i$, we have $f_i(x) \geq f_i(y)$.

Theorem 3. *(This is a generalization of [6, Theorem 2.2])*
Assume Assumptions 1-4, and Algorithm (3.1). Furthermore suppose that the $I^{\varepsilon}_{i,f,t+1}$ and $J^{\varepsilon}_{j,f,t+1,m}$ defining Z^{ε}_t in Algorithm (3.1), maximize $\sum_{i\in\mathcal{E}}(Z^{\varepsilon}_{i,t} - \theta^{\varepsilon}_{i,t})/\theta^{\varepsilon}_{i,t}$ subject to some constraints on $I^{\varepsilon}_{i,f,t+1}$ and $J_{j,f,t+1,m}$, or maximize

$$\sum_{i\in\mathcal{E}} \frac{\sum_{f\in\mathcal{F}} r^e_{i,f,t+1} I^{\varepsilon}_{i,f,t+1} - \theta^{\varepsilon}_{i,t}}{\theta^{\varepsilon}_{i,t}} \tag{3.6}$$

subject to some constraints on $I^{\varepsilon}_{i,f,t+1}$, and where the hijacking policy defining the values of $J^{\varepsilon}_{j,f,t+1,m}$ is independent of the values of $I^{\varepsilon}_{j,f,t+1}$. Also assume that $\dot{\theta} = f(\theta) = \bar{g}(\theta) - \theta$ satisfies the K-condition and is Lipschitz continuous. Then the limit point $\bar{\theta}$ of (3.5) is unique, and does not depend on the initial condition $\theta^{\varepsilon}(0)$. I.e. the process $\theta^{\varepsilon}(t)$ converges to $\bar{\theta}$ as $\varepsilon \downarrow 0$ and $t \to \infty$.

Theorem 4. *(This is a generalization of [6, Theorem 2.3])*
Assume Assumptions 1-4, and algorithm (3.1). Furthermore suppose that the $I^{\varepsilon}_{i,f,t+1}$ and $J^{\varepsilon}_{j,f,t+1,m}$ defining Z^{ε}_t in Algorithm (3.1), maximize $\sum_{i\in\mathcal{E}}(Z^{\varepsilon}_{i,t} - \theta^{\varepsilon}_{i,t})/\theta^{\varepsilon}_{i,t}$ subject to some constraints on $I^{\varepsilon}_{i,f,t+1}$ and $J_{j,f,t+1,m}$, or maximize

$$\sum_{i\in\mathcal{E}} \frac{\sum_{f\in\mathcal{F}} r^e_{i,f,t+1} I^{\varepsilon}_{i,f,t+1} - \theta^{\varepsilon}_{i,t}}{\theta^{\varepsilon}_{i,t}} \tag{3.7}$$

subject to some constraints on $I^{\varepsilon}_{i,f,t+1}$, and where the hijacking policy defining the values of $J^{\varepsilon}_{j,f,t+1,m}$ is independent of the values of $I^{\varepsilon}_{j,f,t+1}$. Let $\bar{\theta}$ be the limit point of (3.5). Then there is no non-anticipating assignment policy which yields a limit throughput $\widetilde{\theta} \neq \bar{\theta}$ such that $U(\widetilde{\theta}) \geq U(\bar{\theta})$.

Theorem 5. *(This is [6, Theorem 4.1] which refers to [12, Proposition 1.1])*
Let $\theta(t|x)$ be the solution to $\dot{\theta} = f(\theta)$ with initial condition x where $f(\cdot)$ is Lipschitz continuous and satisfies the K-condition. If $x \geq y$ (respectively $\gg$), then $\theta(t|x) \geq \theta(t|y)$ (respectively $\gg$).

As Theorems 1 and 2 are different formulations of [11, Theorems 2.1 and 2.2, Chapter 8], and Theorem 5 is [6, Theorem 4.1] which refers to [12, Proposition 1.1], we refer to the references for the proof of the theorems.

Proof of Theorem 3
Let $\widetilde{\theta}(0) \gg 0$ be a starting point arbitrarily close to the origin. Then $\theta(t|\widetilde{\theta}(0))$ is initially increasing in each coordinate. Now let $s > 0$ be small, then $\theta(s|\widetilde{\theta}(0)) \geq \widetilde{\theta}(0)$ since $\theta(t|\widetilde{\theta}(0))$ is initially increasing in each coordinate. So Theorem 5 now gives that $\theta(t+s|\widetilde{\theta}(0)) = \theta(t|\theta(s|\widetilde{\theta}(0))) \geq \theta(t|\widetilde{\theta}(0))$. Therefore we conclude that $\theta(t|\widetilde{\theta}(0))$ is non-decreasing (in each coordinate) for all t. Because $\bar{g}$ is bounded, the path $\theta(t|\widetilde{\theta}(0))$ is also bounded. Therefore there is a unique limit point for the path $\theta(t|\widetilde{\theta}(0))$.

Now we will show that there is a unique limit point for all paths starting near the origin. To do this suppose that $\widetilde{\theta}$ and $\widehat{\theta}$, with $\widetilde{\theta} \neq \widehat{\theta}$ are two limit points with initial conditions $\widetilde{\theta}(0)$ and $\widehat{\theta}(0)$ respectively, with $\widetilde{\theta}(0)$ and $\widehat{\theta}(0)$ arbitrarily close to the origin. As we start arbitrarily close to the origin, all components of both paths $\theta(t|\widetilde{\theta}(0))$ and $\theta(t|\widehat{\theta}(0))$ are initially increasing. Thus for small enough $\widetilde{\theta}(0)$ there is $t_0 > 0$

such that $\theta(t_0|\widehat{\theta}(0)) \gg \widetilde{\theta}(0)$. Then by Theorem 5 we have $\theta(t+t_0|\widehat{\theta}(0)) = \theta(t|\theta(t_0|\widehat{\theta}(0))) \geq \theta(t|\widetilde{\theta}(0))$ which implies that $\widehat{\theta} \geq \widetilde{\theta}$. Now with a similar argument we get $\widehat{\theta} \leq \widetilde{\theta}$. Thus we conclude that there is a unique limit point, say $\bar{\theta}$.

Define $Q = \{x \mid x \geq \bar{\theta}\}$. Suppose an arbitrary initial condition $\widehat{\theta}(0) \gg 0$. Now let $\widetilde{\theta}(0)$ be arbitrarily close to the origin, and such that $\widehat{\theta}(0) \gg \widetilde{\theta}(0) \gg 0$, then we know that $\bar{\theta}$ is the limit point of $\theta(t|\widetilde{\theta}(0))$. Then by Theorem 5 we have that $\theta(t|\widehat{\theta}(0)) \geq \theta(t|\widetilde{\theta}(0))$, therefore we get $\lim_{t\to\infty} \theta(t|\widehat{\theta}(0)) \geq \bar{\theta}$. Thus we have $\lim_{t\to\infty} \theta(t|\widehat{\theta}(0)) \in Q$.

Next we show that all paths starting in Q will converge to $\bar{\theta}$. Suppose there is a point $\widetilde{\theta} \geq \bar{\theta}$ with $\widetilde{\theta} \neq \bar{\theta}$ (then $\widetilde{\theta} \in Q$) such that

$$\dot{U}(\widetilde{\theta}) = \sum_{i\in\mathcal{E}} \frac{\bar{g}_i(\widetilde{\theta}) - \widetilde{\theta}_i}{\widetilde{\theta}_i} \geq 0. \tag{3.8}$$

This means that there is a path $\theta(t|\widetilde{\theta})$ that by concavity of $U(\cdot)$ stays away from $\bar{\theta}$ since $U(\widetilde{\theta}) > U(\bar{\theta})$. Combining Equation (3.8) and $\widetilde{\theta} \geq \bar{\theta}$ with $\widetilde{\theta} \neq \bar{\theta}$ we get that

$$\sum_{i\in\mathcal{E}} \frac{\bar{g}_i(\widetilde{\theta}) - \bar{\theta}_i}{\bar{\theta}_i} > 0. \tag{3.9}$$

To show that Equation (3.9) is not true we will consider two algorithms. For the first algorithm we use a scheduling rule (denoted by the $\widetilde{I}^{\varepsilon}_{i,f,t}$ and $\widetilde{J}^{\varepsilon}_{j,f,t,m}$) that satisfies all the constraints given by Equations (2.7)-(2.11) but only depends on the rates $r^e_{i,f,t}$, $r^u_{i,f,t}$, the URLLC demands $D_{j,t,m}$ and $\widetilde{\theta}$ and update $\theta^{\varepsilon}_{i,t}$ according to Equation (2.4) with initial condition $\bar{\theta}$. Let $\widetilde{Z}^{\varepsilon}_t$ be defined by Equation (3.2) with $\widetilde{I}^{\varepsilon}_{i,f,t}$ and $\widetilde{J}^{\varepsilon}_{j,f,t,m}$ (see Equation (2.3)).

For our second algorithm we could have two possible scenarios (see conditions of the theorem), namely

1. The $I^{\varepsilon}_{i,f,t}$ and $J^{\varepsilon}_{j,f,t,m}$ are defined by the solution of (2.6)-(2.11);
2. The $I^{\varepsilon}_{j,f,t}$ are defined by the solution of (2.12)-(2.14), and the hijacking policy defining the values of $J^{\varepsilon}_{j,f,t,m}$ is independent of the values of $I^{\varepsilon}_{j,f,t}$.

Also for this algorithm we update $\theta^{\varepsilon}_{i,t}$ according to Equation (2.4) with initial condition $\bar{\theta}$.

In the first case we know that $\sum_{i\in\mathcal{E}}(Z^{\varepsilon}_{i,t} - \theta^{\varepsilon}_{i,t})/\theta^{\varepsilon}_{i,t} \geq \sum_{i\in\mathcal{E}}(\widetilde{Z}^{\varepsilon}_{i,t} - \theta^{\varepsilon}_{i,t})/\theta^{\varepsilon}_{i,t}$. This is because the $I^{\varepsilon}_{i,f,t}$ and $J^{\varepsilon}_{j,f,t,m}$ are defined by the solution of (2.6)-(2.11), which is meant to maximize $\sum_{i\in\mathcal{E}} Z^{\varepsilon}_{i,t-1}/\theta^{\varepsilon}_{i,t-1}$ subject to the same constraints that $\widetilde{I}^{\varepsilon}_{i,f,t}$ and $\widetilde{J}^{\varepsilon}_{j,f,t,m}$ have to satisfy.

In the second case, we know that

$$\sum_{i\in\mathcal{E}}\sum_{f\in\mathcal{F}} \frac{r^e_{i,f,t} I^{\varepsilon}_{i,f,t}}{\theta^{\varepsilon}_{i,t-1}} \geq \sum_{i\in\mathcal{E}}\sum_{f\in\mathcal{F}} \frac{r^e_{i,f,t} \widetilde{I}^{\varepsilon}_{i,f,t}}{\theta^{\varepsilon}_{i,t-1}} \tag{3.10}$$

as $I^{\varepsilon}_{i,f,t}$ and $\widetilde{I}^{\varepsilon}_{i,f,t}$ are subject to the same constraints, and the $I^{\varepsilon}_{i,f,t}$ maximize this expression under these constraints. This implies

$$\sum_{i\in\mathcal{E}}\sum_{f\in\mathcal{F}} \frac{r^e_{i,f,t} I^{\varepsilon}_{i,f,t}\left(1 - \frac{1}{M}\sum_{m=1}^{M}\sum_{j\in\mathcal{U}} J^{\varepsilon}_{j,f,t,m}\right)}{\theta^{\varepsilon}_{i,t-1}} \geq \sum_{i\in\mathcal{E}}\sum_{f\in\mathcal{F}} \frac{r^e_{i,f,t} \widetilde{I}^{\varepsilon}_{i,f,t}\left(1 - \frac{1}{M}\sum_{m=1}^{M}\sum_{j\in\mathcal{U}} J^{\varepsilon}_{j,f,t,m}\right)}{\theta^{\varepsilon}_{i,t-1}}. \tag{3.11}$$

As we do not know which frequencies to hijack for our second algorithm, we assume that we hijack the same frequencies as our first algorithm would (i.e. $J^{\varepsilon}_{j,f,t,m} = \widetilde{J}^{\varepsilon}_{j,f,t,m}$ for all j, f, t, m), this way the $J^{\varepsilon}_{j,f,t,m}$ do not depend on $I_{i,f,t}$. So now we have

$$\begin{aligned}\sum_{i\in\mathcal{E}} \frac{Z^{\varepsilon}_{i,t} - \theta^{\varepsilon}_{i,t}}{\theta^{\varepsilon}_{i,t}} &= \sum_{i\in\mathcal{E}} \frac{\sum_{f\in\mathcal{F}} r^{e}_{i,f,t+1} I^{\varepsilon}_{i,f,t+1}\left(1 - \frac{1}{M}\sum_{m=1}^{M}\sum_{j\in\mathcal{U}} J^{\varepsilon}_{j,f,t+1,m}\right) - \theta^{\varepsilon}_{i,t}}{\theta^{\varepsilon}_{i,t}} \\ &\geq \sum_{i\in\mathcal{E}} \frac{\sum_{f\in\mathcal{F}} r^{e}_{i,f,t+1} \widetilde{I}^{\varepsilon}_{i,f,t+1}\left(1 - \frac{1}{M}\sum_{m=1}^{M}\sum_{j\in\mathcal{U}} J^{\varepsilon}_{j,f,t+1,m}\right) - \theta^{\varepsilon}_{i,t}}{\theta^{\varepsilon}_{i,t}} \\ &= \sum_{i\in\mathcal{E}} \frac{\sum_{f\in\mathcal{F}} r^{e}_{i,f,t+1} \widetilde{I}^{\varepsilon}_{i,f,t+1}\left(1 - \frac{1}{M}\sum_{m=1}^{M}\sum_{j\in\mathcal{U}} \widetilde{J}^{\varepsilon}_{j,f,t+1,m}\right) - \theta^{\varepsilon}_{i,t}}{\theta^{\varepsilon}_{i,t}} = \sum_{i\in\mathcal{E}} \frac{\widetilde{Z}^{\varepsilon}_{i,t} - \theta^{\varepsilon}_{i,t}}{\theta^{\varepsilon}_{i,t}},\end{aligned} \tag{3.12}$$

where the first and last equality are by definition of $Z^{\varepsilon}_{i,t}$ (see Equation (3.2)). The second equality is because we assumed $J_{j,f,t,m} = \widetilde{J}_{j,f,t,m}$ for all j, f, t, m, and the inequality is because of Equation (3.11).

So in both cases we have $\sum_{i\in\mathcal{E}}(Z^{\varepsilon}_{i,t} - \theta^{\varepsilon}_{i,t})/\theta^{\varepsilon}_{i,t} \geq \sum_{i\in\mathcal{E}}(\widetilde{Z}^{\varepsilon}_{i,t} - \theta^{\varepsilon}_{i,t})/\theta^{\varepsilon}_{i,t}$, now let $\lfloor x \rfloor$ denote the integer part of x, then for small enough $\varepsilon > 0$ we can write

$$\begin{aligned}U(\theta^{\varepsilon}(t)) - U(\bar{\theta}) &= U\left(\theta_{\lfloor t/\varepsilon \rfloor}\right) - U(\theta_0) \\ &= \varepsilon \sum_{\tau=0}^{\lfloor t/\varepsilon \rfloor - 1} \sum_{i\in\mathcal{E}} \left(\frac{Z^{\varepsilon}_{i,\tau} - \theta^{\varepsilon}_{i,\tau}}{\theta^{\varepsilon}_{i,\tau}} + \mathcal{O}(\varepsilon^2) \right) \\ &\geq \varepsilon \sum_{\tau=0}^{\lfloor t/\varepsilon \rfloor - 1} \sum_{i\in\mathcal{E}} \left(\frac{\widetilde{Z}^{\varepsilon}_{i,\tau} - \theta^{\varepsilon}_{i,\tau}}{\theta^{\varepsilon}_{i,\tau}} + \mathcal{O}(\varepsilon^2) \right).\end{aligned} \tag{3.13}$$

The first equality is by definition of the interpolated process and the initial condition. By repeatedly applying a Taylor expansion we get the second equality. The inequality follows from the fact that $\sum_{i\in\mathcal{E}}(Z^{\varepsilon}_{i,t} - \theta^{\varepsilon}_{i,t})/\theta^{\varepsilon}_{i,t} \geq \sum_{i\in\mathcal{E}}(\widetilde{Z}^{\varepsilon}_{i,t} - \theta^{\varepsilon}_{i,t})/\theta^{\varepsilon}_{i,t}$. Now if we let $\varepsilon \downarrow 0$, we can use a stochastic approximation argument to get

$$U(\theta(t)) - U(\bar{\theta}) = \int_0^t \sum_{i\in\mathcal{E}} \frac{\bar{g}_i(\theta(s)) - \theta_i(s)}{\theta_i(s)} ds \geq \int_0^t \sum_{i\in\mathcal{E}} \frac{\bar{g}_i(\widetilde{\theta}) - \theta_i(s)}{\theta_i(s)} ds \tag{3.14}$$

Now taking derivatives with respect to t yields

$$\dot{U}(\theta(t)) = \sum_{i\in\mathcal{E}} \frac{\bar{g}_i(\theta(t)) - \theta_i(t)}{\theta_i(t)} \geq \sum_{i\in\mathcal{E}} \frac{\bar{g}_i(\widetilde{\theta}) - \theta_i(t)}{\theta_i(t)}. \tag{3.15}$$

Now substituting $t = 0$ gives us (because $\bar{g}(\bar{\theta}) = \bar{\theta}$) that

$$0 = \sum_{i\in\mathcal{E}} \frac{\bar{g}_i(\bar{\theta}) - \bar{\theta}_i}{\bar{\theta}_i} \geq \sum_{i\in\mathcal{E}} \frac{\bar{g}_i(\widetilde{\theta}) - \bar{\theta}_i}{\bar{\theta}_i} > 0, \tag{3.16}$$

where the strict inequality follows from (3.9). Therefore we conclude that $\dot{U}(\theta) < 0$ for all $\theta \in Q \setminus \{\bar{\theta}\}$ which implies that any path starting in Q must end up in $\bar{\theta}$. Therefore $\bar{\theta}$ is the unique limit point which is independent of the initial condition. ■

Proof of Theorem 4

Suppose there is an assignment policy ($\widetilde{I}^{\varepsilon}_{i,f,t}$ and $\widetilde{J}^{\varepsilon}_{i,f,t}$) that attains limit point $\widetilde{\theta} \neq \bar{\theta}$ such that $U(\widetilde{\theta}) \geq U(\bar{\theta})$. Now when we use this assignment policy with starting point $\bar{\theta}$ we have that

$$\widetilde{\theta}^{\varepsilon}_i(t) = (1-\varepsilon)^{\lfloor t/\varepsilon \rfloor}\bar{\theta}_i + \varepsilon \sum_{k=1}^{\lfloor t/\varepsilon \rfloor} (1-\varepsilon)^{\lfloor t/\varepsilon \rfloor - k} \sum_{f\in\mathcal{F}} r^{e}_{i,f,t+1}\widetilde{I}^{\varepsilon}_{i,f,t+1}\left(1 - \frac{1}{M}\sum_{m=1}^{M}\sum_{j\in\mathcal{U}} \widetilde{J}^{\varepsilon}_{j,f,t+1,m}\right). \tag{3.17}$$

Now by Theorem 1 this converges weakly to $\widetilde{\theta}(t) = e^{-t}\bar{\theta} + (1-e^{-t})\,\widetilde{\theta}$ as $\varepsilon \downarrow 0$. Similarly we get that

$$\theta^{\varepsilon}_i(t) = (1-\varepsilon)^{\lfloor t/\varepsilon \rfloor}\bar{\theta}_i + \varepsilon \sum_{k=1}^{\lfloor t/\varepsilon \rfloor} (1-\varepsilon)^{\lfloor t/\varepsilon \rfloor - k} \sum_{f\in\mathcal{F}} r^{e}_{i,f,t+1}I^{\varepsilon}_{i,f,t+1}\left(1 - \frac{1}{M}\sum_{m=1}^{M}\sum_{j\in\mathcal{U}} J^{\varepsilon}_{j,f,t+1,m}\right) \tag{3.18}$$

converges weakly to $\theta(t) = \bar{\theta}$ as $\varepsilon \downarrow 0$ when we use assignment policy ($I^{\varepsilon}_{i,f,t}$ and $J^{\varepsilon}_{i,f,t}$).

Using the exact same argument as in the proof of Theorem 3, we get that for assignment policy ($\widetilde{I}_{i,f,t}$ and $\widetilde{J}_{i,f,t}$) we have that $\sum_{i\in\mathcal{E}}(Z^{\varepsilon}_{i,t} - \theta^{\varepsilon}_{i,t})/\theta^{\varepsilon}_{i,t} \geq \sum_{i\in\mathcal{E}}(\widetilde{Z}^{\varepsilon}_{i,t} - \theta^{\varepsilon}_{i,t})/\theta^{\varepsilon}_{i,t}$. So for small enough ε, we can write

$$\begin{aligned}
U(\theta^{\varepsilon}(t)) - U(\bar{\theta}) &= U\left(\theta_{\lfloor t/\varepsilon \rfloor}\right) - U(\theta_0) \\
&= \varepsilon \sum_{\tau=0}^{\lfloor t/\varepsilon \rfloor - 1} \sum_{i\in\mathcal{E}} \left(\frac{Z_{i,\tau} - \theta^{\varepsilon}_{i,\tau}}{\theta^{\varepsilon}_{i,\tau}} + \mathcal{O}(\varepsilon^2)\right) \\
&\geq \varepsilon \sum_{\tau=0}^{\lfloor t/\varepsilon \rfloor - 1} \sum_{i\in\mathcal{E}} \left(\frac{\widetilde{Z}^{\varepsilon}_{i,\tau} - \theta^{\varepsilon}_{i,\tau}}{\theta^{\varepsilon}_{i,\tau}} + \mathcal{O}(\varepsilon^2)\right) \\
&= U\left(\widetilde{\theta}_{\lfloor t/\varepsilon \rfloor}\right) - U(\theta_0) \\
&= U(\widetilde{\theta}^{\varepsilon}(t)) - U(\bar{\theta}).
\end{aligned} \tag{3.19}$$

Therefore as $\varepsilon \downarrow 0$ we have that

$$0 = U(\bar{\theta}) - U(\bar{\theta}) = U(\theta(t)) - U(\bar{\theta}) \geq U(\widetilde{\theta}(t)) - U(\bar{\theta}).$$

Now taking the derivative with respect to t yields

$$0 \geq \dot{U}(\widetilde{\theta}(t)).$$

However, strict concavity of $U(\cdot)$ implies that

$$\dot{U}(\widetilde{\theta}(t)) = \sum_{i\in\mathcal{E}} \frac{\widetilde{\theta}_i - \bar{\theta}_i}{(e^t - 1)\,\widetilde{\theta}_i + \bar{\theta}_i} > 0 \qquad \forall_{t\geq 0}, \tag{3.20}$$

which gives a contradiction, and therefore there can not be a limit point $\widetilde{\theta} \neq \bar{\theta}$ with $U(\widetilde{\theta}) \geq U(\bar{\theta})$. ■

Chapter 4

Independent exponential model

In reality, rates can often be modelled by exponential random variables. Therefore we will in this chapter consider a model where the rates of each user-frequency pair are independent exponentially distributed. This means that the rates of each user-frequency pair are independent of all other user-frequency pairs, but also the rates at time t are independent of the rates at time $s \neq t$.

In this chapter we will first consider a scenario without hijacking in Section 4.1. For this scenario we will show that we can use Theorem 1, and derive the ODE. In Section 4.2 we will consider a scenario where we use a random hijacking policy. For this scenario we will show that we can still use Theorem 1 and that under some conditions can also derive the ODE. In Section 4.3 we will formulate a more sophisticated hijacking policy. Finally we will formulate a hijacking policy that should outperform all other hijacking policies in Section 4.4.

4.1 No hijacking

To be able to use Theorems 1 and 2, we should confirm that this setting satisfies Assumptions 1-4. As the exponential distribution takes values in $(0, \infty)$, Assumption 1 would not be valid. However, if we truncate the exponential distribution such that the mass of the truncated part is almost 0, then Assumption 1 is valid. Because we truncate the exponential distribution such that the truncated part has arbitrary small mass, the truncated distribution has approximately an exponential distribution, so for convenience we will use the exponential distribution since the results will be approximately the same.

We will work with the assignment policy given by (2.15). As the rates are independent exponentials, we will write $r^e_{i,f,t+1} = s^e_{i,f} X^e_{i,f,t+1}$ for the rates of eMBB users, where $s^e_{i,f}$ is a constant that represents the average rate eMBB user i would achieve on frequency f if it is always selected, and $X^e_{i,f,t}$ is an exponential random variable with mean 1 representing the channel state.

For convenience we will drop the time slot subscript t (we still write the subscript m indicating the mini-slots) and superscripts e indicating that the variable corresponds to an eMBB user and the smoothing parameter ε in the remainder of this section.

As all rates are independent, we get that the history ξ has no influence on $g(\theta, \xi)$. So for user $i \in \mathcal{E}$ we get that

$$
\begin{aligned}
g_i(\theta, \xi) &= \mathbb{E}\left[Z_i \mid \theta\right] \\
&= \mathbb{E}\left[\sum_{f \in \mathcal{F}} r_{i,f} I_{i,f} \left(1 - \frac{1}{M} \sum_{m=1}^{M} \sum_{j \in \mathcal{U}} J_{j,f,m}\right) \;\middle|\; \theta\right] \\
&= \sum_{f \in \mathcal{F}} \mathbb{E}\left[r_{i,f} I_{i,f} \mid \theta\right] \\
&= \sum_{f \in \mathcal{F}} \mathbb{E}\left[s_{i,f} X_{i,f} I_{i,f} \mid \theta\right] \\
&= \sum_{f \in \mathcal{F}} \mathbb{E}\left[s_{i,f} X_{i,f} \mathbb{1}_{\left\{\frac{s_{i,f} X_{i,f}}{\theta_i} \geq \frac{s_{k,f} X_{k,f}}{\theta_k},\ k \in \mathcal{E}, k \neq i\right\}} \;\middle|\; \theta\right].
\end{aligned} \tag{4.1}
$$

Here the first and second equality are by definition of $g(\theta, \xi)$ and Z_i. For the third equality we use the linearity of expectations and the fact that there is no hijacking, which implies that all $J_{j,f,m}$ should be zero for an optimal assignment. Next we rewrite $r_{i,f} = s_{i,f} X_{i,f}$. In the last equality we replace $I_{i,f}$ by a function that corresponds to decision rule (2.15).

Now we will rewrite the indicator function in the expectation. To do this we denote the event that user k is preferred over user i on frequency f by $A_{i,k}^f$, i.e. $A_{i,k}^f := \{s_{i,f} X_{i,f}/\theta_i < s_{k,f} X_{k,f}/\theta_k\}$. Then we can write

$$
\begin{aligned}
\mathbb{1}_{\left\{\frac{s_{i,f} X_{i,f}}{\theta_i} \geq \frac{s_{k,f} X_{k,f}}{\theta_k},\ k \in \mathcal{E}, k \neq i\right\}} &= \prod_{\substack{k \in \mathcal{E},\\ k \neq i}} \mathbb{1}_{\left\{\frac{s_{i,f} X_{i,f}}{\theta_i} \geq \frac{s_{k,f} X_{k,f}}{\theta_k}\right\}} \\
&= \prod_{\substack{k \in \mathcal{E},\\ k \neq i}} \left(1 - \mathbb{1}_{\left\{\frac{s_{i,f} X_{i,f}}{\theta_i} < \frac{s_{k,f} X_{k,f}}{\theta_k}\right\}}\right) \\
&= \prod_{\substack{k \in \mathcal{E},\\ k \neq i}} \left(1 - \mathbb{1}_{\{A_{i,k}^f\}}\right).
\end{aligned} \tag{4.2}
$$

As the last product implies a sum over all subsets of $\mathcal{E} \setminus \{i\}$, we denote the set of all subsets of $\mathcal{E} \setminus \{i\}$ by Q_i. Then we get that

$$
\prod_{\substack{k \in \mathcal{E},\\ k \neq i}} \left(1 - \mathbb{1}_{\{A_{i,k}^f\}}\right) = \sum_{J \in Q_i} (-1)^{|J|} \prod_{k \in J} \mathbb{1}_{\{A_{i,k}^f\}}. \tag{4.3}
$$

Now suppose that we condition on the value of $X_{i,f}$ to be x, then we can write

$$
\begin{aligned}
\mathbb{P}\left(\prod_{k \in J} \mathbb{1}_{\{A_{i,k}^f\}} \;\middle|\; X_{i,f} = x\right) &= \prod_{k \in J} \mathbb{P}\left(\mathbb{1}_{\{A_{i,k}^f\}} \;\middle|\; X_{i,f} = x\right) \\
&= \prod_{k \in J} \mathbb{P}\left(\frac{s_{i,f}}{\theta_i} x < \frac{s_{k,f} X_{k,f}}{\theta_k}\right) \\
&= \prod_{k \in J} \mathbb{P}\left(\frac{s_{i,f} \theta_k}{s_{k,f} \theta_i} x < X_{k,f}\right) \\
&= \prod_{k \in J} \exp\left(-\frac{s_{i,f} \theta_k}{s_{k,f} \theta_i} x\right) \\
&= \exp\left(-\frac{s_{i,f} \sum_{k \in J} \theta_k \prod_{\substack{m \in J,\\ m \neq k}} s_{m,f}}{\theta_i \prod_{k \in J} s_{k,f}} x\right).
\end{aligned} \tag{4.4}
$$

For the first equality we use the independence of the $X_{k,f}$. To get the second equality we replace the indicator of the event with the event itself where we also use the conditioning on $X_{i,f}$. For the third equality we rewrite the event such that the random variable $X_{k,f}$ is on one side of the inequality. This allows us to easily use the cumulative distribution function of an exponential random variable with mean 1 in the fourth equality. For the last equality we rewrite the obtained expression.

Now we can write

$$\begin{aligned}
\mathbb{E}\left[X_{i,f}\prod_{k\in J}\mathbb{1}_{\{A^f_{i,k}\}}\;\middle|\;\theta\right] &= \int_0^\infty x\mathbb{P}\left(\prod_{k\in J}\mathbb{1}_{\{A^f_{i,k}\}}\;\middle|\;X_{i,f}=x\right)\exp(-x)\;dx \\
&= \int_0^\infty x\exp\left(-\frac{s_{i,f}\sum_{k\in J}\theta_k\prod_{\substack{m\in J,\\ m\neq k}}s_{m,f}}{\theta_i\prod_{k\in J}s_{k,f}}x\right)\exp(-x)\;dx \\
&= \int_0^\infty x\exp\left(-\frac{\theta_i\prod_{k\in J}s_{k,f}+s_{i,f}\sum_{k\in J}\theta_k\prod_{\substack{m\in J,\\ m\neq k}}s_{m,f}}{\theta_i\prod_{k\in J}s_{k,f}}x\right)\;dx.
\end{aligned} \tag{4.5}$$

For the first equality we conditioned on the value of $X_{i,f}$, which allows us to use Equation (4.4) for the second equality. To get the last equality we combined the exponentials.

Now let

$$\lambda := \frac{\theta_i\prod_{k\in J}s_{k,f}+s_{i,f}\sum_{k\in J}\theta_k\prod_{\substack{m\in J,\\ m\neq k}}s_{m,f}}{\theta_i\prod_{k\in J}s_{k,f}},$$

then we get

$$\begin{aligned}
\mathbb{E}\left[X_{i,f}\prod_{k\in J}\mathbb{1}_{\{A^f_{i,k}\}}\;\middle|\;\theta\right] &= \int_0^\infty x\exp\left(-\lambda x\right)\;dx \\
&= \frac{1}{\lambda}\int_0^\infty x\lambda\exp\left(-\lambda x\right)\;dx \\
&= \left(\frac{1}{\lambda}\right)^2 \\
&= \left(\frac{\theta_i\prod_{k\in J}s_{k,f}}{\theta_i\prod_{k\in J}s_{k,f}+s_{i,f}\sum_{k\in J}\theta_k\prod_{\substack{m\in J,\\ m\neq k}}s_{m,f}}\right)^2,
\end{aligned} \tag{4.6}$$

where we used the definition of λ and Equation (4.5) to obtain the first equality. Multiplying by a 'smart' 1 yields the second equality, which allows us to recognize that the integral is the expectation of an exponential random variable with mean $1/\lambda$, which gives the third equality. For the final equality we substitute λ.

Now the expectation in Equation (4.1) is given by

$$\begin{aligned}\mathbb{E}\left[s_{i,f}X_{i,f}\mathbb{1}_{\left\{\frac{s_{i,f}X_{i,f}}{\theta_i}\geq\frac{s_{k,f}X_{k,f}}{\theta_k},\ k\in\mathcal{E},k\neq i\right\}}\ \Big|\ \theta\right] &= \mathbb{E}\left[s_{i,f}X_{i,f}\sum_{J\in Q_i}(-1)^{|J|}\prod_{k\in J}\mathbb{1}_{\left\{A^f_{i,k}\right\}}\ \Big|\ \theta\right]\\ &= s_{i,f}\sum_{J\in Q_i}(-1)^{|J|}\mathbb{E}\left[X_{i,f}\prod_{k\in J}\mathbb{1}_{\left\{A^f_{i,k}\right\}}\ \Big|\ \theta\right]\\ &= s_{i,f}\sum_{J\in Q_i}(-1)^{|J|}\left(\frac{\theta_i\prod\limits_{k\in J}s_{k,f}}{\theta_i\prod\limits_{k\in J}s_{k,f}+s_{i,f}\sum\limits_{k\in J}\theta_k\prod\limits_{\substack{m\in J,\\ m\neq k}}s_{m,f}}\right)^2,\end{aligned} \tag{4.7}$$

where we use Equations (4.2) and (4.3) for the first equality. For the second equality we use the linearity of the expectation, and Equation (4.6) gives us the last equality.

So combining Equations (4.1) and (4.7) give us

$$\begin{aligned}g_i(\theta,\xi) &= \sum_{f\in\mathcal{F}}\mathbb{E}\left[s_{i,f}X_{i,f}\mathbb{1}_{\left\{\frac{s_{i,f}X_{i,f}}{\theta_i}\geq\frac{s_{k,f}X_{k,f}}{\theta_k},\ k\in\mathcal{E},k\neq i\right\}}\ \Big|\ \theta\right]\\ &= \sum_{f\in\mathcal{F}}s_{i,f}\sum_{J\in Q_i}(-1)^{|J|}\left(\frac{\theta_i\prod\limits_{k\in J}s_{k,f}}{\theta_i\prod\limits_{k\in J}s_{k,f}+s_{i,f}\sum\limits_{k\in J}\theta_k\prod\limits_{\substack{m\in J,\\ m\neq k}}s_{m,f}}\right)^2.\end{aligned} \tag{4.8}$$

Because $\theta_i > 0$ for all $i \in \mathcal{E}$ and $s_{i,f} > 0$ for all $i \in \mathcal{E}$, $f \in \mathcal{F}$, the fraction exists and is continuous in θ. Therefore it is not difficult to see that $g_i(\theta, \xi)$ satisfies Assumption 2.

Assumption 3 is a technical assumption, so we will assume that it satisfied.

Since $g(\theta, \xi)$ does not depend on ξ, we can take $\bar{g}(\theta) = g(\theta, \xi)$ which ensures that Assumption 4 is satisfied.

Given the system parameters ($\mathcal{E}$, $\mathcal{F}$, all $s_{i,f}$ and initial value $\theta(0) = \theta_0$), we know by Theorem 1 that the ODE for scenarios with multiple frequencies and exponential rates is given by

$$\dot{\theta}_i = \sum_{f\in\mathcal{F}}s_{i,f}\sum_{J\in Q_i}(-1)^{|J|}\left(\frac{\theta_i\prod\limits_{k\in J}s_{k,f}}{\theta_i\prod\limits_{k\in J}s_{k,f}+s_{i,f}\sum\limits_{k\in J}\theta_k\prod\limits_{\substack{m\in J,\\ m\neq k}}s_{m,f}}\right)^2-\theta_i. \tag{4.9}$$

Now we want to show that (4.9) has a unique limit point, and that this limit point maximizes our utility function (2.1). So first let $f(\theta) = \dot{\theta} = \bar{g}(\theta) - \theta$ where

$$\bar{g}_i(\theta) = \sum_{f\in\mathcal{F}}s_{i,f}\sum_{J\in Q_i}(-1)^{|J|}\left(\frac{\theta_i\prod\limits_{k\in J}s_{k,f}}{\theta_i\prod\limits_{k\in J}s_{k,f}+s_{i,f}\sum\limits_{k\in J}\theta_k\prod\limits_{\substack{m\in J,\\ m\neq k}}s_{m,f}}\right)^2 \tag{4.10}$$

$$= \sum_{f\in\mathcal{F}}\mathbb{E}\left[s_{i,f}X_{i,f}\mathbb{1}_{\left\{\frac{s_{i,f}X_{i,f}}{\theta_i}\geq\frac{s_{k,f}X_{k,f}}{\theta_k},\ k\in\mathcal{E},k\neq i\right\}}\right]. \tag{4.11}$$

For $a \leq b$ with $a_i = b_i$ we know that $\mathbb{1}_{\left\{\frac{s_{i,f}X_{i,f}}{a_i} \geq \frac{s_{k,f}X_{k,f}}{a_k},\ k\in\mathcal{E},k\neq i\right\}} \leq \mathbb{1}_{\left\{\frac{s_{i,f}X_{i,f}}{b_i} \geq \frac{s_{k,f}X_{k,f}}{b_k},\ k\in\mathcal{E},k\neq i\right\}}$, so we have $\bar{g}_i(a) \leq \bar{g}_i(b)$ and therefore

$$f_i(a) = \bar{g}_i(a) - a_i = \bar{g}_i(a) - b_i \leq \bar{g}_i(b) - b_i = f_i(b). \tag{4.12}$$

From this we conclude that the K-condition is satisfied, and we notice that $f(\theta)$ is Lipschitz continuous on $[c, \infty)$ for any $c > 0$. Now by Theorems 3 and 4 we know that (4.9) has a unique limit point, and this limit point maximizes our utility function given by (2.1).

4.2 Random hijacking

Because we want to satisfy URLLC demands as well, we should immediately schedule/hijack frequencies during the next mini-slot to satisfy the URLLC demand when such a demand arrives. To do this we will assume that we hijack the frequencies uniformly at random. This means that if URLLC user j has a demand of size $D_{j,t,m}$ bits ($D_{j,t,m}$ is a random variable) during mini-slot m of slot t, we choose a frequency (that is still assigned to eMBB users) to hijack at random, where each frequency has equal probability to be chosen. If this frequency cannot satisfy the demand, i.e. $r^u_{j,f,t}/M < D_{j,t,m}$, we hijack another frequency, and keep doing this until the hijacked frequencies together satisfy the demand or there are no frequencies left to hijack.

4.2.1 One hijacker

Before we complicate the scenario we will first look at a relatively simple case, where there is only one hijacking URLLC user. As we keep hijacking frequencies until the hijacked frequencies together satisfy the demand, the probability that frequency f gets hijacked depends on the order of hijacking. Denote H_f as the event that frequency f is hijacked during mini-slot m.

Let S be an arbitrary hijacking sequence, which is a permutation of the elements of $\mathcal{F}$. Denote the k^{th} element of this hijacking sequence by S_k. Let S^f denote the index of frequency f in sequence S. Assuming that our only URLLC user is user j, we get

$$\begin{aligned}
\mathbb{P}\left(H_f \mid S\right) &= \mathbb{P}\left(\text{frequencies hijacked before } f \text{ in } S \text{ together do not satisfy the demand}\right) \\
&= \mathbb{P}\left(\frac{1}{M}\sum_{k=1}^{S^f-1} r^u_{j,S_k,t} < D_{j,t,m}\right) \\
&= \int_0^\infty \mathbb{P}\left(\frac{1}{M}\sum_{k=1}^{S^f-1} r^u_{j,S_k,t} < x\right) f_{D_{j,t,m}}(x)\, dx.
\end{aligned} \tag{4.13}$$

where $f_{D_{j,t,m}}$ is the probability density function of $D_{j,t,m}$. Given a hijacking sequence S, we will only hijack frequency f when the frequencies that we hijack before f together cannot satisfy the demand. This observation gives us the first equality. For the second equality, we write the expression from words to symbols where we note that $r^u_{j,f,t}$ denotes the rate in bits/slot instead of bits/mini-slot, to correct for this we multiply with $1/M$. To get the last equality we condition on the demand $D_{j,t,m}$.

We should also know the probability of a certain hijacking sequence S. As each frequency is hijacked with equal probability, the probability to hijack a certain frequency (that is not yet hijacked) when m frequencies have already been hijacked is given by $1/(|\mathcal{F}| - m)$. Therefore we have

$$\mathbb{P}\left(S\right) = \prod_{m=0}^{|\mathcal{F}|-1} \frac{1}{|\mathcal{F}| - m}. \tag{4.14}$$

Now let P denote the set of all possible hijacking sequences i.e. the set of all possible permutations of the elements of $\mathcal{F}$. Then we get

$$\begin{aligned}
\mathbb{P}(H_f) &= \sum_{S \in P} \mathbb{P}(H_f \mid S) \mathbb{P}(S) \\
&= \sum_{S \in P} \mathbb{P}(H_f \mid S) \prod_{m=0}^{|\mathcal{F}|-1} \frac{1}{|\mathcal{F}| - m} \\
&= \left(\prod_{m=0}^{|\mathcal{F}|-1} \frac{1}{|\mathcal{F}| - m} \right) \sum_{S \in P} \mathbb{P}(H_f \mid S) \\
&= \left(\prod_{m=0}^{|\mathcal{F}|-1} \frac{1}{|\mathcal{F}| - m} \right) \sum_{S \in P} \int_0^\infty \mathbb{P}\left(\frac{1}{M} \sum_{k=1}^{S^f - 1} r^u_{j,S_k,t} < x \right) f_{D_{j,t,m}}(x)\, dx.
\end{aligned} \tag{4.15}$$

Because the order in which frequencies are hijacked matters, we determine the probability that frequency f is hijacked by conditioning on all possible hijacking sequences, which gives the first equality. The second equality follows by substituting Equation (4.13). Now we recognise all hijacking sequences have equal probability and therefore the product can be taken out of the sum in the third equality. For the last equality we substitute Equation (4.14). Here we are assuming that URLLC users are always present, but could have zero demand with non-zero probability.

Again for convenience we will drop the time subscript t and superscripts ε for the smoothing parameter e indicating that variables correspond to eMBB users (if needed we will write superscript u when variables correspond to URLLC users).

Because we now need to take hijacking of frequencies into account, we know that $g(\theta, \xi) = \mathbb{E}[Z]$ will differ from the no-hijacking scenario (see Section 4.1). In this case we can write

$$\begin{aligned}
g_i(\theta, \xi) &= \mathbb{E}[Z_i \mid \theta] \\
&= \mathbb{E}\left[\sum_{f \in \mathcal{F}} r_{i,f} I_{i,f} \left(1 - \frac{1}{M} \sum_{m=1}^{M} \sum_{j \in \mathcal{U}} J_{j,f,m} \right) \;\middle|\; \theta \right] \\
&= \sum_{f \in \mathcal{F}} \left(\mathbb{E}\left[r_{i,f} I_{i,f} \;\middle|\; \theta \right] - \frac{1}{M} \sum_{m=1}^{M} \sum_{j \in \mathcal{U}} \mathbb{E}\left[r_{i,f} I_{i,f} J_{j,f,m} \;\middle|\; \theta \right] \right) \\
&= \sum_{f \in \mathcal{F}} \left(\mathbb{E}\left[r_{i,f} I_{i,f} \;\middle|\; \theta \right] - \frac{1}{M} \sum_{m=1}^{M} \sum_{j \in \mathcal{U}} \mathbb{E}\left[r_{i,f} I_{i,f} \;\middle|\; \theta \right] \mathbb{P}(J_{j,f,m} = 1) \right) \\
&= \sum_{f \in \mathcal{F}} \left(1 - \frac{1}{M} \sum_{m=1}^{M} \sum_{j \in \mathcal{U}} \mathbb{P}(J_{j,f,m} = 1) \right) \mathbb{E}\left[r_{i,f} I_{i,f} \;\middle|\; \theta \right] \\
&= \sum_{f \in \mathcal{F}} \left(1 - \sum_{j \in \mathcal{U}} \mathbb{P}(J_{j,f,1} = 1) \right) \mathbb{E}\left[r_{i,f} I_{i,f} \;\middle|\; \theta \right] \\
&= \sum_{f \in \mathcal{F}} \left(1 - \sum_{j \in \mathcal{U}} \mathbb{P}(J_{j,f,1} = 1) \right) \mathbb{E}\left[s_{i,f} X_{i,f} \mathbb{1}_{\left\{ \frac{s_{i,f} X_{i,f}}{\theta_i} \geq \frac{s_{k,f} X_{k,f}}{\theta_k},\ k \in \mathcal{E}, k \neq i \right\}} \;\middle|\; \theta \right],
\end{aligned} \tag{4.16}$$

where the first equality is by definition of $g(\theta, \xi)$. The second equality follows by definition of Z (see Equation (3.2)). Using linearity of the expectation yields the third equality, and conditioning on the value of $J_{j,f,m}$ gives the fourth equality. Rewriting yields the fifth equality. For the sixth equality we notice that $\mathbb{P}(J_{j,f,m} = 1)$ is equal for all mini-slots, this is because hijacking a frequency is a uniform decision on a mini-slot. Therefore the $1/M$ cancels the sum over all M mini-slots. In the last equality we substitute $I_{i,f}$ for the indicator function corresponding to the assignment policy given by (2.15), and rewrite $r_{i,f} = s_{i,f} X_{i,f}$.

Now we notice that we are only considering one hijacking user. Therefore we have that

$$\sum_{j\in\mathcal{U}} \mathbb{P}\left(J_{j,f,1} = 1\right) = \mathbb{P}\left(J_{1,f,1} = 1\right) = \mathbb{P}\left(H_f\right). \tag{4.17}$$

Next to this we also know that Equation (4.7) is still valid since we still use (as in Section 4.1) assignment policy (2.15). So combining Equations (4.7), (4.16) and (4.17) we get

$$g_i(\theta,\xi) = \sum_{f\in\mathcal{F}} \left(1 - \mathbb{P}\left(H_f\right)\right) s_{i,f} \sum_{J\in Q_i} (-1)^{|J|} \left(\frac{\theta_i \prod_{k\in J} s_{k,f}}{\theta_i \prod_{k\in J} s_{k,f} + s_{i,f} \sum_{k\in J} \theta_k \prod_{\substack{m\in J,\\ m\neq k}} s_{m,f}} \right)^2. \tag{4.18}$$

Again since $\theta_i > 0$ for all $i \in \mathcal{E}$ and $s_{i,f} > 0$ for all $i \in \mathcal{E}$, $f \in \mathcal{F}$, the fraction exists and is continuous in θ. Therefore we can conclude that Assumption 2 is satisfied.

Similar to the no-hijacking scenario in Section 4.1, we can take $\bar{g}(\theta) = g(\theta,\xi)$ as $g(\theta,\xi)$ does not depend on the history ξ. This way we have that Assumption 4 is satisfied. Assumptions 1 and 3 are satisfied for the same reasons as in Section 4.1.

Because Assumptions 1-4 are satisfied, Theorem 1 tells us that the ODE for a scenario with random hijacking is given by

$$\dot{\theta}_i = \sum_{f\in\mathcal{F}} \left(1 - \mathbb{P}\left(H_f\right)\right) s_{i,f} \sum_{J\in Q_i} (-1)^{|J|} \left(\frac{\theta_i \prod_{k\in J} s_{k,f}}{\theta_i \prod_{k\in J} s_{k,f} + s_{i,f} \sum_{k\in J} \theta_k \prod_{\substack{m\in J,\\ m\neq k}} s_{m,f}} \right)^2 - \theta_i. \tag{4.19}$$

Using the same arguments as in Section 4.1 can show that $f(\theta) = \dot{\theta} = \bar{g}(\theta) - \theta$ satisfies the K-condition, and is Lipschitz continuous on $[c,\infty)$ for any $c > 0$. So by Theorem 3 and 4 we have that (4.19) has a unique limit point which maximizes our utility function (2.1).

4.2.2 Multiple hijackers

In a situation with multiple hijackers it is more difficult to calculate $\mathbb{P}\left(H_f\right)$, and therefore the problem becomes a lot more complicated. To avoid this more complicated analysis, we assume that there are more frequencies than hijacking URLLC users. Now we assign a subset $\mathcal{F}_u$ of the frequencies to each hijacking user such that $\mathcal{F}_j \cap \mathcal{F}_k = \emptyset$ for all $j,k \in \mathcal{U}$. Assuming that hijacker $u \in \mathcal{U}$ can only hijack frequencies from $\mathcal{F}_u$, we can calculate $\mathbb{P}\left(H_f\right)$ in a similar way as in Section 4.2.1.

Essentially we simplified the problem to calculate $\mathbb{P}\left(H_f\right)$, so the same results as for the one-hijacker case will hold. However, the partitioning of $\mathcal{F}$ influences the performance. Because a random partitioning does not take advantage of any information, we will consider an assignment based on the following integer program:

$$\begin{aligned}
\max \quad & \sum_{j\in\mathcal{U}}\sum_{f\in\mathcal{F}} s^u_{j,f} x_{j,f} && (4.20)\\
\text{subject to} \quad & x_{j,f} \in \{0,1\} \quad \forall_{j\in\mathcal{U}}\ \forall_{f\in\mathcal{F}}, && (4.21)\\
& \sum_{j\in\mathcal{U}} x_{j,f} \le 1 \quad \forall_{f\in\mathcal{F}}, && (4.22)\\
& \sum_{f\in\mathcal{F}} x_{j,f} \ge K \quad \forall_{j\in\mathcal{U}}. && (4.23)
\end{aligned}$$

In this integer program the $x_{j,f}$ are the decision variables which equal 1 if frequency f is in $\mathcal{F}_j$, and 0 otherwise. We chose objective function (4.20) since it assigns the frequencies to the users such that the average achievable rates of all hijacking URLLC users are maximized. The decision variables should be 1 or 0 since we can only assign a frequency to a set $\mathcal{F}_j$ or not, this is represented by Constraint (4.21). Constraint (4.22) ensures that a frequency is only assigned to one of the URLLC users, otherwise two URLLC users might try to hijack the same frequency. Constraint (4.23) ensures that each $\mathcal{F}_j$ contains at least K frequencies. Constraint (4.23) can be changed to represent other desirable properties, but also the objective function (4.20) can be changed to get better results.

We should note that partitioning the frequencies, decreases the reliability of the system to satisfy URLLC demands since a URLLC user can only hijack a predetermined subset of the frequencies, while using an ideal policy it could hijack all frequencies.

4.3 Score based hijacking

Instead of random hijacking, we now consider a more sophisticated hijacking policy. As we assign the frequencies to users according to $\arg\max_i r^e_{i,f,t+1}/\theta^\varepsilon_{i,t}$ (see assignment policy (2.15)), we define the score of a frequency as $\max_i r^e_{i,f,t+1}/\theta^\varepsilon_{i,t}$. Then we could sacrifice the frequencies with lowest scores to satisfy the demands of URLLC users as these contribute the least in terms of utility. Before we dive into details (how to assign hijacked frequencies to URLLC users) of the exact hijacking policy, we will first consider a scenario where giving up only one frequency would suffice.

4.3.1 Sacrifice one frequency

Suppose that we must sacrifice one frequency during each slot, then we should add a constraint to the optimization problem given by (2.12)-(2.14) to exclude one frequency. So the optimization problem for slot t now becomes

$$\begin{aligned}
\max \quad & \sum_{i\in\mathcal{E}}\sum_{f\in\mathcal{F}} \frac{r^e_{i,f,t+1} I^\varepsilon_{i,f,t+1}}{\theta^\varepsilon_{i,t}} && (4.24)\\
\text{subject to} \quad & \sum_{i\in\mathcal{E}} I^\varepsilon_{i,f,t+1} \le 1 \quad \forall_{f\in\mathcal{F}}, && (4.25)\\
& I^\varepsilon_{i,f,t+1} \in \{0,1\} \quad \forall_{i\in\mathcal{E}}\ \forall_{f\in\mathcal{F}}, && (4.26)\\
& \sum_{f\in\mathcal{F}}\sum_{i\in\mathcal{E}} I^\varepsilon_{i,f,t+1} \le |\mathcal{F}| - 1. && (4.27)
\end{aligned}$$

The solution to this optimization problem is given by

$$I^{\varepsilon}_{i,f,t} = \begin{cases} 1 & \text{if } i \in \arg\max_{e \in \mathcal{E}} \frac{r_{e,f,t}}{\theta^{\varepsilon}_{e,t-1}} \text{ and } \frac{r_{i,f,t}}{\theta^{\varepsilon}_{i,t-1}} > \min_{f \in \mathcal{F}} \max_{i \in \mathcal{E}} \frac{r_{i,f,t}}{\theta^{\varepsilon}_{i,t-1}}, \\ 0 & \text{otherwise.} \end{cases} \tag{4.28}$$

This assignment is the same as (2.15) except that the frequency with the lowest score, which is assumed to be unique, is no longer selected.

This particular scenario is similar to the scenario in Section 4.1. There is one difference though. That is, in the analysis of $g^{\varepsilon}_t(\theta^{\varepsilon}_t, \xi^{\varepsilon}_t)$. We should now replace $I^{\varepsilon}_{i,f,t+1}$ by

$$\mathbb{1}_{\left\{\frac{s^e_{i,f} X^e_{i,f,t+1}}{\theta^{\varepsilon}_{i,t}} \geq \frac{s^e_{k,f} X^e_{k,f,t+1}}{\theta^{\varepsilon}_{k,t}},\ k \in \mathcal{E}, k \neq i\right\}} \mathbb{1}_{\left\{\frac{s^e_{i,f} X^e_{i,f,t+1}}{\theta^{\varepsilon}_{i,t}} > \min_{f \in \mathcal{F}} \max_{k \in \mathcal{E}} \frac{s^e_{k,f} X^e_{k,f,t+1}}{\theta^{\varepsilon}_{k,t}}\right\}} \tag{4.29}$$

instead of

$$\mathbb{1}_{\left\{\frac{s^e_{i,f} X^e_{i,f,t+1}}{\theta^{\varepsilon}_{i,t}} \geq \frac{s^e_{k,f} X^e_{k,f,t+1}}{\theta^{\varepsilon}_{k,t}},\ k \in \mathcal{E}, k \neq i\right\}}. \tag{4.30}$$

But even with this change $g^{\varepsilon}_t(\theta^{\varepsilon}_t, \xi^{\varepsilon}_t)$ will satisfy Assumption 2 since $\theta^{\varepsilon}_i > 0$ for all $i \in \mathcal{E}$ and $s^e_{i,f} > 0$ for all $i \in \mathcal{E}$ and $f \in \mathcal{F}$.

So we conclude that Theorems 1-4 are still valid. Because of Theorem 4 we conclude that if we have to sacrifice one frequency we should do this based on the score. The reason for this is that score based hijacking minimizes loss in utility.

4.3.2 Naive score based algorithm

Now that we have a method to determine which frequency to sacrifice, we need to determine which URLLC user will get this frequency. To do this we will maximize the data that will be transmitted on this frequency. In summary we have the following steps, where $D_{j,t,m}$ is the remaining demand of URLLC user j during mini-slot m of slot t.

1. Determine frequency with lowest score - say frequency f;
2. Assign frequency f to the URLLC user with highest $\min\{r^u_{j,f,t}/M,\ D_{j,t,m}\}$;
3. If user j is chosen, reduce $D_{j,t,m}$ with $\min\{r^u_{j,f,t}/M,\ D_{j,t,m}\}$;
4. If there is still a user with positive demand and there are still frequencies assigned to eMBB users return to step 1. Otherwise terminate.

Note that we already know the scores as these are needed to assign frequencies to eMBB users. Therefore this hijacking algorithm has complexity $\mathcal{O}(|\mathcal{F}|^2)$, since each iteration of the steps has complexity $\mathcal{O}(|\mathcal{F}|)$ because of step 1, and there can at most be $|\mathcal{F}|$ iterations since there are only $|\mathcal{F}|$ frequencies. So this is a polynomial time hijacking algorithm. Therefore we can use this algorithm to determine which frequencies we will hijack and to which URLLC user each of these hijacked frequencies should be assigned.

Because of the method to hijack frequencies, it is difficult to determine $g^{\varepsilon}_t(\theta^{\varepsilon}_t, \xi^{\varepsilon}_t)$, but as long as it satisfies Assumption 2, we conclude that Theorems 1 and 2 will hold for the same reasons as in Section 4.1. However, we cannot apply Theorems 3 and 4 to show that there is a unique equilibrium that maximizes the utility function because the assignment of the $J^{\varepsilon}_{j,f,t,m}$ depends on the assignment of $I^{\varepsilon}_{i,f,t}$, and these $J^{\varepsilon}_{j,f,t,m}$ are not necessarily optimal. For example consider the scenario in Table 4.1 with one URLLC user. Suppose that the URLLC user has a demand of 50 bits during the mini-slot, then the algorithm will select both frequencies, while it could do better for the eMBB users by only selecting frequency 2.

Frequency	Score	Rate in bits/mini-slot (URLLC user)
1	0.85	40
2	1.1	60

Table 4.1: Example of suboptimality of the score based hijacking policy

4.4 Optimal score based hijacking

To get a feeling what the best is that we can do (in a non-anticipating scenario) we will consider the following approach, where we solve an integer program every time there is at least one non-zero URLLC demand. We will refer to this approach as the optimal score based or OSB policy. Let $D_{j,t,m}$ denote the demand of URLLC user j during mini-slot m of slot t. Then the optimal assignment of frequencies during a slot will be the solution of

$$\begin{aligned}
\max \quad & \sum_{i\in\mathcal{E}}\sum_{f\in\mathcal{F}} \frac{r^e_{i,f,t} I^\varepsilon_{i,f,t}\left(1-\frac{1}{M}\sum_{m=1}^{M}\sum_{j\in\mathcal{U}} J^\varepsilon_{j,f,t,m}\right)}{\theta^\varepsilon_{i,t-1}} \\
\text{subject to} \quad & I^\varepsilon_{i,f,t}\in\{0,1\} \quad \forall_{i\in\mathcal{E}}\,\forall_{f\in\mathcal{F}}, \\
& J^\varepsilon_{j,f,t,m}\in\{0,1\} \quad \forall_{j\in\mathcal{U}}\,\forall_{f\in\mathcal{F}}\,\forall_{m\in\{1,\dots,M\}}, \\
& \sum_{i\in\mathcal{E}} I^\varepsilon_{i,f,t}\le 1 \quad \forall_{f\in\mathcal{F}}, \\
& \sum_{j\in\mathcal{U}} J^\varepsilon_{j,f,t,m}\le 1 \quad \forall_{f\in\mathcal{F}}\,\forall_{m\in\{1,\dots,M\}}, \\
& \sum_{f\in\mathcal{F}} \frac{r^u_{j,f,t}}{M} J^\varepsilon_{j,f,t,m} \ge D_{j,t,m}\mathbb{1}_{\left\{\sum\limits_{k\in\mathcal{U}}\sum\limits_{f\in\mathcal{F}} J^\varepsilon_{k,f,t,m}<|\mathcal{U}|\right\}} \quad \forall_{j\in\mathcal{U}}\,\forall_{m\in\{1,\dots,M\}},
\end{aligned}$$

(this is the problem given by (2.6)-(2.11)).

Since the URLLC demands are known at most a mini-slot in advance, we schedule the eMBB users according to the solution of the integer program given by (2.12)-(2.14) each slot (which is (2.6)-(2.11) but with all demands $D_{j,t,m}=0$ for all j,t,m). When URLLC demands for mini-slot m arrive, we will hijack frequencies during mini-slot m to satisfy these demands. To determine which frequencies get hijacked, we solve the following integer program for each mini-slot m.

$$\min \quad \sum_{f\in\mathcal{F}}\sum_{j\in\mathcal{U}} J^\varepsilon_{j,f,t,m} \max_{i\in\mathcal{E}} \frac{r^e_{i,f,t}}{\theta^\varepsilon_{i,t-1}} \tag{4.31}$$

$$\text{subject to} \quad J^\varepsilon_{j,f,t,m}\in\{0,1\} \quad \forall_{j\in\mathcal{U}}\,\forall_{f\in\mathcal{F}}, \tag{4.32}$$

$$\sum_{j\in\mathcal{U}} J^\varepsilon_{j,f,t,m}\le 1 \quad \forall_{f\in\mathcal{F}}, \tag{4.33}$$

$$\sum_{f\in\mathcal{F}} \frac{r^u_{j,f,t}}{M} J^\varepsilon_{j,f,t,m} \ge D_{j,t,m}\mathbb{1}_{\left\{\sum\limits_{k\in\mathcal{U}}\sum\limits_{f\in\mathcal{F}} J^\varepsilon_{k,f,t,m}<|\mathcal{U}|\right\}} \quad \forall_{j\in\mathcal{U}}. \tag{4.34}$$

Note that we use the score of the frequencies as a measure of loss in the objective function (4.31). We chose for this because we concluded in Section 4.3.1 that a score based hijacking policy is optimal since this minimizes the loss in terms of the utility function.

Because binary integer linear programming is NP-complete, we know that it could be difficult to determine the optimal solution of (4.31)-(4.34), where we note that the indicator function in (4.34) is only there to ensure feasibility. However, we could remove this indicator in most cases as the URLLC demands must be satisfied with high reliability.

If we would try to solve the optimization problem given by (4.31)-(4.34) using a brute force method, we have to consider $2^{|\mathcal{U}||\mathcal{F}|}$ solutions since there are $|\mathcal{U}||\mathcal{F}|$ binary decision variables. Fortunately Constraint (4.33) reduces the number of possibly feasible solutions to $\sum_{k=0}^{|\mathcal{F}|} |\mathcal{U}|^k \binom{|\mathcal{F}|}{k} = (|\mathcal{U}| + 1)^{|\mathcal{F}|}$. However, in practical situations this solution space will still be too large to solve in real time. Therefore it will not be possible to find the optimal solution in the little amount of time available to the scheduler.

Chapter 5

Simulations

By Theorem 1, we know that the continuous-time interpolation of the process $\{\theta_t^\varepsilon,\ t = 0, 1, 2, \ldots\}$ converges weakly to

$$\theta(t) = \theta(0) + \int_0^t \bar{g}(\theta(s)) - \theta(s)\ ds \tag{5.1}$$

as $\varepsilon \downarrow 0$. However, as we cannot simulate the continuous-time process we will compare our simulation results to a discrete-time approximation of Equation (5.1), given by

$$\theta_t^\varepsilon = \theta_0^\varepsilon + \varepsilon \sum_{n=0}^{t-1} \left(\bar{g}(\theta_n^\varepsilon) - \theta_n^\varepsilon \right). \tag{5.2}$$

In Equation (5.2), the term $\bar{g}(\theta_n^\varepsilon) - \theta_n^\varepsilon$ defines the expected gain in throughput during slot n, which corresponds to Y_n^ε in our model. Therefore we expect the simulated throughputs to follow the approximated throughputs produced using Equation (5.2) closely. To verify this we will consider three scenarios.

5.1 Scenario 1

In this scenario we consider a system with two eMBB users, one URLLC user and two frequencies. Suppose that the users can achieve average throughputs (in bits/slot) using the frequencies given by

$$s^e = \begin{pmatrix} 572 & 256 \\ 128 & 632 \end{pmatrix},$$
$$s^u = \begin{pmatrix} 442 & 310 \end{pmatrix},$$

where the row indicates the user and the column indicates the frequency. In this scenario we assume that all users have an initial throughput of 500 bits/slot.

Furthermore, we assume that the hijacking URLLC user has a demand distribution given by

$$\mathbb{P}\left(D_{1,t,m} = 0\right) = 0.95,$$
$$\mathbb{P}\left(D_{1,t,m} = 20\right) = 0.05,$$

where $D_{j,t,m}$ is given in bits. Here we assume that the demand of each mini-slot is independent of the other mini-slots, and that the demand must be satisfied during the indicated mini-slot.

We will consider three smoothing parameters $\varepsilon = 10^{-4}$, 10^{-5} and 10^{-6}. For each case we will simulate $10/\varepsilon$ slots consisting of 8 mini-slots each. For these cases we expect that the simulated results for the no and random hijacking scenario follow the approximation of the ODE given by (5.2) closely. Since a smaller smoothing parameter implies a smaller update of the throughputs, we expect less variation around the approximation of the ODE when ε is smaller.

Logically, we expect that the no-hijacking case will give highest throughputs. Further we expect the OSB policy to perform best followed by the score based policy, and expect the random policy to perform worst. We expect this order of performance because the OSB policy is most advanced, and the random policy is least advanced among the hijacking policies.

In Figures 5.1-5.3 we show the results of simulations with $\varepsilon = 10^{-4}$, 10^{-5} and 10^{-6} respectively. In these figures, the blue line shows the approximation of the ODE for the no-hijacking case, where we use that $\bar{g}_i(\theta) = g_i(\theta)$ which is given by Equation (4.8). The red line represents the approximation of the ODE for the random hijacking case, here we use that $\bar{g}_i(\theta) = g_i(\theta)$ given by Equation (4.18). The cyan, magenta, black and green lines represent the values of θ_t for the no, random, score based and OSB hijacking policies respectively.

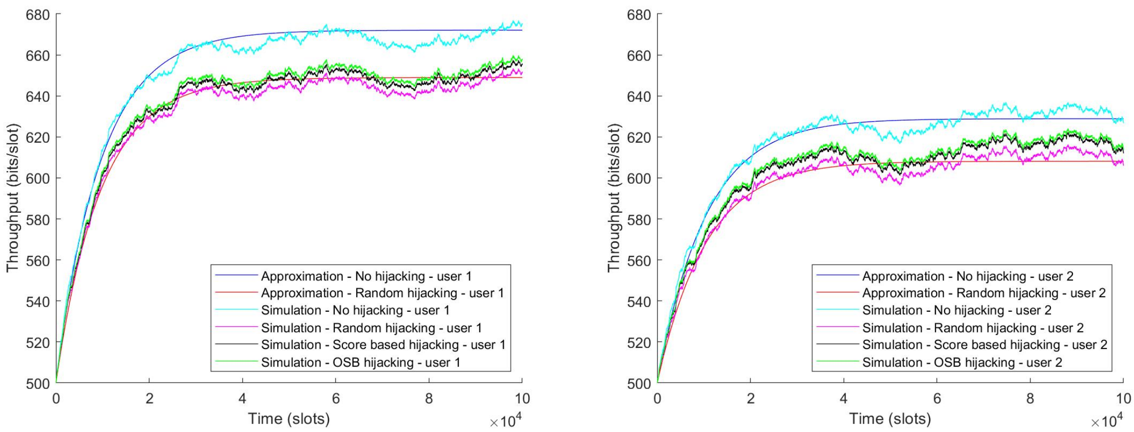

(a) User 1 (b) User 2

Figure 5.1: Average throughputs over time for scenario 1 with $\varepsilon = 10^{-4}$

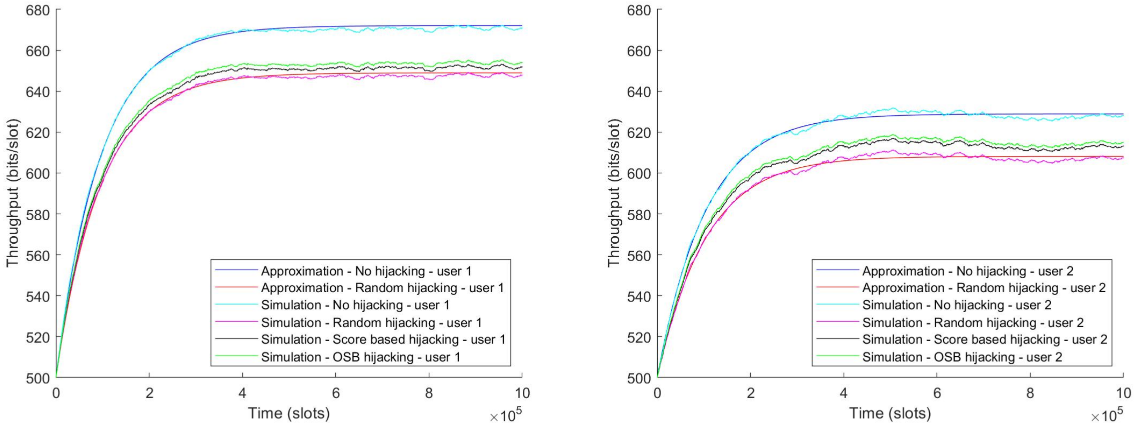

(a) User 1 (b) User 2

Figure 5.2: Average throughputs over time for scenario 1 with $\varepsilon = 10^{-5}$

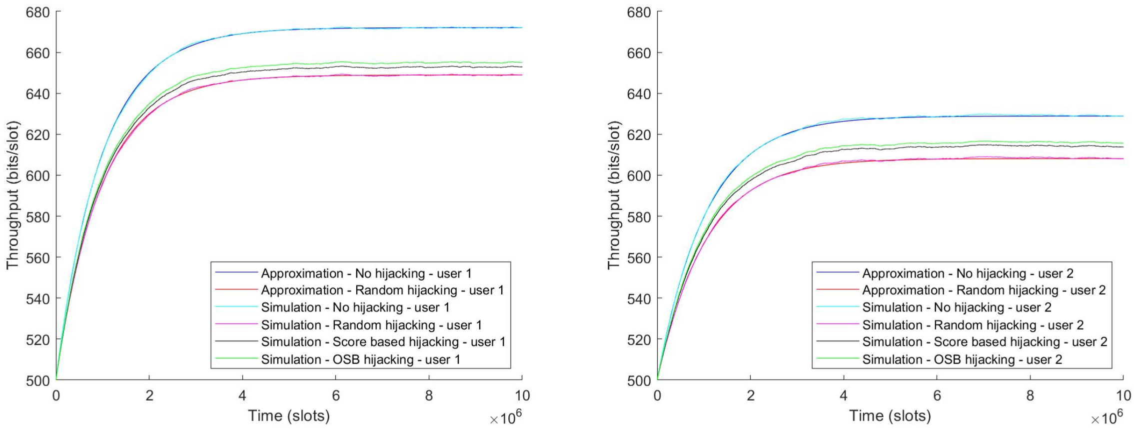

(a) User 1 (b) User 2

Figure 5.3: Average throughputs over time for scenario 1 with $\varepsilon = 10^{-6}$

If we compare Figures 5.1-5.3, we see that the simulation results confirm our expectation that the values of θ vary the least for the scenario with $\varepsilon = 10^{-6}$, and vary the most for the scenario with $\varepsilon = 10^{-4}$. This less varying behaviour for smaller values of ε show that the sample paths of the simulation indeed converge to the ODE which confirms Theorems 1 and 2. Furthermore we see that for all three values of ε it takes approximately $4/\varepsilon$ slots to converge. This indicates that the time (number of slots) needed for convergence is of the order $1/\varepsilon$.

Figures 5.1-5.3 also confirm our expectation that the OSB policy (green curve) performs best among the hijacking policies followed by the score based policy (black curve), and that the random policy (magenta curve) performs worst.

In these figures we see that the score based policy performs only slightly worse then the OSB policy, which we believe to perform near-optimal in a non-anticipating setting. This is remarkable since it is much easier to determine which frequencies to hijack for the score based then for the OSB policy.

In Figures 5.1-5.3, we see that all hijacking policies follow a similar curve as the no-hijacking case, and therefore show approximately the same amount of variation over time. To investigate the amount of variation between different simulations for a converged system, we will do 500 simulations for the no-hijacking case with $\varepsilon = 10^{-5}$ and plot the approximated ODE, the average throughput (of the 500 runs), and 95% and 99% confidence bounds. The results of these simulations can be found in Figure 5.4, here we only plot the results for the slots after slot $5 \cdot 10^5$, since the system should (almost) be converged for these slots.

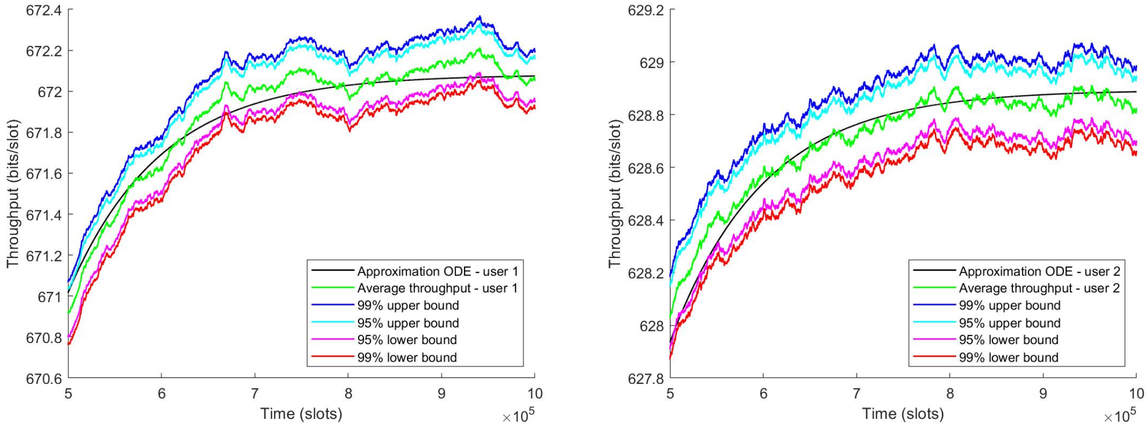

(a) User 1

(b) User 2

Figure 5.4: Average throughputs, and confidence bounds for scenario 1 without hijacking with $\varepsilon = 10^{-5}$

The results in Figure 5.4 show that the Approximation of the ODE (black line) for user 1 is outside the 95% confidence band (the magenta and cyan lines) a few times but only for a short time period. For user 2 we see that the average throughputs (green line) match quite well with the approximation of the ODE (black line). Furthermore the approximation of the ODE for user 2 is approximately in the middle of the both the 95% and 99% confidence bands. So we have no reason to believe that our theoretical results are wrong.

5.2 Scenario 2

In this scenario we consider a system with three eMBB users, two URLLC users and three frequencies. Suppose that the average throughputs (in bits/slot) are given by

$$s^e = \begin{pmatrix} 560 & 70 & 420 \\ 210 & 350 & 490 \\ 280 & 630 & 140 \end{pmatrix},$$

$$s^u = \begin{pmatrix} 182 & 576 & 332 \\ 694 & 244 & 376 \end{pmatrix},$$

where the row indicates the user and the column indicates the frequency. In this scenario we assume that all users have an initial throughput of 570 bits/slot.

For hijacking, we assume that the demand $D_{j,t,m}$ of URLLC user j during mini-slot m of slot t is independent from any other demand. Further more we assume that the demand distributions for mini-slot m during slot t for the two URLLC users are given by

$$\mathbb{P}(D_{1,t,m} = 0) = 0.95, \qquad \mathbb{P}(D_{1,t,m} = 20) = 0.05,$$
$$\mathbb{P}(D_{2,t,m} = 0) = 0.95, \qquad \mathbb{P}(D_{2,t,m} = 25) = 0.05,$$

where $D_{j,t,m}$ is given in bits.

Since there are two URLLC users, we need to partition the frequencies for our random hijacking policy. If we partition the frequencies according to the solution of (4.20)-(4.23), URLLC user 1 would be able to hijack frequency 2, and URLLC user 2 would be able to hijack frequencies 1 and 3 (this partitioning is only for the random hijacking policy).

As we did for scenario 1 we will again consider the three smoothing parameters $\varepsilon = 10^{-4}$, 10^{-5} and 10^{-6}, and simulate $10/\varepsilon$ slots consisting of 8 mini-slots for each value of ε.

Again we expect that a smaller value of ε gives simulation results that match the approximation of the ODE better, and thus expect less varying behaviour. We also expect that the OSB policy outperforms the other hijacking policies, but that the score based still performs better than the random policy.

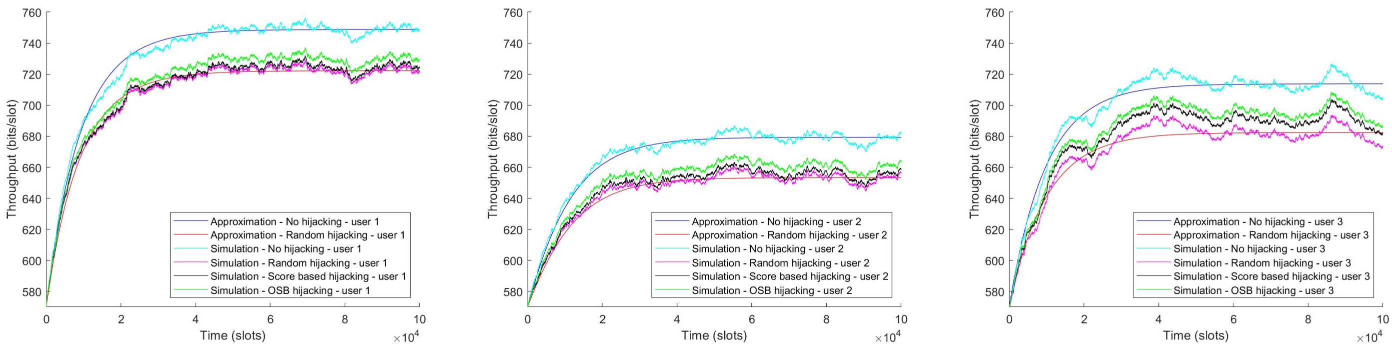

(a) User 1 (b) User 2 (c) User 3

Figure 5.5: Average throughputs over time for scenario 2 with $\varepsilon = 10^{-4}$

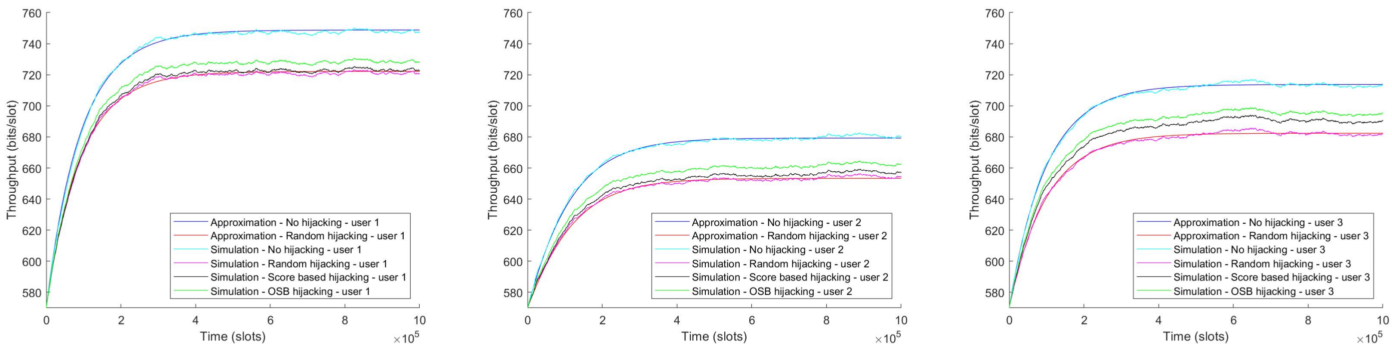

(a) User 1 (b) User 2 (c) User 3

Figure 5.6: Average throughputs over time for scenario 2 with $\varepsilon = 10^{-5}$

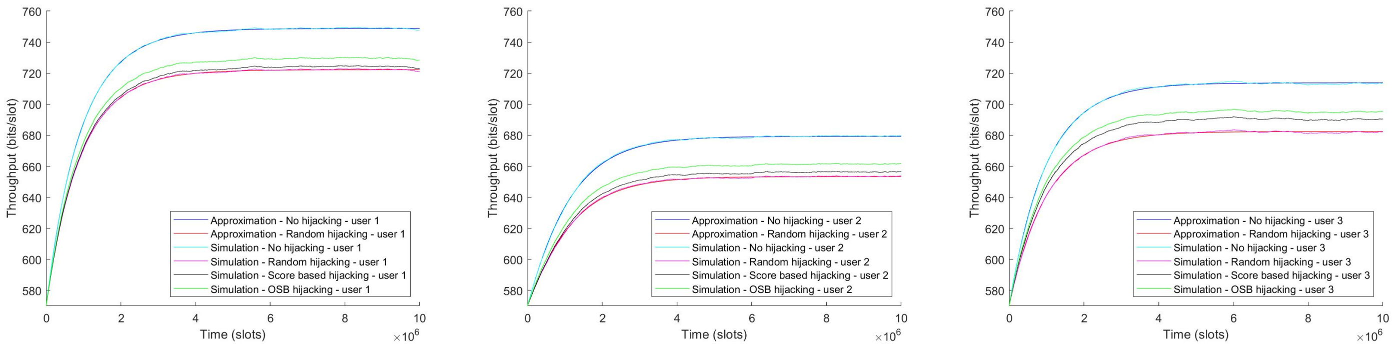

(a) User 1 (b) User 2 (c) User 3

Figure 5.7: Average throughputs over time for scenario 2 with $\varepsilon = 10^{-6}$

In Figures 5.5-5.7, we again see that the simulation results are less varying for smaller values of ε. Also for this scenario we see that the throughputs converge in approximately $4/\varepsilon$ slots, indicating that again the convergence time is of the order $1/\varepsilon$.

As expected we see that the OSB policy performs best among the hijacking policies, followed by the score based policy. However, the gap between the OSB and the score based policy is larger then it was for scenario 1. An explanation for this is that situations like the example in Table 4.1 occur more frequently since there are more frequencies, which implies that there is a better set of frequencies to hijack (which the OSB policy hijacks) than the set selected by the score based policy.

In Figures 5.5-5.7, we again see that all hijacking policies follow a similar curve as the no-hijacking scenario. Therefore the hijacking policies show approximately the same amount of variation over time. To investigate the amount of variation between different simulations for a converged system, we will do 500 simulations for the no-hijacking case with $\varepsilon = 10^{-5}$ and plot the approximated ODE, the average throughput (of the 500 runs), and 95% and 99% confidence bounds. The results of these simulations can be found in Figure 5.8, here we only plot the results for the slots after slot $5 \cdot 10^5$, since the system should (almost) be converged for these slots.

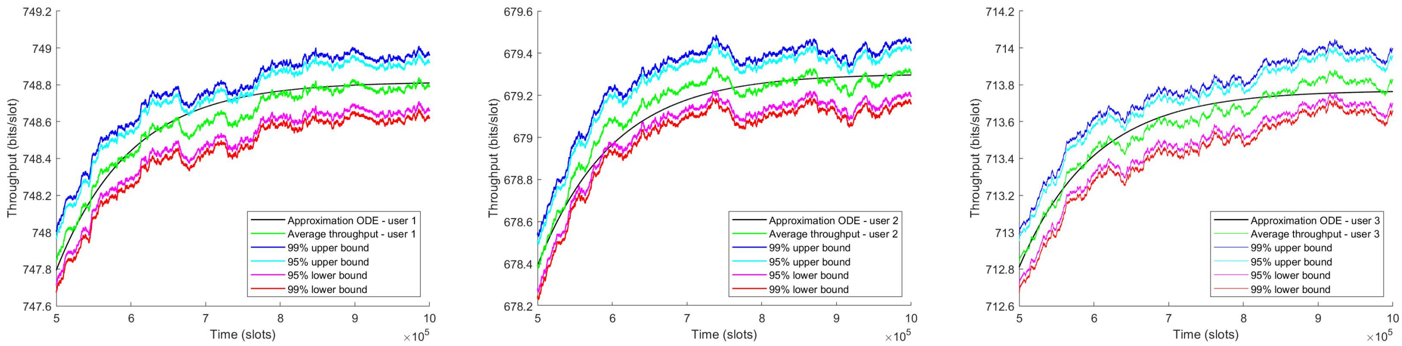

(a) User 1 (b) User 2 (c) User 3

Figure 5.8: Average throughputs, and confidence bounds for scenario 2 without hijacking with $\varepsilon = 10^{-5}$

In Figure 5.8, we see that the approximation of the ODE (black line) is almost always within the 95% confidence band (cyan and magenta lines), and always within the 99% confidence band (blue and red lines). Furthermore, we see that the average throughputs (green line) follows the approximation of the ODE quite well for all three users. So also this experiment confirms our theoretical results.

5.3 Scenario 3

For our third scenario, we will consider three eMBB users that have different average rates, namely 800, 450 and 300 bits/slot. In reality, big differences could be due to the location of the user, e.g. close to the transmitter, or in an urban environment. Next to the eMBB users, we consider two URLLC users. For this scenario we will consider six frequencies, where the average rates of the users on each frequency is given by

$$s^e = \begin{pmatrix} 789 & 856 & 735 & 888 & 754 & 778 \\ 496 & 417 & 391 & 482 & 398 & 516 \\ 267 & 346 & 372 & 248 & 233 & 334 \end{pmatrix},$$
$$s^u = \begin{pmatrix} 564 & 351 & 594 & 634 & 402 & 563 \\ 347 & 331 & 523 & 342 & 321 & 411 \end{pmatrix},$$

where the row indicates the user and the column indicates the frequency. In this scenario we assume that the user 1, 2 and 3 have initial throughputs of 2800, 1550 and 1000 bits/slot respectively.

For hijacking, we assume that the demand $D_{j,t,m}$ of URLLC user j during mini-slot m of slot t is independent from any other demand. Further more we assume that the demand distributions for mini-slot m during slot t for the two URLLC users are given by

$$\mathbb{P}\left(D_{1,t,m} = 0\right) = 0.95, \qquad \mathbb{P}\left(D_{1,t,m} = 20\right) = 0.05,$$
$$\mathbb{P}\left(D_{2,t,m} = 0\right) = 0.95, \qquad \mathbb{P}\left(D_{2,t,m} = 25\right) = 0.05,$$

where $D_{j,t,m}$ is given in bits.

Again there are multiple URLLC users, therefore we need to partition the frequencies for the random hijacking policy. When we partition the frequencies according to the solution of (4.20)-(4.23), URLLC user 1 would be able to hijack frequencies 1, 4 and 6, and URLLC user 2 would be able to hijack frequencies 2, 3 and 5 (this partitioning is only for the random hijacking policy).

Similar to scenarios 1 and 2 we will consider the three smoothing parameters $\varepsilon = 10^{-4}$, 10^{-5} and 10^{-6}, and simulate $10/\varepsilon$ slots consisting of 8 mini-slots for each value of ε.

Also for this scenario we expect to see less variability over time for smaller values of ε, and therefore expect that the simulated throughputs follow the approximation of the ODE more closely. We also expect that the case without hijacking has highest throughputs followed by the OSB and score based policies, and the random policy performing worst, as before.

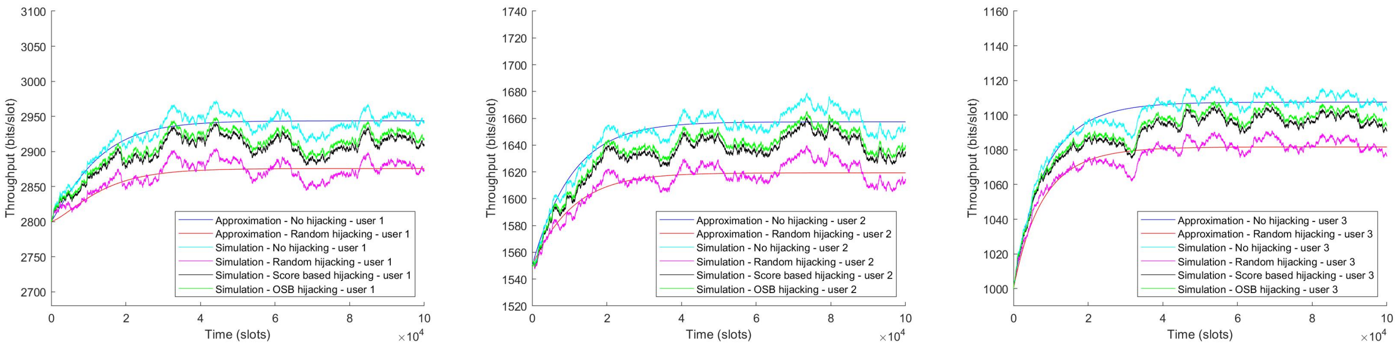

(a) User 1 (b) User 2 (c) User 3

Figure 5.9: Average throughputs over time for scenario 3 with $\varepsilon = 10^{-4}$

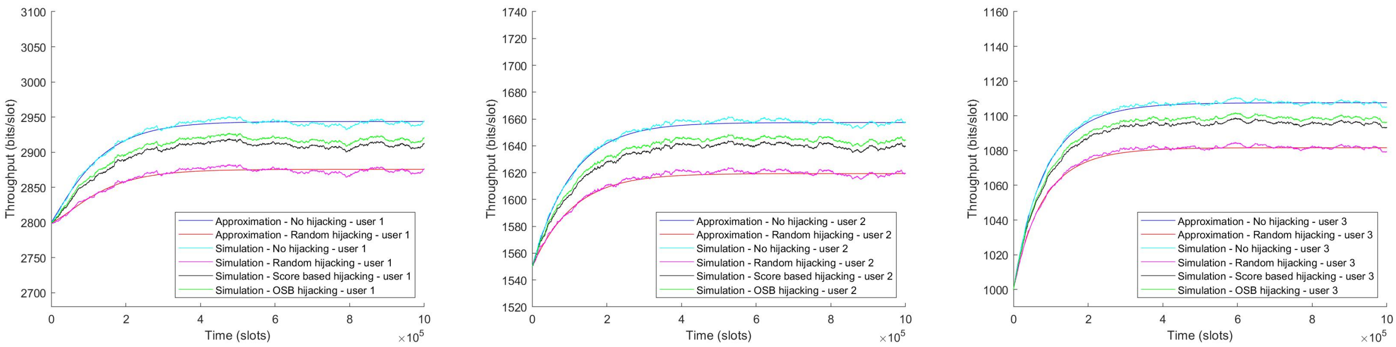

(a) User 1 (b) User 2 (c) User 3

Figure 5.10: Average throughputs over time for scenario 3 with $\varepsilon = 10^{-5}$

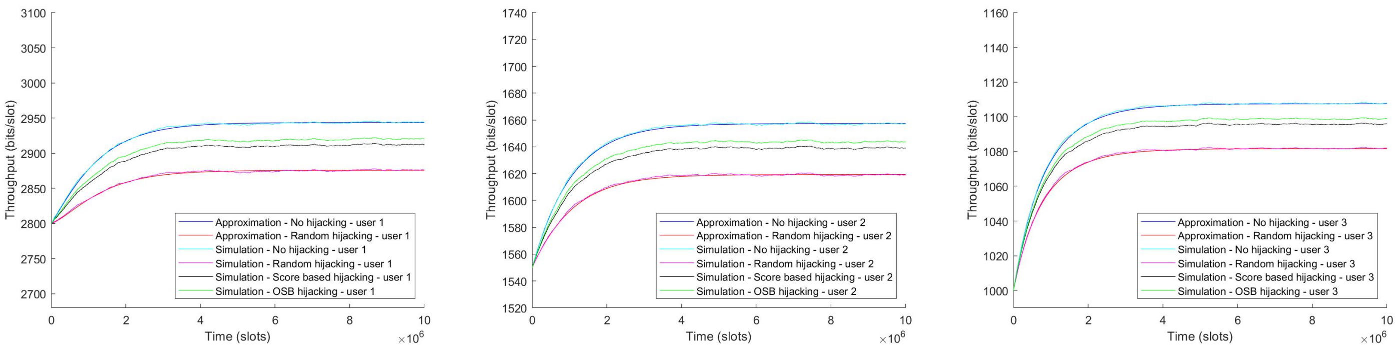

(a) User 1 (b) User 2 (c) User 3

Figure 5.11: Average throughputs over time for scenario 3 with $\varepsilon = 10^{-6}$

In Figures 5.9-5.11 we see that the results are in line with our expectations.

Similar to scenarios 1 and 2 we also want to investigate average behaviour of the system when the throughputs should be converged. Therefore we 500 simulated the no hijacking case with $\varepsilon = 10^{-5}$ and plot the approximated ODE, the average throughput (of the 500 runs), and 95% and 99% confidence bounds. The results of these simulations can be found in Figure 5.12, here we only plot the results for the slots after slot $5 \cdot 10^5$, since the system should (almost) be converged for these slots.

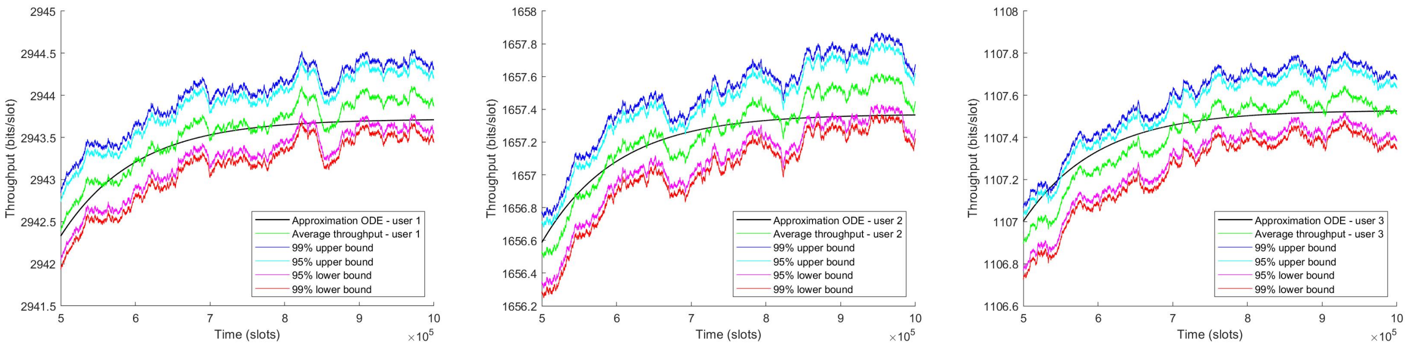

(a) User 1 (b) User 2 (c) User 3

Figure 5.12: Average throughputs, and confidence bounds for scenario 3 without hijacking with $\varepsilon = 10^{-5}$

In Figure 5.12, we see that the approximation of the ODE is almost always within the 95% confidence band. So again the experiment gives us no reason to doubt our theoretical results.

Chapter 6

Rayleigh fading

Because it is not very realistic that all rates are independent over time as we assumed in Chapter 4, we will now be considering a Rayleigh fading model, which implies that the rates are correlated over time. In Section 6.1 we will first discuss this model. We will discuss some results for this fading scenario in Section 6.2.

6.1 Fading model

In general, the base station transmitting a signal to a receiver (e.g. a mobile phone) is not in sight (e.g. blocked by a building). This implies that there is not a direct signal from the transmitter to the receiver. As the signal bounces off all kind of scatterers like buildings, the signal received by the receiver is a combination of all these scattered signals.

Jakes [13] proposes to model this as follows, assume that the receiver moves with a velocity of v m/s, and that there are N scatterers placed uniformly in a circle around the receiver. As the receiver moves, the scattered signals are subject to a Doppler shift. For the k^{th} scattered signal this shift is given by

$$\omega_k = \frac{v}{\lambda}\cos(\alpha_k), \tag{6.1}$$

with λ being the wavelength of the carrier frequency, and α_k the angle between the incoming wave from the scatterer and direction in which the receiver moves. An illustration of this can be found in Figure 6.1, where the red line represents the signal that gets scattered. Notice that the maximum Doppler shift is given by $\omega_{\max} = v/\lambda$.

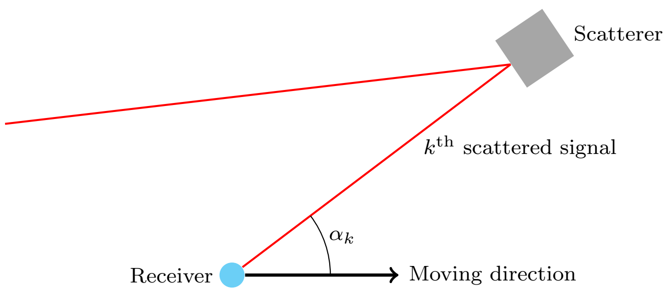

Figure 6.1: Incoming wave in the horizontal plane

All scattered signals can be seen as a waves with initial phases φ_k that are uniformly distributed over $(0, 2\pi]$. So at time t the in-phase component of wave k can be represented by

$$\cos\left(2\pi\omega_k t + \varphi_k\right), \tag{6.2}$$

for the quadrature component of wave k we have

$$\sin\left(2\pi\omega_k t + \varphi_k\right). \tag{6.3}$$

Following [14] the in-phase respectively quadrature components of the fading waveforms are given by

$$T_c(t) = \sqrt{\frac{2}{N}} \sum_{k=1}^{N} \cos\left(2\pi\omega_k t + \varphi_k\right), \tag{6.4}$$

$$T_s(t) = \sqrt{\frac{2}{N}} \sum_{k=1}^{N} \sin\left(2\pi\omega_k t + \varphi_k\right), \tag{6.5}$$

with $T_c(t)$ and $T_s(t)$ being approximately random Gaussian processes with zero mean and variance $1/2$. Now the Rayleigh fading waveform is given by

$$\mu(t) = T_c(t) + \mathbf{i}T_s(t), \tag{6.6}$$

where $\mathbf{i} = \sqrt{-1}$. Now we know that the signal power is proportional to the square of the magnitude of $\mu(t)$. So let $E = \sqrt{T_c(t)^2 + T_s(t)^2}$, now we want to know the density of E^2, as this is proportional to the power of the signal. According to [13], we have that the density $p_E(\cdot)$ of E is given by

$$p_E(x) = \begin{cases} \frac{x}{\sigma^2} \exp\left(-\frac{x^2}{2\sigma^2}\right) & \text{if } x \geq 0, \\ 0 & \text{otherwise,} \end{cases} \tag{6.7}$$

which is the Rayleigh density formula. Because the variance of $T_c(t)$ and $T_s(t)$ was $1/2$, we have that $\sigma^2 = 1/2$. This gives us

$$p_E(x) = \begin{cases} 2x \exp\left(-x^2\right) & \text{if } x \geq 0, \\ 0 & \text{otherwise,} \end{cases} \tag{6.8}$$

which implies that the cumulative distribution of E is given by

$$\mathbb{P}\left(E \leq x\right) = \begin{cases} 1 - \exp\left(-x^2\right) & \text{if } x \geq 0, \\ 0 & \text{otherwise.} \end{cases} \tag{6.9}$$

Therefore we know that the cumulative distribution of E^2 is given by

$$\begin{aligned} \mathbb{P}\left(E^2 \leq x\right) &= \begin{cases} \mathbb{P}\left(E \leq \sqrt{x}\right) & \text{if } x \geq 0, \\ 0 & \text{otherwise,} \end{cases} \\ &= \begin{cases} 1 - \exp\left(-x\right) & \text{if } x \geq 0, \\ 0 & \text{otherwise,} \end{cases} \end{aligned} \tag{6.10}$$

which is the cumulative distribution of an exponential random variable with mean 1. So as in the independent exponential case, the channel state is an exponential random variable with mean 1. Because the rates are correlated over time, knowing the rates during previous slots gives us some information about the rate during the next slot. Therefore $g_t(\theta_t^\varepsilon, \xi_t^\varepsilon)$ now depends on ξ_t^ε (which it did not in Chapter 4). However, there is no reason to believe that $g_t(\theta_t^\varepsilon, \xi_t^\varepsilon)$ would no longer be continuous since all θ_i and $s_{i,f}$ will still be larger than zero. This indicates that Assumption 2 holds.

For the same reasons as in Chapter 4, we conclude that Assumptions 1 and 3 hold. For Assumption 4, we notice that averaging over a long time horizon implies that we average over fades (channel states), which means that $\bar{g}(\theta)$ should average over all values of ξ_t^ε. Therefore we can assume that it is independent of ξ_t^ε, implying that $\bar{g}(\theta)$ for this fading model is the same as it was for the independent exponential model of Chapter 4. Similar to the results in Chapter 4, we conclude that Theorems 1-4 hold when we do not hijack and when we hijack according to the random or OSB policy. As in Chapter 4, for the score based policy we can only conclude that Theorems 1 and 2 hold.

Since the $\bar{g}(\theta)$ are the same as in Chapter 4, we know that the ODE for a Rayleigh fading model without hijacking is given by

$$\dot{\theta}_i = \sum_{f\in\mathcal{F}} s_{i,f} \sum_{J\in Q_i} (-1)^{|J|} \left(\frac{\theta_i \prod_{k\in J} s_{k,f}}{\theta_i \prod_{k\in J} s_{k,f} + s_{i,f} \sum_{k\in J} \theta_k \prod_{\substack{m\in J,\\ m\neq k}} s_{m,f}} \right)^2 - \theta_i, \tag{6.11}$$

which is the same as Equation (4.9). For a Rayleigh fading model with hijacking according to the random policy we have that the ODE is given by

$$\dot{\theta}_i = \sum_{f\in\mathcal{F}} (1-\mathbb{P}(H_f))\, s_{i,f} \sum_{J\in Q_i} (-1)^{|J|} \left(\frac{\theta_i \prod_{k\in J} s_{k,f}}{\theta_i \prod_{k\in J} s_{k,f} + s_{i,f} \sum_{k\in J} \theta_k \prod_{\substack{m\in J,\\ m\neq k}} s_{m,f}} \right)^2 - \theta_i, \tag{6.12}$$

which is the same as Equation (4.19).

6.2 Simulations

To be able to simulate the scenarios with Rayleigh fading, we need functionality that generates the channel states. For this we decided to use a built-in Rayleigh fading simulator from Matlab. We will first perform some simple checks to verify that the simulator gives good results in Section 6.2.1. In Section 6.2.2 we will show results for Scenarios 1-3 described in Sections 5.1-5.3, but now using our fading model.

6.2.1 Fading simulator

To generate the channel states according to the above described Rayleigh fading model, we use a built-in Rayleigh fading simulator in Matlab. This simulator generates the channel states using the GMEDS$_1$ algorithm described in [14].

The simulator will give us the Rayleigh waveforms $\mu(t) = T_c(t) + \mathbf{i}T_s(t)$. If we have samples covering a long enough time horizon, we know that the density of $E = \sqrt{T_c(t)^2 + T_s(t)^2}$ should be Rayleigh distributed with parameter $\sigma^2 = 1/2$. To verify this we generate 1,000,000 samples with sample frequency of 600 Hz, we will do this for three different values for the maximum Doppler shift $\omega_{\max}$, namely 6 Hz, 25 Hz and 60 Hz. One can think of these maximum Doppler shifts as if these correspond to receivers moving at approximately 6, 30 and 70 km/h.

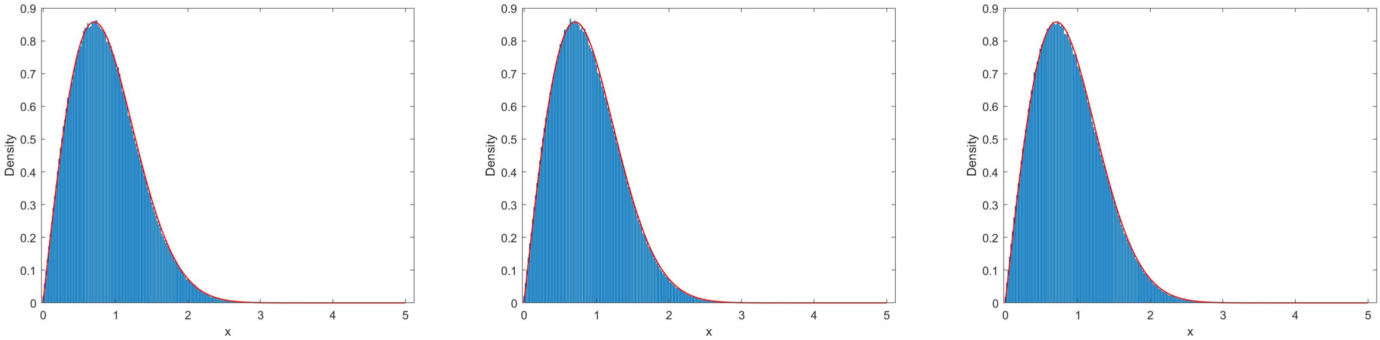

(a) Maximum Doppler shift $\omega_{\max} = 6$ Hz (b) Maximum Doppler shift $\omega_{\max} = 25$ Hz (c) Maximum Doppler shift $\omega_{\max} = 60$ Hz

Figure 6.2: Density of channel state using a Rayleigh fading simulator

In Figures 6.2a-6.2c we plotted the normalized histogram (in blue) of the channel states generated using the fading simulator. Furthermore we added the theoretical density (red line) according to the Rayleigh distribution. Even though all histograms match the theoretical density almost perfectly, we will perform another test. Jakes [13] shows that the autocorrelation of the in-phase component can be approximated by $J_0(2\pi\omega_{\max}t)$ where $J_0(\cdot)$ denotes the zeroth-order Bessel function. In a similar way one can show that the autocorrelation of the quadrature component can also be approximated by $J_0(2\pi\omega_{\max}t)$. So we can also test whether the correlation between the samples is approximately correct. To do this we use the simulated waveforms of 1,000,000 samples assuming 600 samples per second, with maximum Doppler shifts of 6, 25 and 60 Hz that we used to check the Rayleigh density.

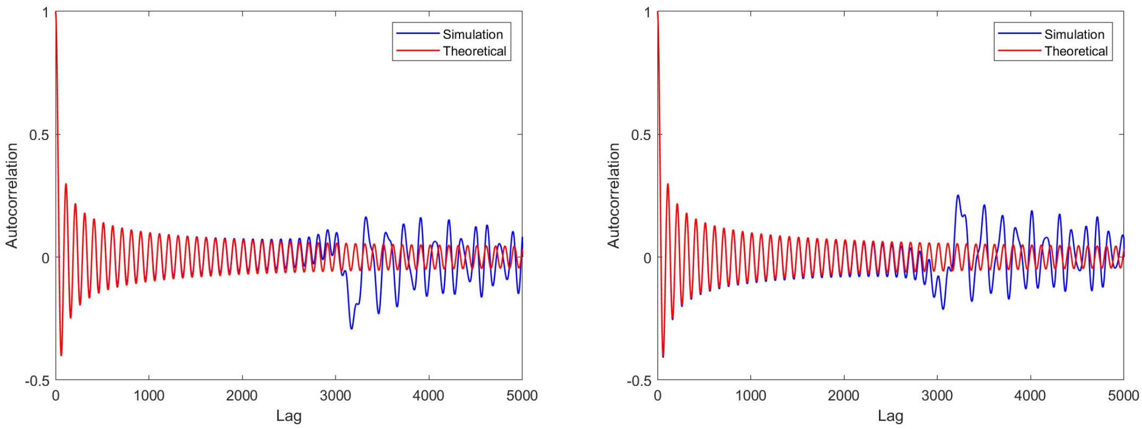

(a) Correlation of the in-phase component $T_c(t)$ (b) Correlation of the in-phase component $T_s(t)$

Figure 6.3: Correlation simulated Rayleigh fading process with maximum Doppler shift $\omega_{\max} = 6$ Hz

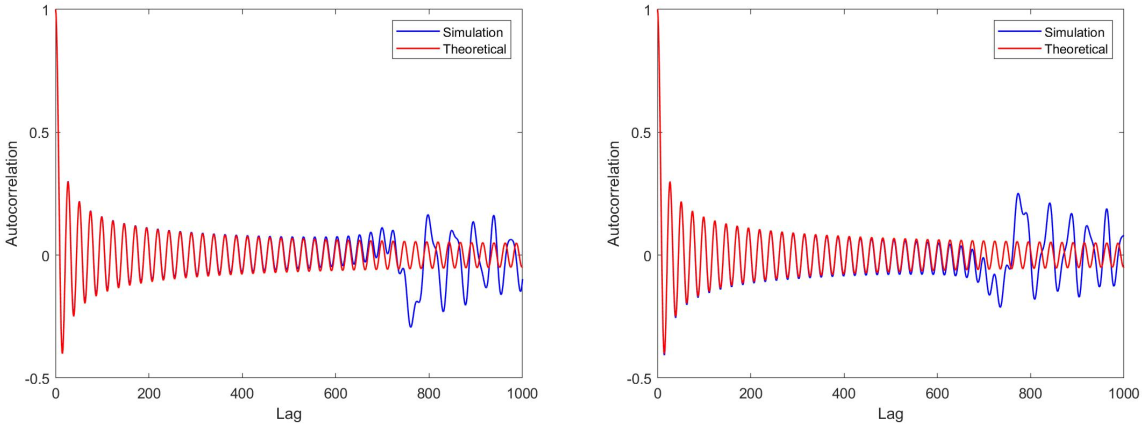

(a) Correlation of the in-phase component $T_c(t)$ (b) Correlation of the in-phase component $T_s(t)$

Figure 6.4: Correlation simulated Rayleigh fading process with maximum Doppler shift $\omega_{\max} = 25$ Hz

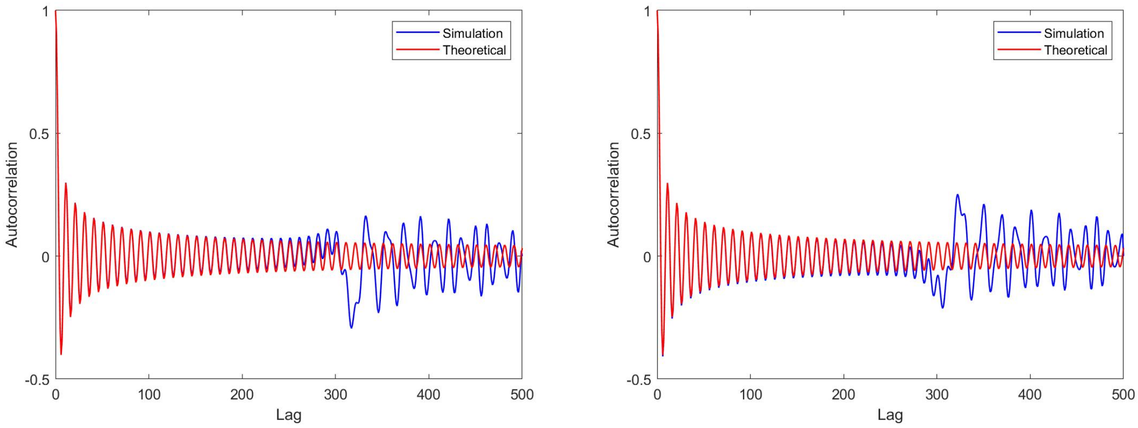

(a) Correlation of the in-phase component $T_c(t)$ (b) Correlation of the in-phase component $T_s(t)$

Figure 6.5: Correlation simulated Rayleigh fading process with maximum Doppler shift $\omega_{\max} = 60$ Hz

In Figures 6.3-6.5 we see that the correlation of the processes match the theoretical correlation almost exactly in the beginning. When the correlation starts to differ significantly at lag τ from the theoretical correlation, the process sees more than 10 fades between sample t and $t + \tau$, therefore we have little reason to believe that correlation should still match the theoretical value.

So we conclude that there is no reason to believe that the simulator performs poorly. Therefore we will use this simulator for our simulations in Section 6.2.2.

6.2.2 Results

In this section we consider the same scenarios as described in Sections 5.1-5.3, but now we will use a fading simulator to generate the channel states. Similar to the scenarios with independent exponential rates, we will compare simulation results against an asymptotic approximation of the ODE (see Equation

(5.2)) for the no-hijacking and random hijacking cases. We will consider the same values of ε with corresponding simulation times as in Sections 5.1-5.3. For the fading model we need to specify the slot duration, therefore we assume that there are 600 slots per second. Furthermore we will simulate different maximum Doppler shifts, namely $\omega_{\max} = 6$, 25 and 60 Hz, where we assume that all users travel with the same speed. Since this results in many figures, we will only present the results for user 1 in each scenario. For the results of the other users we refer to Appendix B.

The results of scenario 1, 2 and 3 can be found in Figures 6.6-6.8.

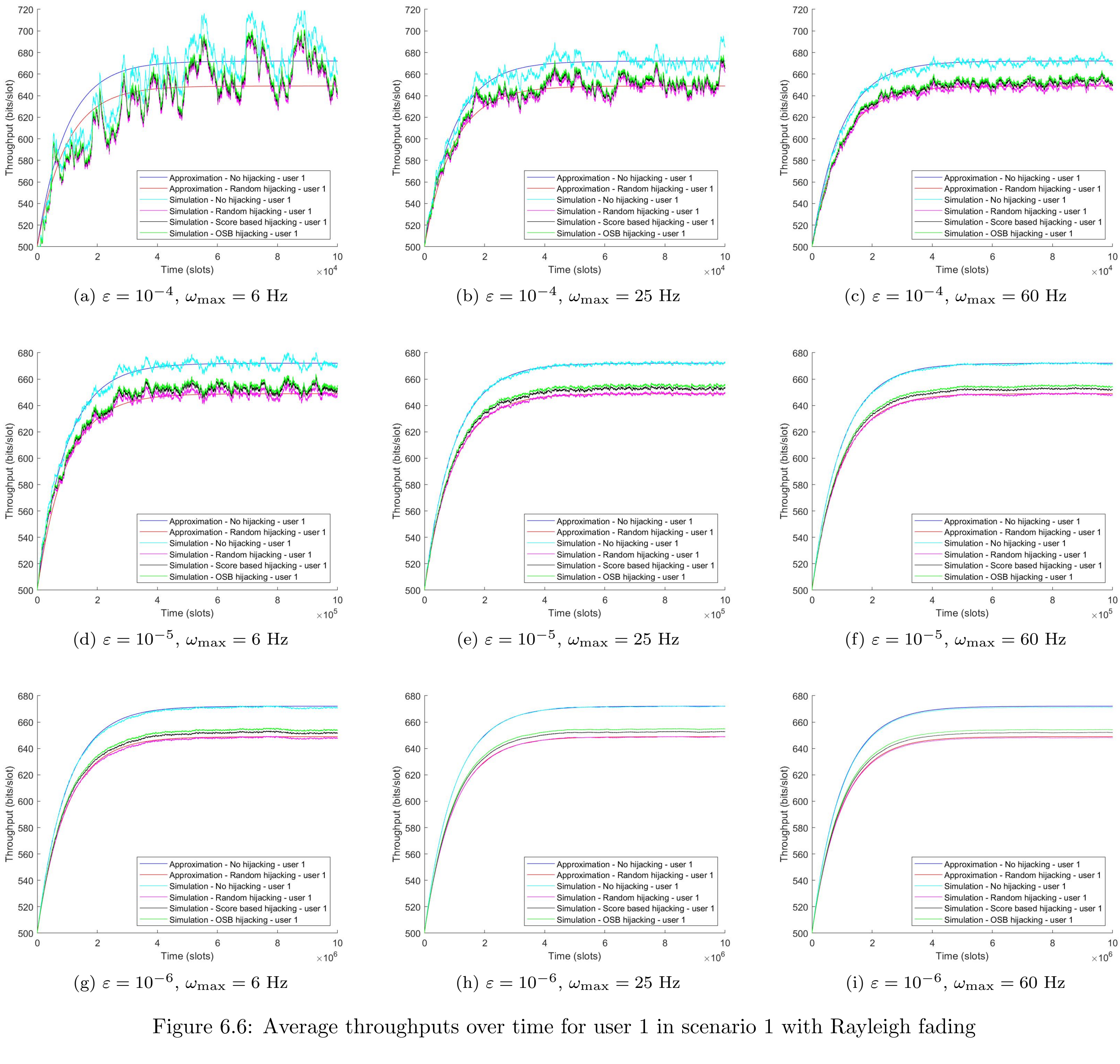

(a) $\varepsilon = 10^{-4}$, $\omega_{\max} = 6$ Hz
(b) $\varepsilon = 10^{-4}$, $\omega_{\max} = 25$ Hz
(c) $\varepsilon = 10^{-4}$, $\omega_{\max} = 60$ Hz
(d) $\varepsilon = 10^{-5}$, $\omega_{\max} = 6$ Hz
(e) $\varepsilon = 10^{-5}$, $\omega_{\max} = 25$ Hz
(f) $\varepsilon = 10^{-5}$, $\omega_{\max} = 60$ Hz
(g) $\varepsilon = 10^{-6}$, $\omega_{\max} = 6$ Hz
(h) $\varepsilon = 10^{-6}$, $\omega_{\max} = 25$ Hz
(i) $\varepsilon = 10^{-6}$, $\omega_{\max} = 60$ Hz

Figure 6.6: Average throughputs over time for user 1 in scenario 1 with Rayleigh fading

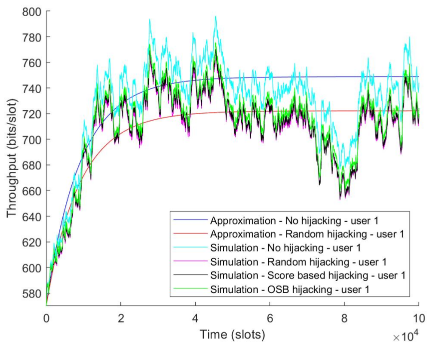

(a) $\varepsilon = 10^{-4}$, $\omega_{\max} = 6$ Hz

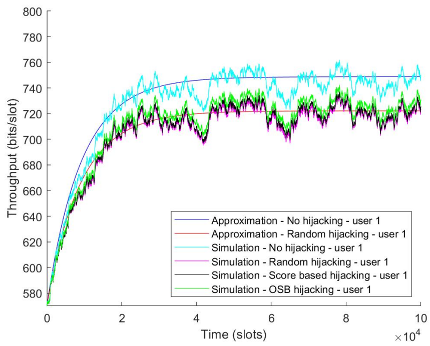

(b) $\varepsilon = 10^{-4}$, $\omega_{\max} = 25$ Hz

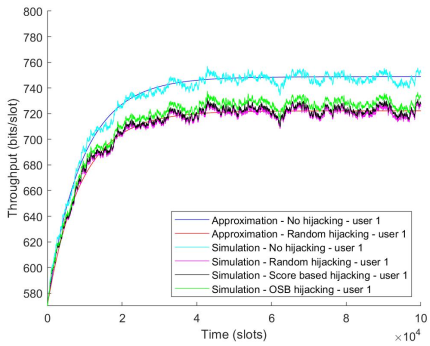

(c) $\varepsilon = 10^{-4}$, $\omega_{\max} = 60$ Hz

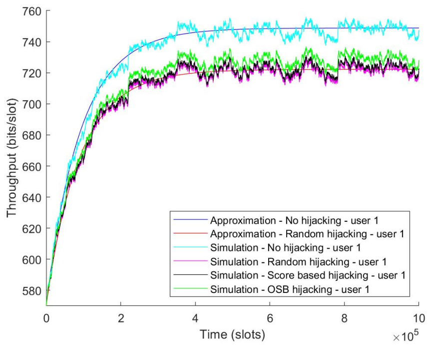

(d) $\varepsilon = 10^{-5}$, $\omega_{\max} = 6$ Hz

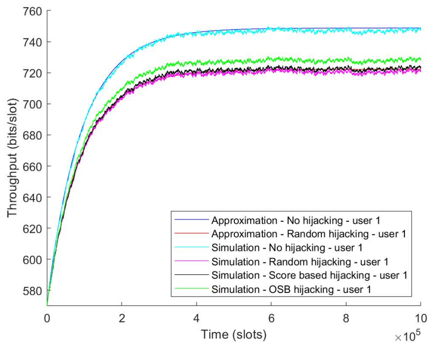

(e) $\varepsilon = 10^{-5}$, $\omega_{\max} = 25$ Hz

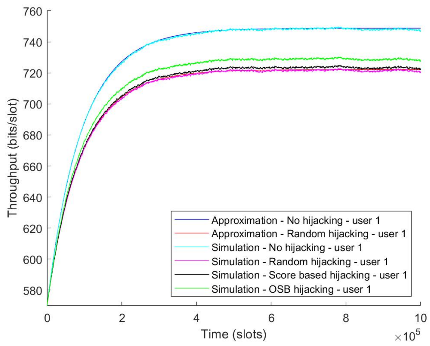

(f) $\varepsilon = 10^{-5}$, $\omega_{\max} = 60$ Hz

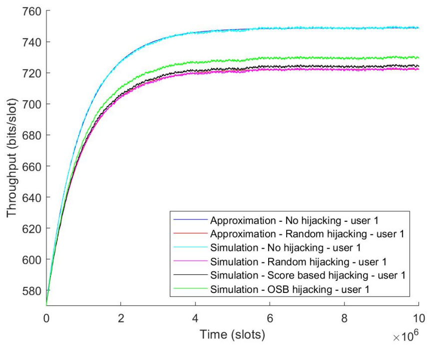

(g) $\varepsilon = 10^{-6}$, $\omega_{\max} = 6$ Hz

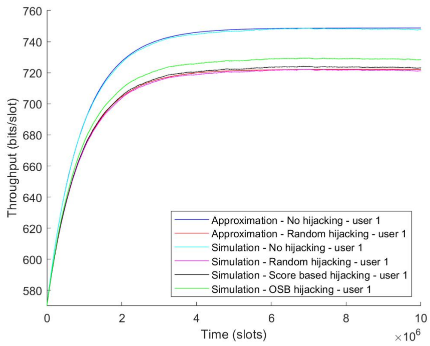

(h) $\varepsilon = 10^{-6}$, $\omega_{\max} = 25$ Hz

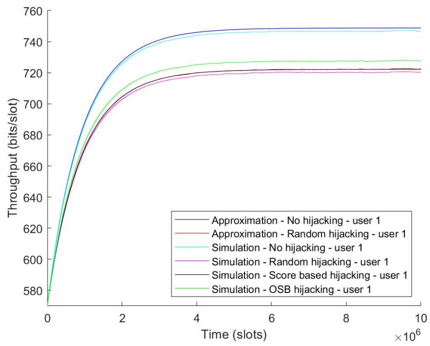

(i) $\varepsilon = 10^{-6}$, $\omega_{\max} = 60$ Hz

Figure 6.7: Average throughputs over time for user 1 in scenario 2 with Rayleigh fading

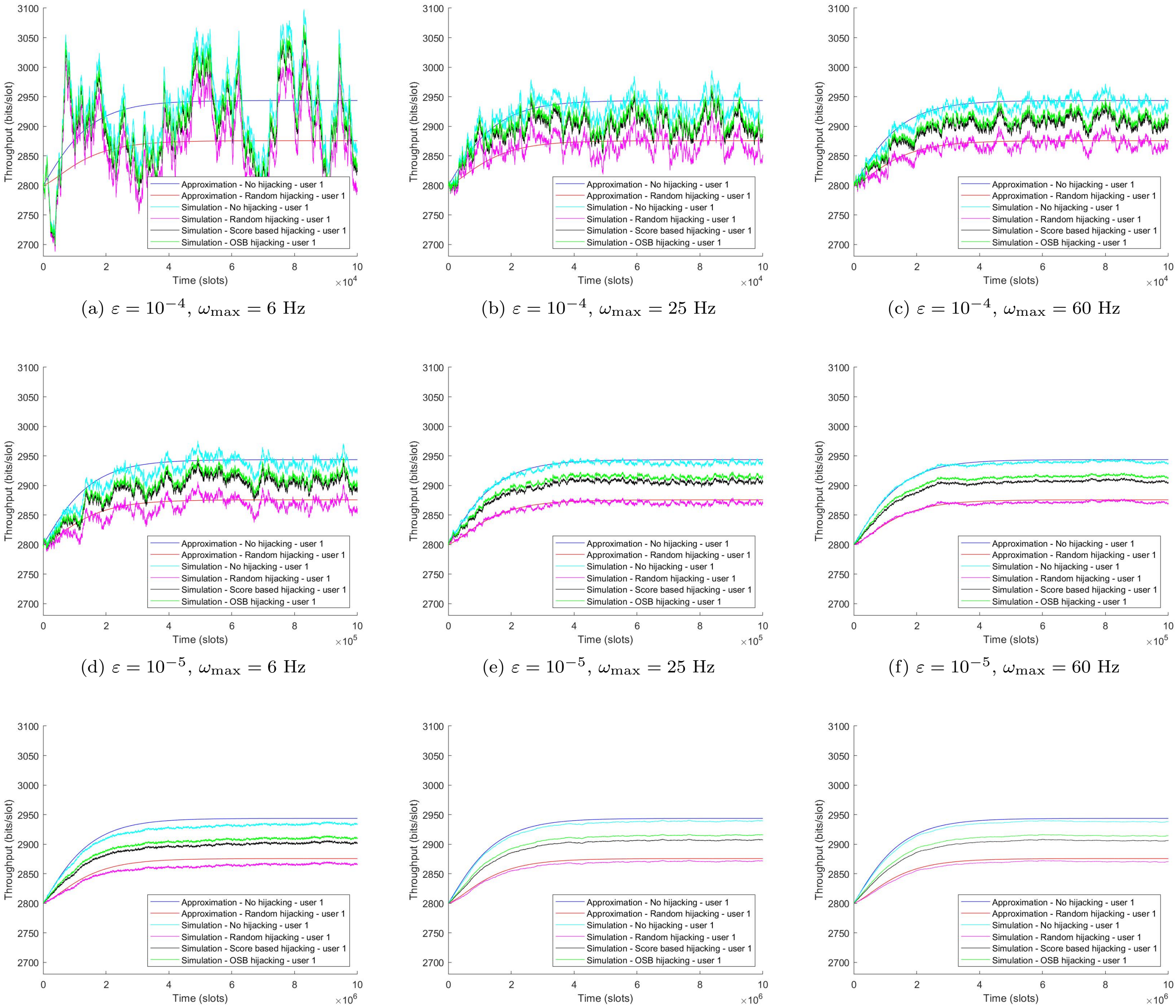

(a) $\varepsilon = 10^{-4}$, $\omega_{\max} = 6$ Hz
(b) $\varepsilon = 10^{-4}$, $\omega_{\max} = 25$ Hz
(c) $\varepsilon = 10^{-4}$, $\omega_{\max} = 60$ Hz

(d) $\varepsilon = 10^{-5}$, $\omega_{\max} = 6$ Hz
(e) $\varepsilon = 10^{-5}$, $\omega_{\max} = 25$ Hz
(f) $\varepsilon = 10^{-5}$, $\omega_{\max} = 60$ Hz

(g) $\varepsilon = 10^{-6}$, $\omega_{\max} = 6$ Hz
(h) $\varepsilon = 10^{-6}$, $\omega_{\max} = 25$ Hz
(i) $\varepsilon = 10^{-6}$, $\omega_{\max} = 60$ Hz

Figure 6.8: Average throughputs over time for user 1 in scenario 3 with Rayleigh fading

In Figures 6.6-6.8 we see that the simulated throughputs vary less when ε decreases for a fixed maximum Doppler shift $\omega_{\max}$. This is not surprising since we have seen that the simulated results vary less when ε decreases in the independent exponential model. Similar to the exponential model, we see that the convergence time is again of the order $1/\varepsilon$. Figures 6.6-6.8 also show that for fixed ε but increasing maximum Doppler shift $\omega_{\max}$ the simulation results vary less. An explanation, is that the higher $\omega_{\max}$ implies more rapidly changing channel states. Therefore we will have a better averaging over the channel states, which makes us less vulnerable for extreme channel states. Thus we will have less variation in the results.

So when we would like to use this model in practice, we should determine a good value for the smoothing parameter ε (note that we have no influence on the velocity of users and therefore the maximum Doppler shift). In reality, users join or leave the system every second. However, considering eMBB users that want to transmit large files, they stay in the system for longer periods of time, therefore we can still use these results. To be able to give a good indication of the remaining service time of a user, we would like to have convergence in a reasonably short time. For this we need to use a large smoothing parameter ε. However, if ε is too big, the throughputs will vary a lot over time, which makes it difficult to give a good approximation of the remaining service time of a user. Furthermore we have seen that the velocity at which the users travel also influences the variation in throughput over time, so if many users travel at high speed (high $\omega_{\max}$), the smoothing parameter ε can be smaller.

In some of the sub-figures of Figures 6.6-6.8 we see that the Approximation of the ODE is slightly above the corresponding simulated results. This behaviour is best visible when there is little variability in throughputs over time, i.e. small values of ε and high values of $\omega_{\max}$. Therefore we are interested in the average behaviour of the system when the throughputs should be converged. Since the hijacking policies follow a similar curve as the case without hijacking, we will only investigate the average behaviour of the case without hijacking. To do this we will simulate 500 independent runs for both scenario 1 and 2 without hijacking, for $\omega_{\max} = 6$, 25 and 60 Hz with $\varepsilon = 10^{-5}$. For these 500 runs we will calculate the average throughput, and 95% and 99% confidence bounds. The results for user 1 are shown in Figures 6.9-6.11, for the results of the other users we refer to Appendix B.

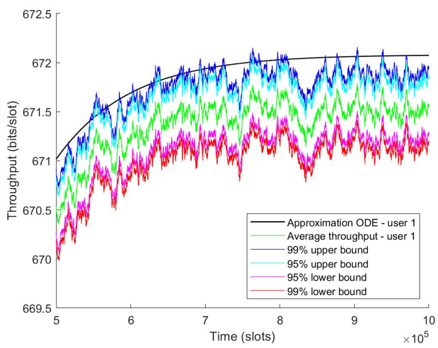

(a) $\omega_{\max} = 6$ Hz

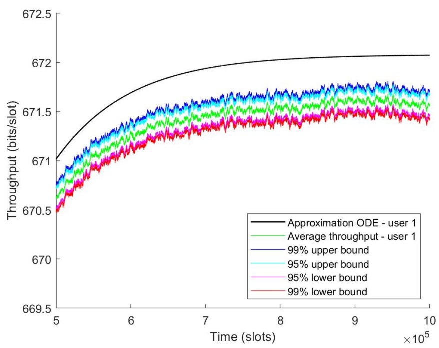

(b) $\omega_{\max} = 25$ Hz

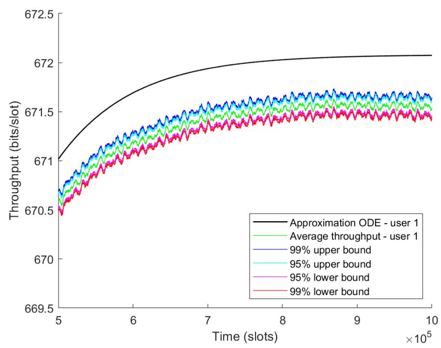

(c) $\omega_{\max} = 60$ Hz

Figure 6.9: Average throughput and confidence bounds over time for user 1 in scenario 1 with Rayleigh fading and $\varepsilon = 10^{-5}$

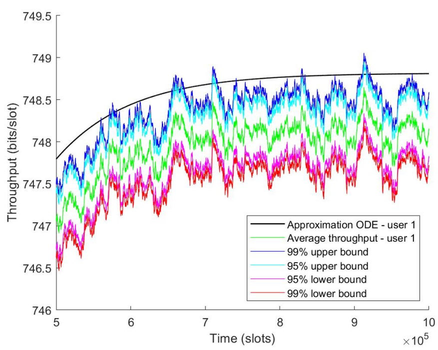

(a) $\omega_{\max} = 6$ Hz

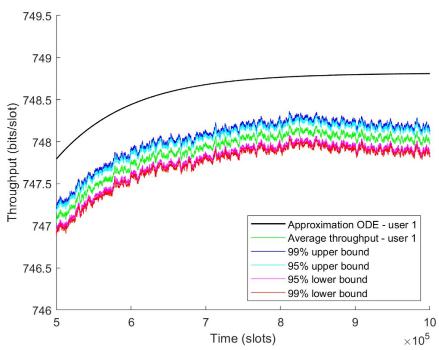

(b) $\omega_{\max} = 25$ Hz

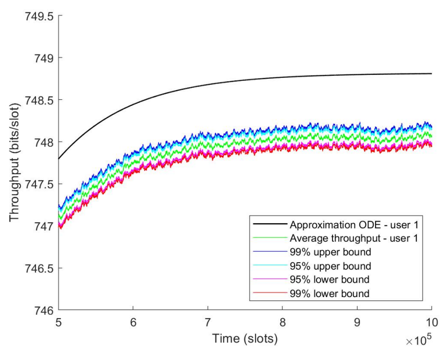

(c) $\omega_{\max} = 60$ Hz

Figure 6.10: Average throughput and confidence bounds over time for user 1 in scenario 2 with Rayleigh fading and $\varepsilon = 10^{-5}$

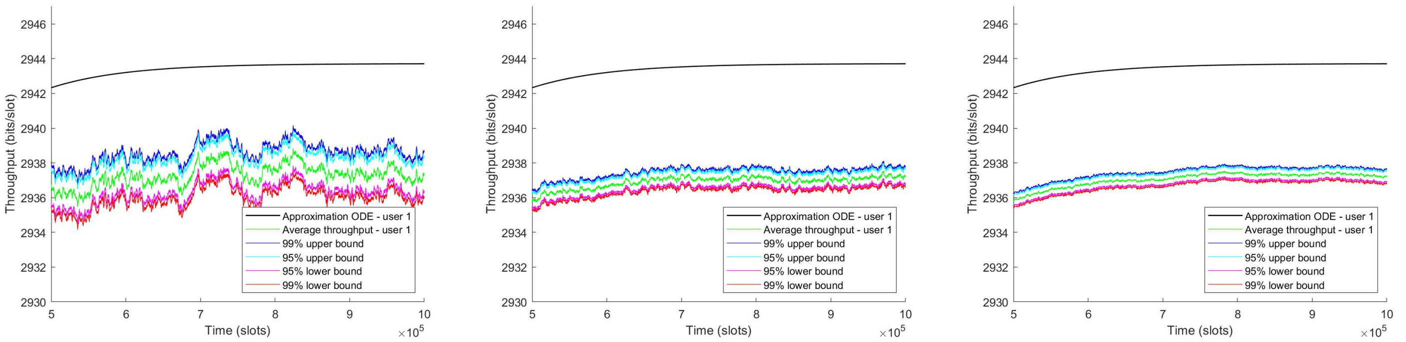

(a) $\omega_{\max} = 6$ Hz (b) $\omega_{\max} = 25$ Hz (c) $\omega_{\max} = 60$ Hz

Figure 6.11: Average throughput and confidence bounds over time for user 1 in scenario 3 with Rayleigh fading and $\varepsilon = 10^{-5}$

In Figures 6.9-6.11 we see that the confidence bands get smaller as $\omega_{\max}$ increases, this is logical since the throughputs vary more over time when $\omega_{\max}$ is smaller (see Figures 6.6-6.8). More interesting in Figures 6.9-6.11 is that the average throughputs (green line) are always slightly below the approximation of the ODE (black line). Furthermore, the approximation of the ODE is even outside the 99% confidence band. This is strange since we would expect the approximation of the ODE to be within the confidence bands, and we have seen that it was for the scenarios with independent exponential rates. A possible explanation could be that the correlation of the channel states over times causes this. Since a higher maximum Doppler shift $\omega_{\max}$ implies that the channel states change more quickly. Therefore the average throughputs are expected to behave more like the scenario with independent exponential rates. So, we expect the average throughput to shift towards the approximation of the ODE as $\omega_{\max}$ increases. However, Figures 6.9-6.11 do not show this behaviour. Therefore we believe that something else is going on.

So our next guess is that the fading simulator causes these lower throughputs. To investigate this we note that the channel states ($E^2 = T_c(t)^2 + T_s(t)^2$) should be exponentially distributed with mean 1. We verified this by checking that E was Rayleigh distributed with parameter $\sigma^2 = 1/2$. However, our algorithm prefers good channel states (high values of E^2), so it might be the case that the tail of the distribution is too thin. To test this we will generate 10,000 Rayleigh fading waves of $N = 1,000,000$ samples assuming 600 samples per second for a fixed maximum Doppler shift $\omega_{\max}$. We will consider three values $\omega_{\max} = 6$, 25 and 60 Hz.

Given that E^2 is exponential with mean 1, we know that

$$\mathbb{P}\left(E^2 \geq x\right) = e^{-x} = p \iff x = \log\left(\frac{1}{p}\right). \tag{6.13}$$

Now suppose that we are interested in the largest p% of the samples (in our experiment we chose p to be 10, 5 and 2.5), then we know that approximately pN samples of each wave should be larger than $\log(1/p)$. In Figure 6.12, we made a normalized histogram of the number of samples that are larger than $\log(1/p)$. The red line in this histogram indicates the number of samples that theoretically should be larger then $\log(1/p)$, which is pN.

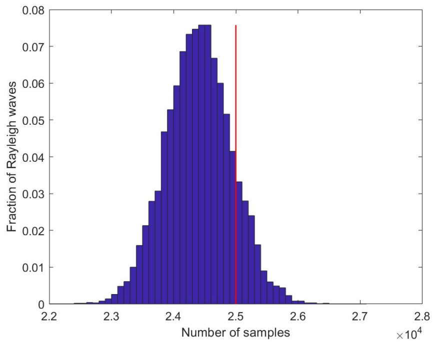

(a) $\omega_{\max} = 6$ Hz, $p = 2.5$

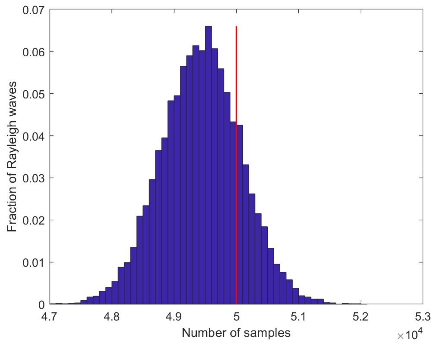

(b) $\omega_{\max} = 6$ Hz, $p = 5$

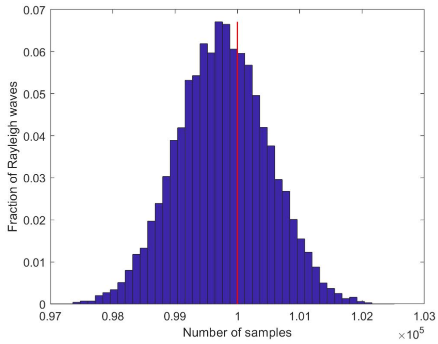

(c) $\omega_{\max} = 6$ Hz, $p = 10$

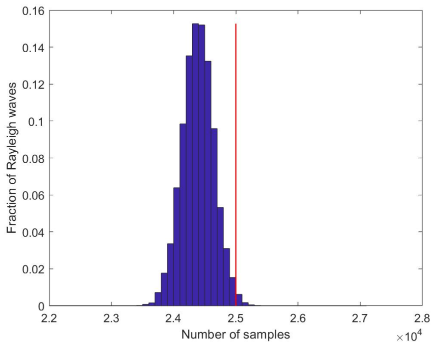

(d) $\omega_{\max} = 25$ Hz, $p = 2.5$

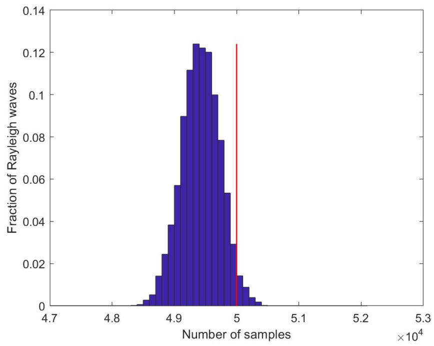

(e) $\omega_{\max} = 25$ Hz, $p = 5$

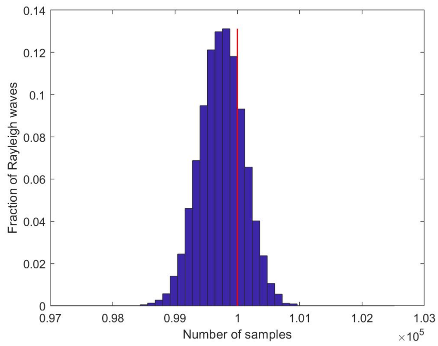

(f) $\omega_{\max} = 25$ Hz, $p = 10$

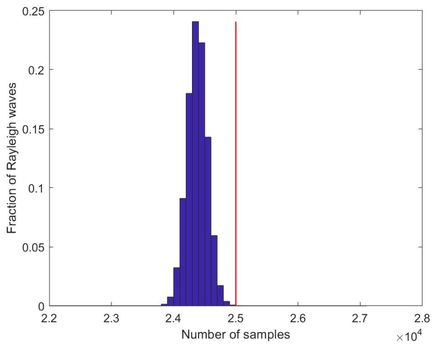

(g) $\omega_{\max} = 60$ Hz, $p = 2.5$

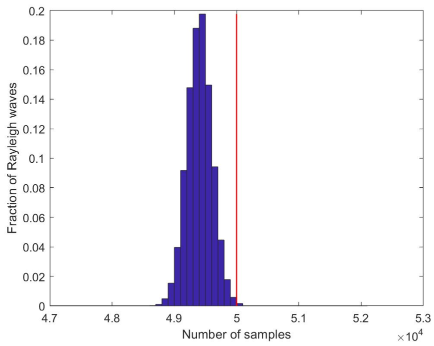

(h) $\omega_{\max} = 60$ Hz, $p = 5$

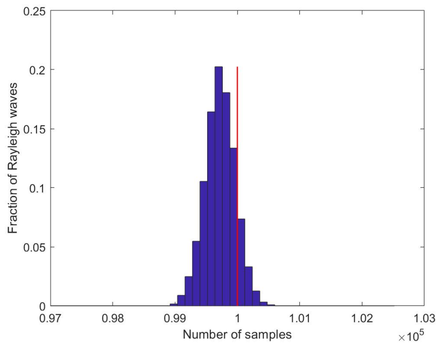

(i) $\omega_{\max} = 60$ Hz, $p = 10$

Figure 6.12: Histograms of the number of samples $\geq \log(1/p)$ per Rayleigh wave

In Figure 6.12 we see that the biggest part of each histogram is on the left of the theoretical number of samples that should be greater than $\log(1/p)$ (the red line) indicating that most of the Rayleigh fading waves have too few samples greater than $\log(1/p)$. This already indicates that there probably is something wrong with the tail of the distribution. One interesting thing to notice is that there is less variation in the number of samples greater than $\log(1/p)$ as $\omega_{\max}$ increases.

If we would only consider the part of the distribution greater than $\log(1/p)$, and denote this new distribution by $E^2_{\geq \log(1/p)}$, we know that

$$
\begin{aligned}
\mathbb{E}\left[E^2_{\geq \log(1/p)}\right] &= \int\limits_{\log(1/p)}^{\infty} \frac{1}{p} x \exp(-x)\; dx \\
&= -\frac{x+1}{p}\exp(-x)\Big|_{x=\log(1/p)}^{\infty} \\
&= \log(1/p) + 1 \qquad (6.14)
\end{aligned}
$$

So if we only consider the samples of the fading waves with channel state $E^2 \geq \log(1/p)$ for each Rayleigh fading wave. Then we can calculate the mean, which should approximately be $\log(1/p)+1$. In Figure 6.13 we show a normalized histogram of these means, where the red lines indicates the theoretical values $\log(1/p)+1$.

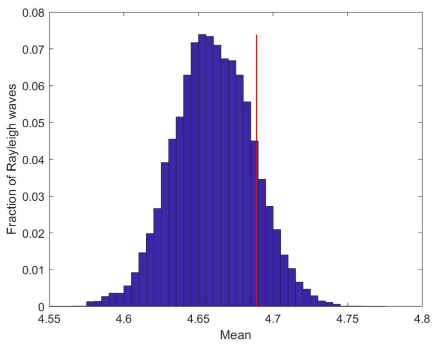

(a) $\omega_{\max} = 6$ Hz, $p = 2.5$

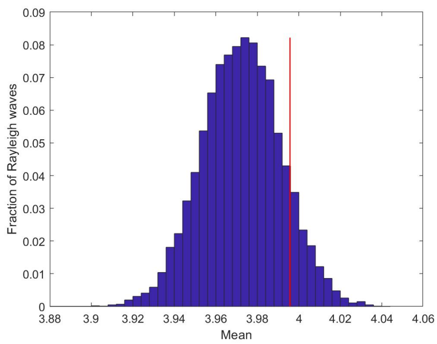

(b) $\omega_{\max} = 6$ Hz, $p = 5$

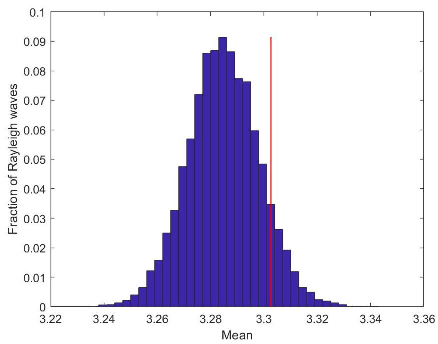

(c) $\omega_{\max} = 6$ Hz, $p = 10$

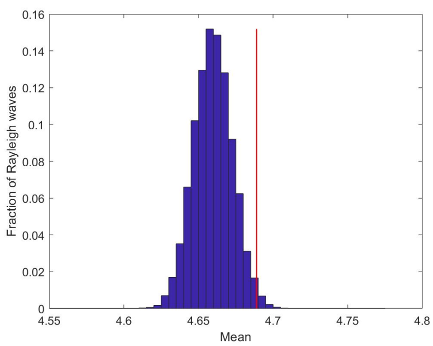

(d) $\omega_{\max} = 25$ Hz, $p = 2.5$

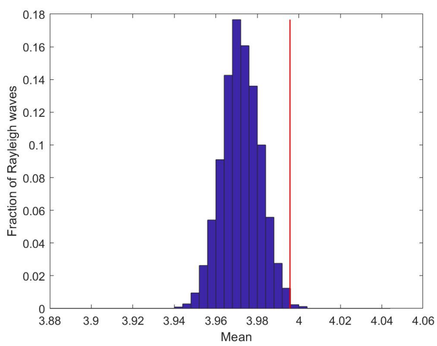

(e) $\omega_{\max} = 25$ Hz, $p = 5$

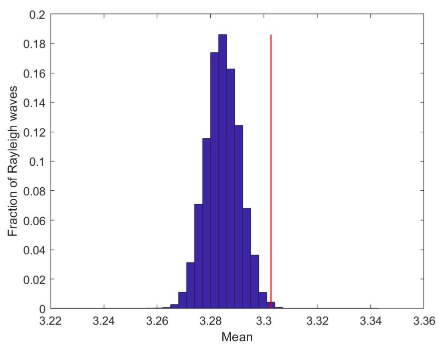

(f) $\omega_{\max} = 25$ Hz, $p = 10$

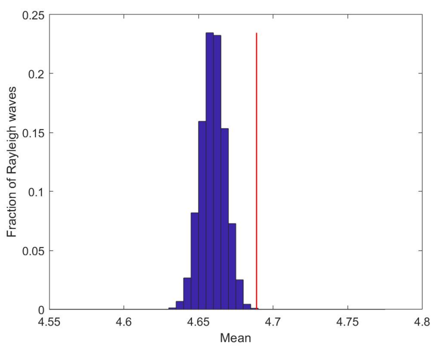

(g) $\omega_{\max} = 60$ Hz, $p = 2.5$

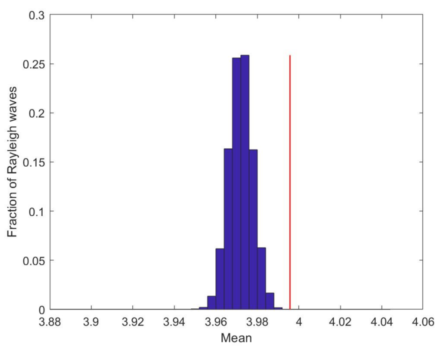

(h) $\omega_{\max} = 60$ Hz, $p = 5$

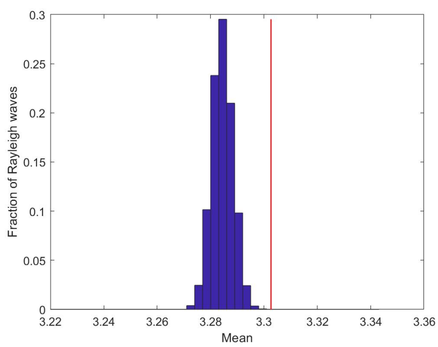

(i) $\omega_{\max} = 60$ Hz, $p = 10$

Figure 6.13: Histograms of the means of the samples $\geq \log(1/p)$ per Rayleigh wave

In Figure 6.13 we see that the biggest part of each histogram is on the left of the theoretical mean (red line), indicating that the mean of the tail is in most cases less than it should be. This together with the fact that in most cases the tail consists of too few samples, indicate that the tail of the distribution is too thin, which is a possible explanation for the fact that the approximation of the ODE fell outside the confidence bands in Figures 6.9-6.11.

Chapter 7

Optimality

Since it is not clear what the optimal performance would be in scenarios with hijacking, we will investigate the performance of the hijacking policies in this chapter. To do this, we will compare the results of our algorithm against the optimal solution in an offline setting (where the channel rates and URLLC demands are known in advance), this is known as competitive analysis. Similar analysis but in the context of different probblems are considered in [8]-[10]. Even though we have asymptotic optimality results (Theorem 4) which use the fact that the algorithm maximizes the gain in utility for each slot, we will first do this kind of analysis for the scenario without hijacking as a warm-up.

As a performance measure we will use the utility function that the algorithm tries to maximize, only now we consider the time-average throughput over a finite time horizon of T slots. So we try to maximize the utility given by

$$\sum_{i \in \mathcal{E}} \log\left(\bar{R}_i\right), \tag{7.1}$$

where $\bar{R}_i$ is the time-average throughput of user i, i.e.

$$\bar{R}_i = \frac{1}{T}\sum_{t=1}^{T}\sum_{f\in\mathcal{F}} r^e_{i,f,t} I^{\varepsilon}_{i,f,t}\left(1 - \frac{1}{M}\sum_{m=1}^{M}\sum_{j\in\mathcal{U}} J^{\varepsilon}_{j,f,t,m}\right). \tag{7.2}$$

In this chapter we will drop the superscript ε for notational convenience.

7.1 No hijacking

When we do not consider any hijacking in the offline setting, we want to solve the following optimization problem:

$$\begin{aligned}
\max \quad & \sum_{i\in\mathcal{E}} \log\left(\frac{1}{T}\sum_{t=1}^{T}\sum_{f\in\mathcal{F}} r^e_{i,f,t} I_{i,f,t}\right) && (7.3)\\
\text{subject to} \quad & \sum_{i\in\mathcal{E}} I_{i,f,t} \le 1 \quad \forall_{f\in\mathcal{F}}\ \forall_{t\in\{1,\ldots,T\}}, && (7.4)\\
& I_{i,f,t} \in \{0,1\} \quad \forall_{i\in\mathcal{E}}\ \forall_{f\in\mathcal{F}}\ \forall_{t\in\{1,\ldots,T\}}. && (7.5)
\end{aligned}$$

However, it could be difficult to solve this problem. To see why it could be difficult, we will show that the NP-hard optimization variant of the set partitioning problem reduces to the problem defined above. The optimization variant of the partitioning problem can be written as

$$\min \quad \left| \sum_{k=1}^{K} a_k \left(x_{1,k} - x_{2,k} \right) \right| \tag{7.6}$$

$$\text{subject to} \quad x_{1,k} + x_{2,k} = 1 \qquad \forall_{k \in \{1,\dots,K\}}, \tag{7.7}$$

$$x_{i,k} \in \{0,1\} \qquad \forall_{k \in \{1,\dots,K\}} \; \forall_{i \in \{1,2\}}, \tag{7.8}$$

where $x_{1,k}$ and $x_{2,k}$ are the decision variables indicating to which set element k belongs. Now let each k correspond to a unique combination of f and t, and suppose that $|\mathcal{E}| = 2$ and that $r^e_{1,f,t} = r^e_{2,f,t} = a_k$. Notice that to maximize (7.3), we should assign all resources and therefore Constraint (7.4) should be met with equality. This implies that the optimal solution to both problems should satisfy the same constraints. Now we notice that (7.3) is maximal when $\left| \sum_{t=1}^{T} \sum_{f \in \mathcal{F}} r^e_{1,f,t} \left(I_{1,f,t} - I_{2,f,t} \right) \right|$ is minimal, but this is the equivalent of (7.6). So this implies that these problems have the same optimal solution. Therefore we conclude that the problem defined by (7.3)-(7.5) is NP-hard because the set partitioning problem is NP-hard.

To simplify the problem given by (7.3)-(7.5) a bit, we will consider the continuous relaxation, where Constraint (7.5) is relaxed to

$$I^{\varepsilon}_{i,f,t} \geq 0 \quad \forall_{i \in \mathcal{E}}, \; \forall_{f \in \mathcal{F}}, \; \forall_{t \in \{1,\dots,T\}}. \tag{7.9}$$

Because of this relaxation, the solution space expands. Therefore the objective value corresponding to the optimal solution will be an upper bound to our original problem.

Since the solution space is defined by a set of linear constraints, it is convex. To see why this is true, we notice that each linear constraint C_k defines a hyperplane, that is the boundary between the feasible and infeasible solutions. So on one side of this hyperplane we have a convex set S_k with the feasible solutions corresponding to constraint C_k. Boyd and Vandenberghe [15, Section 2.3.1] state that the intersection of any number of convex sets is convex. Using this we know that the intersection of all S_k, which defines the feasible region, is convex.

Lemma 1. *The optimal solution to the optimization problem with objective function (7.3), and Constraints (7.4) and (7.9) satisfies Constraint (7.4) with equality, implying that the optimal solution is found at the boundary of the solution space. Furthermore, there exists an optimal solution with at least $|\mathcal{E}||\mathcal{F}|T - |\mathcal{F}|T - |\mathcal{E}| + 1$ variables $I_{i,f,t} = 0$, at least $|\mathcal{F}|T - |\mathcal{E}| + 1$ variables $I_{i,f,t} = 1$, at most $2|\mathcal{E}| - 2$ variables $I_{i,f,t} \in (0,1)$, and no variables $I_{i,f,t} < 0$ or $I_{i,f,t} > 1$.*

Proof of Lemma 1

For notational convenience we will drop the superscript e and ε in this proof. The KKT-conditions tell us that a local optimal solution (all variables $I_{i,f,t}$) satisfies

$$0 = \nabla \sum_{e\in\mathcal{E}} \log\left(\frac{1}{T}\sum_{\tau=1}^{T}\sum_{k\in\mathcal{F}} r_{e,k,\tau} I_{e,k,\tau}\right) - \sum_{f\in\mathcal{F}}\sum_{\tau=1}^{T} \lambda_{f,t}\nabla\left(\sum_{e\in\mathcal{E}} I_{e,f,\tau} - 1\right) - \sum_{e\in\mathcal{E}}\sum_{f\in\mathcal{F}}\sum_{\tau=1}^{T} \mu_{e,f,\tau}\nabla\left(-I_{e,f,\tau}\right), \tag{7.10}$$

$$0 = \lambda_{f,t}\left(\sum_{e\in\mathcal{E}} I_{e,f,t} - 1\right) \qquad \forall_{f\in\mathcal{F}}\ \forall_{t\in\{1,\dots,T\}} \tag{7.11}$$

$$0 = \mu_{i,f,t}\left(-I_{i,f,t}\right) \qquad \forall_{i\in\mathcal{E}}\ \forall_{f\in\mathcal{F}}\ \forall_{t\in\{1,\dots,T\}} \tag{7.12}$$

$$0 \geq \sum_{e\in\mathcal{E}} I_{e,f,t} - 1 \qquad \forall_{f\in\mathcal{F}}\ \forall_{t\in\{1,\dots,T\}} \tag{7.13}$$

$$0 \geq -I_{i,f,t} \qquad \forall_{i\in\mathcal{E}}\ \forall_{f\in\mathcal{F}}\ \forall_{t\in\{1,\dots,T\}} \tag{7.14}$$

$$0 \leq \lambda_{f,t} \qquad \forall_{f\in\mathcal{F}}\ \forall_{t\in\{1,\dots,T\}} \tag{7.15}$$

$$0 \leq \mu_{i,f,t} \qquad \forall_{i\in\mathcal{E}}\ \forall_{f\in\mathcal{F}}\ \forall_{t\in\{1,\dots,T\}} \tag{7.16}$$

where the $\lambda_{f,t}$ and $\mu_{i,f,t}$ are real numbers that are not all zero. Writing out Equation (7.10) gives

$$0 = w_i r_{i,f,t} - \lambda_{f,t} + \mu_{i,f,t} \qquad \forall_{i\in\mathcal{E}}\ \forall_{f\in\mathcal{F}}\ \forall_{t\in\{1,\dots,T\}}, \tag{7.17}$$

where

$$w_i = \frac{1}{\sum\limits_{\tau=1}^{T}\sum\limits_{k\in\mathcal{F}} r_{i,k,\tau} I_{i,k,\tau}}. \tag{7.18}$$

Since $r_{i,f,t} > 0$, $I_{i,f,t} \geq 0$ and $\mu_{i,f,t} \geq 0$ for all i, f and t, Equation (7.17) gives us that

$$\lambda_{f,t} \geq \max_{e\in\mathcal{E}} w_e r_{e,f,t} > 0 \qquad \forall_{f\in\mathcal{F}}\ \forall_{t\in\{1,\dots,T\}}. \tag{7.19}$$

Because of Constraint (7.11), we know that we must have $\sum_{e\in\mathcal{E}} I_{e,f,t} - 1 = 0$ for all f and t, and thus get that Constraint (7.13) and therefore Constraint (7.4) is met with equality for all f and t. So we conclude that the optimal solution must be at the boundary of the solution space. Using this, the problem becomes

$$w_i r_{i,f,t} - \lambda_{f,t} + \mu_{i,f,t} = 0 \qquad \forall_{i\in\mathcal{E}}\ \forall_{f\in\mathcal{F}}\ \forall_{t\in\{1,\dots,T\}} \tag{7.20}$$

$$\mu_{i,f,t} I_{i,f,t} = 0 \qquad \forall_{i\in\mathcal{E}}\ \forall_{f\in\mathcal{F}}\ \forall_{t\in\{1,\dots,T\}} \tag{7.21}$$

$$\sum_{e\in\mathcal{E}} I_{e,f,t} = 1 \qquad \forall_{f\in\mathcal{F}}\ \forall_{t\in\{1,\dots,T\}} \tag{7.22}$$

$$\frac{1}{\sum\limits_{\tau=1}^{T}\sum\limits_{k\in\mathcal{F}} r_{i,k,\tau} I_{i,k,\tau}} = w_i \qquad \forall_{i\in\mathcal{E}} \tag{7.23}$$

$$I_{i,f,t} \geq 0 \qquad \forall_{i\in\mathcal{E}}\ \forall_{f\in\mathcal{F}}\ \forall_{t\in\{1,\dots,T\}} \tag{7.24}$$

$$\lambda_{f,t} \geq \max_{e\in\mathcal{E}} w_e r_{e,f,t} \qquad \forall_{f\in\mathcal{F}}\ \forall_{t\in\{1,\dots,T\}} \tag{7.25}$$

$$\mu_{i,f,t} \geq 0 \qquad \forall_{i\in\mathcal{E}}\ \forall_{f\in\mathcal{F}}\ \forall_{t\in\{1,\dots,T\}} \tag{7.26}$$

Suppose that we take $\lambda_{f,t}$ such that Equation (7.25) is not met with equality for any choice of f, t. Then Equation (7.20) gives us that $\mu_{i,f,t} > 0$ for all i. This implies that $I_{i,f,t} = 0$ for all i because of Equation (7.21). But this means that $\sum_{e\in\mathcal{E}} I_{e,f,t} = 0$, and therefore does not satisfy Constraint (7.22). Thus we conclude that $\lambda_{f,t}$ must be chosen such that Constraint (7.25) is met with equality for all f and t.

Now that we know all $\lambda_{f,t}$ in terms of the w_i variables, Equation (7.20) gives us

$$\mu_{i,f,t} = \lambda_{f,t} - w_i r_{i,f,t} = \max_{e\in\mathcal{E}}\{w_e r_{e,f,t}\} - w_i r_{i,f,t} \geq 0, \tag{7.27}$$

with equality for all $i \in \arg\max_{e\in\mathcal{E}} w_e r_{e,f,t}$ for all f, t. Thus we know that at least $|\mathcal{F}|T$ of the $\mu_{i,f,t} = 0$. Furthermore Equation (7.21) gives us that $I_{i,f,t} = 0$ if $i \notin \arg\max_{e\in\mathcal{E}} w_e r_{e,f,t}$.

Now assume that we can find an optimal assignment I that satisfies the above derived results. Then consider the bipartite 'assignment graph' which has two sets of vertices, on the left vertices corresponding to combinations of f and t, and on the right vertices corresponding to the eMBB users. Then let there be an edge between the vertices on the left corresponding to (f,t) and the vertices on the right corresponding to user i when $I_{i,f,t} > 0$.

If the assignment graph does not have any simple cycles, we know that it is a forest on $|\mathcal{F}|T + |\mathcal{E}|$ vertices and therefore has at most $|\mathcal{F}|T + |\mathcal{E}| - 1$ edges (this is when it is a tree), implying that I has at most $|\mathcal{F}|T + |\mathcal{E}| - 1$ variables greater than 0. This implies that there are at most $|\mathcal{F}|T + |\mathcal{E}| - 1$ edges. But we also know that for an optimal assignment I satisfies Constraint (7.13) with equality for all f and t, and therefore there are at least $|\mathcal{F}|T$ edges. So we conclude that in the worst case the $|\mathcal{E}| - 1$ resources corresponding to vertices corresponding to combinations of f and t are split over multiple users. Now the sub-graph consisting of the edges and vertices corresponding to variables $I_{i,f,t} \in (0,1)$, has at most $2|\mathcal{E}| - 1$ vertices, and does not contain any simple cycles. Because the assignment graph is a forest, this sub-graph is also a forest, and therefore it has at most $2|\mathcal{E}| - 2$ edges. So there are at most $2|\mathcal{E}| - 2$ variables $I_{i,f,t} \in (0,1)$. Now we notice that the all $I_{i,f,t} \in [0,1]$ because of Constraints (7.22) and (7.24). Since at most $|\mathcal{E}| - 1$ resources are split over multiple users, Constraint (7.22) gives us that at least $|\mathcal{F}|T - |\mathcal{E}| + 1$ variables $I_{i,f,t} = 1$. Because the assignment graph has at most $|\mathcal{F}|T + |\mathcal{E}| - 1$ edges, we know that at least $|\mathcal{E}||\mathcal{F}|T - |\mathcal{F}|T - |\mathcal{E}| + 1$ of the $I_{i,f,t} = 0$.

Now we need to show that there always exists an assignment $\widetilde{I}$ which is optimal, and has an assignment graph without any simple cycles. Suppose that I is an optimal assignment, with an assignment graph that contains at least one simple cycle. Let $\mathcal{C}$ be one of these simple cycles consisting of c edges. Now define Λ_i as the set of combinations of f and t that correspond to the neighbours of the vertex corresponding to user i in cycle $\mathcal{C}$. Similarly, define $\Psi_{f,t}$ as the set of users corresponding to the neighbours of the vertex corresponding to the combination of f and t in cycle $\mathcal{C}$.

Now take $\widetilde{I}_{i,f,t} = I_{i,f,t}$ for all i, f, t that do not correspond to one of the edges in $\mathcal{C}$. Then to ensure that assignment $\widetilde{I}$ has the same objective value as assignment I, we must have

$$\sum_{(f,t)\in\Lambda_i} r_{i,f,t} I_{i,f,t} = \sum_{(f,t)\in\Lambda_i} r_{i,f,t} \widetilde{I}_{i,f,t} \qquad \forall_{i\in\mathcal{E}}. \tag{7.28}$$

We also know that we should utilize as much of each resource as possible, then because I is an optimal solution, this implies

$$\sum_{i\in\Psi_{f,t}} I_{i,f,t} = \sum_{i\in\Psi_{f,t}} \widetilde{I}_{i,f,t} \qquad \forall_{(f,t)\in\mathcal{F}\times\{1,\ldots,T\}}. \tag{7.29}$$

Now we should notice that Equations (7.28) and (7.29) give us a system of c linear equations with c unknowns. The structure in this set of equations allow us to write $c-1$ of the unknowns in terms of the last unknown, say $\widetilde{I}_{i^*,f^*,t^*}$. Now we want $\widetilde{I}$ to have more integer variables than I, so we should find a value for $\widetilde{I}_{i^*,f^*,t^*}$ such that all $\widetilde{I}_{i,f,t} \geq 0$, and at least one of the $\widetilde{I}_{i,f,t}$ corresponding to the edges in the cycle $\mathcal{C}$ equals zero. We know that this is possible since all constraints are linear and there exists a solution (namely I) where all $\widetilde{I}_{i,f,t}$ corresponding to the edges in the cycle $\mathcal{C}$ are greater than zero.

This implies that for each optimal solution with a simple cycle in its assignment graph, there exists a solution that is equally good, but has at least one integer variable more. So by repeatedly eliminating simple cycles in the assignment graphs, we eventually find an optimal solution with at least $|\mathcal{E}||\mathcal{F}|T - |\mathcal{F}|T - |\mathcal{E}| + 1$ variables $I_{i,f,t} = 0$, at least $|\mathcal{F}|T - |\mathcal{E}| + 1$ variables $I_{i,f,t} = 1$, at most $2|\mathcal{E}| - 2$ variables $I_{i,f,t} \in (0,1)$, and no variables $I_{i,f,t} < 0$ or $I_{i,f,t} > 1$.

Furthermore, we know that there exist coefficients w_i such that the optimal solution has the structure we described above. Moreover, the coefficients w_i corresponding to the an optimal solution are reciprocal to the optimal throughput of user i over the entire time horizon. ■

7.1.1 Finding the optimal solution

To find the optimal solution for the relaxed problem, we will use an iterative algorithm. Since the solution space defined by (7.4) and (7.9) is convex and the objective function is strictly concave, we know that a local optimum is globally optimal (see [15, Section 4.2]). Therefore we can iteratively do a local search to improve our solution, and eventually end with the global optimal solution.

First let us introduce some notation. Let I^k be our solution after we improved k times. Let $\mathcal{A}_{I^k}$ denote the set of (possibly non-integer) assignments that are equal to I^k, but with $I^k_{i,f,t} = 1$ and $I^k_{e,f,t} = 0$ for all $e \neq i$ for one combination for f and t. This means that we assign a time-frequency resource that was possibly not assigned to a user or split over multiple users to one user. Then the objective function along the line from I^k to $\widetilde{I}$ as a function of x, i.e. the objective function of assignment $x\widetilde{I} + (1-x)I^k$, is given by

$$h_{I^k,\widetilde{I}}(x) = \sum_{i \in \mathcal{E}} \log \left(\frac{1}{T} \sum_{f \in \mathcal{F}} \sum_{t=1}^{T} \left(I^k_{i,f,t} + x \left(\widetilde{I}_{i,f,t} - I^k_{i,f,t} \right) \right) r^e_{i,f,t} \right). \tag{7.30}$$

This implies that the derivative is given by

$$\frac{d}{dx} h_{I^k,\widetilde{I}}(x) = \sum_{i \in \mathcal{E}} \frac{\sum\limits_{f \in \mathcal{F}} \sum\limits_{t=1}^{T} \left(\widetilde{I}_{i,f,t} - I^k_{i,f,t} \right) r^e_{i,f,t}}{\sum\limits_{f \in \mathcal{F}} \sum\limits_{t=1}^{T} \left(I^k_{i,f,t} + x \left(\widetilde{I}_{i,f,t} - I^k_{i,f,t} \right) \right) r^e_{i,f,t}}. \tag{7.31}$$

Now we can determine the optimal solution using Algorithm 1.

Algorithm 1: Algorithm to find the optimal assignment to the problem given by (7.3), (7.4) and (7.9)

Input : Rates $r^e_{i,f,t}$ and an initial assignment I^0
Output: The optimal assignment for all $I_{i,f,t}$

$done = false$
$k = 0$
while $done == false$ **do**
  $done = true$
  for $\widetilde{I} \in \mathcal{A}_{I^k}$ **do**
    if $\frac{d}{dx} h_{I^k,\widetilde{I}}(x)|_{x=0} > 0$ **then**
      if $\frac{d}{dx} h_{I^k,\widetilde{I}}(x)|_{x=1} \geq 0$ **then**
        $I^{k+1} = \widetilde{I}$
        $k = k + 1$
        $done = false$
        break
      else
        Determine y such that $\frac{d}{dx} h_{I^k,\widetilde{I}}(x)|_{x=y} = 0$ using the bisection method
        $I^{k+1} = y\widetilde{I} + (1-y)I^k$
        $k = k + 1$
        $done = false$
        break
      end
    end
  end
end
return I^k

In each iteration k, Algorithm 1 considers all possible directions of improvement (that is in the direction of the elements of $\mathcal{A}_{I^k}$). If an improvement is possible, i.e. $\frac{d}{dx}h_{I^k,\widetilde{I}}(x)|_{x=0} > 0$, with $\widetilde{I} \in \mathcal{A}_{I^k}$, then we update our solution to be the best solution along the line from I^k to $\widetilde{I}$. Since we consider all directions of improvement, we know that there is at least one assignment $\widetilde{I} \in \mathcal{A}_{I^k}$ for which $\frac{d}{dx}h_{I^k,\widetilde{I}}(x)|_{x=0} > 0$ when I^k is not optimal. Because the objective function is concave, and the feasible region is convex, we know that a local optimum is globally optimal [15, Section 4.2]. Therefore this method where we improve our solution locally will eventual give us a globally optimal solution.

7.1.2 Example

To illustrate how Algorithm 1 finds an optimal solution to the problem given by (7.3)(7.4) and (7.9), we will consider the example form Table 7.1 with three eMBB users, two frequencies for three timeslots.

t	1	1	2	2	3	3
f	1	2	1	2	1	2
$r^e_{1,f,t}$	495	510	485	450	522	515
$r^e_{2,f,t}$	526	478	502	553	470	431
$r^e_{3,f,t}$	503	434	555	499	542	469

Table 7.1: Rates $r^e_{i,f,t}$ of the eMBB users in our example

Suppose that we start with initial assignment I^0 given in Table 7.2. This assignment has objective value $h_{I^0,I^0}(0) = 17.3297$.

t	1	1	2	2	3	3
f	1	2	1	2	1	2
$I^0_{1,f,t}$	0	1	0	0	0	1
$I^0_{2,f,t}$	0	0	0	1	0	0
$I^0_{3,f,t}$	1	0	1	0	1	0

Table 7.2: Initial assignment I^0 for our example

Iterating over the assignments in $\mathcal{A}_{I^0}$ gives us that the first assignment $\widetilde{I} \in \mathcal{A}_{I^0}$ with $\frac{d}{dx}h_{I^k,\widetilde{I}}(x)|_{x=0} > 0$ increases $I_{1,1,1}$ at the expense of $I_{3,1,1}$. So define $\widetilde{I}$ as I^0, but with $\widetilde{I}_{1,1,1} = 1$ and $\widetilde{I}_{3,1,1} = 0$. Using the bisection method we now find that $\frac{d}{dx}h_{I^0,\widetilde{I}}(x)|_{x=y} = 0$ when $y = 0.5551$. So the assignment in Table 7.3 has highest utility (a utility of 17.3754) when we improve in this direction. Therefore we set I^1 to be the assignment in Table 7.3.

t	1	1	2	2	3	3
f	1	2	1	2	1	2
$I^1_{1,f,t}$	0.5551	1	0	0	0	1
$I^1_{2,f,t}$	0	0	0	1	0	0
$I^1_{3,f,t}$	0.4449	0	1	0	1	0

Table 7.3: Assignment I^1 for our example

Going over the assignments in $\mathcal{A}_{I^1}$ we find that we can improve our solution by assigning the resource corresponding to frequency $f = 1$ during slot $t = 1$ entirely to user 2. Therefore I^2 as specified in Table

7.4, which has a utility of 17.6207.

t	1	1	2	2	3	3
f	1	2	1	2	1	2
$I^2_{1,f,t}$	0	1	0	0	0	1
$I^2_{2,f,t}$	1	0	0	1	0	0
$I^2_{3,f,t}$	0	0	1	0	1	0

Table 7.4: Assignment I^2 for our example

Considering all possible assignments $\mathcal{A}_{I^2}$ we find that we could improve our solution I^2 by increasing $I^2_{1,1,3}$ at the expense of $I^2_{3,1,3}$. So define $\widetilde{I}$ as I^2, but with $\widetilde{I}_{1,1,3} = 1$ and $\widetilde{I}_{3,1,3} = 0$. Using the bisection method we now find that $\frac{d}{dx} h_{I^2,\widetilde{I}}(x)|_{x=y} = 0$ when $y = 0.0302$. So we now take $I^3 = 0.0302\widetilde{I} + 0.9698 I^2$, which is shown in Table 7.5, and has a utility of 17.6210.

t	1	1	2	2	3	3
f	1	2	1	2	1	2
$I^3_{1,f,t}$	0	1	0	0	0.0302	1
$I^3_{2,f,t}$	1	0	0	1	0	0
$I^3_{3,f,t}$	0	0	1	0	0.9698	0

Table 7.5: Assignment I^3 for our example

Going over all assignments in $\mathcal{A}_{I^3}$, we do not find a positive derivative, which implies that I^3 is the optimal solution.

7.2 Hijacking

Considering hijacking, we know the demand $D_{j,t,m}$ of URLLC user $j \in \mathcal{U}$ during each mini-slot m of slot t. So now we need to solve the following optimization for the offline setting

$$\begin{aligned}
\max \quad & \sum_{i\in\mathcal{E}} \log\left(\frac{1}{T}\sum_{t=1}^{T}\sum_{f\in\mathcal{F}} r^e_{i,f,t} I_{i,f,t}\left(1-\frac{1}{M}\sum_{m=1}^{M}\sum_{j\in\mathcal{U}} J_{j,f,t,m}\right)\right) && (7.32)\\
\text{subject to} \quad & I_{i,f,t} \in \{0,1\} \quad \forall_{i\in\mathcal{E}}\ \forall_{f\in\mathcal{F}}\ \forall_{t\in\{1,\dots,T\}}, && (7.33)\\
& J_{j,f,t,m} \in \{0,1\} \quad \forall_{j\in\mathcal{U}}\ \forall_{f\in\mathcal{F}}\ \forall_{t\in\{1,\dots,T\}}\ \forall_{m\in\{1,\dots,M\}}, && (7.34)\\
& \sum_{i\in\mathcal{E}} I_{i,f,t} \le 1 \quad \forall_{f\in\mathcal{F}}\ \forall_{t\in\{1,\dots,T\}}, && (7.35)\\
& \sum_{j\in\mathcal{U}} J_{j,f,t,m} \le 1 \quad \forall_{f\in\mathcal{F}}\ \forall_{t\in\{1,\dots,T\}}\ \forall_{m\in\{1,\dots,M\}}, && (7.36)\\
& \sum_{f\in\mathcal{F}} \frac{r^u_{j,f,t}}{M} J_{j,f,t,m} \ge D_{j,t,m} \mathbb{1}_{\left\{\sum\limits_{k\in\mathcal{U}}\sum\limits_{f\in\mathcal{F}} J_{k,f,t,m} < |\mathcal{U}|\right\}} \quad \forall_{j\in\mathcal{U}}\ \forall_{t\in\{1,\dots,T\}}\ \forall_{m\in\{1,\dots,M\}}. && (7.37)
\end{aligned}$$

Assuming that there is at most one URLLC user demand, which is equal to $\sum_{f\in\mathcal{F}} r^e_{1,f,t}$ during a mini-slot when it is present, we can use a similar argument as in Section 7.1 to see that this problem is NP-hard.

Similar to the no-hijacking case, we consider the continuous relaxation of this problem, and therefore relax Constraints (7.33) and (7.34) to

$$I^{\varepsilon}_{i,f,t} \geq 0 \quad \forall_{i\in\mathcal{E}}\ \forall_{f\in\mathcal{F}}\ \forall_{t\in\{1,\ldots,T\}}, \tag{7.38}$$
$$J^{\varepsilon}_{i,f,t,m} \geq 0 \quad \forall_{j\in\mathcal{U}}\ \forall_{f\in\mathcal{F}}\ \forall_{t\in\{1,\ldots,T\}}\ \forall_{m\in\{1,\ldots,M\}}. \tag{7.39}$$

Unfortunately, the solution space corresponding to Constraints 7.35-7.39 is not necessarily convex. However, as the URLLC demands should be satisfied with high reliability (99.999%), it is reasonable to assume that the URLLC demands can always be met during all mini-slots. So we will consider the following optimization problem

$$\max \quad \sum_{i\in\mathcal{E}} \log\left(\frac{1}{T}\sum_{t=1}^{T}\sum_{f\in\mathcal{F}} r^{e}_{i,f,t} I_{i,f,t}\left(1-\frac{1}{M}\sum_{m=1}^{M}\sum_{j\in\mathcal{U}} J_{j,f,t,m}\right)\right) \tag{7.40}$$
$$\text{subject to} \quad I_{i,f,t} \geq 0 \quad \forall_{i\in\mathcal{E}}\ \forall_{f\in\mathcal{F}}\ \forall_{t\in\{1,\ldots,T\}}, \tag{7.41}$$
$$J_{j,f,t,m} \geq 0 \quad \forall_{j\in\mathcal{U}}\ \forall_{f\in\mathcal{F}}\ \forall_{t\in\{1,\ldots,T\}}\ \forall_{m\in\{1,\ldots,M\}}, \tag{7.42}$$
$$\sum_{i\in\mathcal{E}} I_{i,f,t} \leq 1 \quad \forall_{f\in\mathcal{F}}\ \forall_{t\in\{1,\ldots,T\}}, \tag{7.43}$$
$$\sum_{j\in\mathcal{U}} J_{j,f,t,m} \leq 1 \quad \forall_{f\in\mathcal{F}}\ \forall_{t\in\{1,\ldots,T\}}\ \forall_{m\in\{1,\ldots,M\}}, \tag{7.44}$$
$$\sum_{f\in\mathcal{F}} \frac{r^{u}_{j,f,t}}{M} J_{j,f,t,m} \geq D_{j,t,m} \quad \forall_{j\in\mathcal{U}}\ \forall_{t\in\{1,\ldots,T\}}\ \forall_{m\in\{1,\ldots,M\}}, \tag{7.45}$$

where we assumed that there exists at least one assignment such that Constraint (7.45) is met. Now Constraints (7.41)-(7.45) form a set of linear constraints, using similar reasoning as in Section 7.2, these constraints define a convex solution space.

7.2.1 Finding an upper bound

Since it could be hard to find the optimal solution to the problem given by (7.32)-(7.37), we would like to have an upper bound for the objective value. However, even the relaxed problem defined by (7.40)-(7.45) could be difficult to solve. Therefore we notice that the scenario without hijacking definitely gives us an upper bound for the objective value. So we could use the upper bound that we found for the scenario without hijacking. However, we want to have a sharper bound.

First for each demand $D_{j,t,m}$, we know that in the best case we hijack the frequency f with the highest rate, i.e. with rate $\max_{f\in\mathcal{F}} r^{u}_{j,f,t}$. So when we hijack the frequencies with the highest rates, the fraction of resources we need to hijack is minimized. Therefore denote by $f^{k}_{j,t}$ the frequency with the k^{th} largest value of $r^{u}_{j,f,t}$. Let $d^{k}_{j,t,m}$ be the unsatisfied demand of user j, when we already hijack the k frequencies with the highest rates, i.e.

$$d^{k}_{j,t,m} = \max\left\{0,\ d^{k-1}_{j,t,m} - \frac{r^{u}_{j,f^{k}_{j,t},t}}{M}\max\left\{1,\ \frac{M d^{k-1}_{j,t,m}}{r^{u}_{j,f^{k}_{j,t},t}}\right\}\right\}, \tag{7.46}$$

where $d^{0}_{j,t,m} = D_{j,t,m}$, and k integer. Now let $k^{*}_{j,t,m} = \arg\min\left\{\arg\min_{k\in\{1,\ldots,|\mathcal{F}|\}} d^{k}_{j,t,m}\right\}$, then the number of frequencies we minimally need to hijack during mini-slot m of slot t (which need not be integer) is given by

$$P_{t,m} = \max\left\{|\mathcal{F}|, \sum_{j\in\mathcal{U}}\left(k^{*}_{j,t,m} - 1 + \frac{M d^{k^{*}_{j,t,m}-1}_{j,t,m}}{r^{u}_{j,f^{k^{*}_{j,t,m}}_{j,t},t}}\right)\right\}. \tag{7.47}$$

Now that we know the number of frequencies that we minimally need to hijack during mini-slot m of slot t, we can determine the loss that the eMBB users minimally suffer. Let f_t^k and i_t^k denote the user and frequency corresponding to the k^{th} smallest value of $r^e_{i,f,t}$ during slot t. Then the minimum aggregate loss for the eMBB users is given by

$$L = \sum_{t=1}^{T} \sum_{m=1}^{M} \sum_{k=1}^{\lfloor P_{t,m} \rfloor} \frac{r^e_{i_t^k, f_t^k, t}}{M} + (P_{t,m} - \lfloor P_{t,m} \rfloor) \frac{r^e_{i_t^{\lfloor P_{t,m} \rfloor}, f_t^{\lfloor P_{t,m} \rfloor}, t}}{M}. \tag{7.48}$$

Suppose that we know the optimal assignment in the scenario without hijacking, and that this assignment gives an average rate of R_i to eMBB user i. Then we need to solve the following problem

$$\max \quad \sum_{i \in \mathcal{E}} \log \left(R_i - \frac{x_i L}{T} \right) \tag{7.49}$$

$$\text{subject to} \quad \sum_{i \in \mathcal{E}} x_i = 1, \tag{7.50}$$

$$x_i \geq 0 \qquad \forall_{i \in \mathcal{E}}, \tag{7.51}$$

where (7.50) ensures that the eMBB users together lose precisely L, and (7.51) ensures that none of the eMBB users will receive a higher rate than in the scenario without hijacking. It can easily be seen that (7.50) and (7.51) define a convex solution space. Since the objective function is strictly concave and the solution space is convex, we know that there is a unique solution [15, Section 4.2].

This solution can be found by lowering the average throughput of the user with the highest R_i until its throughput is equal to the throughput of the user with the second highest throughput. Then we lower the throughputs of the two users with highest throughput, until there are three users with highest throughput. We keep on doing this until the we have decreased the sum of the throughputs with L. This way we decrease our objective value the least, since the objective function decreases the least when the throughput of the user with the highest throughput decreases.

To put it more mathematically, the optimal assignment is given by

$$x_{i_k} = \sum_{l=k}^{|\mathcal{E}|} \min \left\{ \frac{1}{l} \left(1 - \sum_{a=1}^{l-1} a \frac{T \left(R_{i_a} - R_{i_{a+1}} \right)}{L} \right), \frac{T \left(R_{i_l} - R_{i_{l+1}} \right)}{L} \right\}, \tag{7.52}$$

where i_k denotes the eMBB user with k^{th} largest average throughput R_i, with $R_{i_{|\mathcal{E}|+1}} = 0$.

Now the upper bound for the objective value of the problem given by (7.32),(7.35)-(7.39) is given by

$$\sum_{i \in \mathcal{E}} \log \left(R_i - \frac{x_i L}{T} \right), \tag{7.53}$$

where we note that $R_i - \frac{x_i L}{T}$ is not necessarily an upper bound for the throughput of eMBB user i in a scenario with hijacking.

7.3 Proportional fair algorithm compared to the upper bound

Theorem 4 gives us some insight in the optimal performance in a non-anticipating (online) scenario. However, for both the score based policy we do not have such an asymptotic optimality result. So to gain some insight in the relative performance of the hijacking policies, we will compare the average throughputs in an online setting (so using our algorithm) to the optimal throughputs in an offline setting (where the channel rates and URLLC demands are known in advance).

Since we cannot (at least not efficiently) determine the optimal assignment for the hijacking scenario, we cannot determine the optimal throughputs $\bar{R}_i$, and thus the utility corresponding to this optimal assignment. As we would like to say something about the relative performance of the algorithm compared to an offline setting, considering the utilities defined by Equation (7.1) can be misleading since a scaling in rates e.g. from bits/slot to bytes/slot gives different results.

Let $\widehat{R}_i = R_i - x_i L/T$ be the average throughputs corresponding to the upper bound (see Section 7.2.1), where R_i denotes the rate of user i corresponding to the assignment for the upper bound without hijacking (see Section 7.1.1). Let $\widetilde{R}$ be the throughputs corresponding to our algorithm.

Unfortunately $\widehat{R}_i$ is not necessarily an upper bound for $\widetilde{R}_i$. However, as we consider the utility function defined by Equation (7.1) we know that

$$\log\left(\prod_{i\in\mathcal{E}} \widehat{R}_i\right) = \sum_{i\in\mathcal{E}} \log\left(\widehat{R}_i\right) \geq \sum_{i\in\mathcal{E}} \log\left(\widetilde{R}_i\right) = \log\left(\prod_{i\in\mathcal{E}} \widetilde{R}_i\right), \tag{7.54}$$

and therefore

$$\prod_{i\in\mathcal{E}} \widehat{R}_i \geq \prod_{i\in\mathcal{E}} \widetilde{R}_i. \tag{7.55}$$

So to get an impression of the performance, we can consider the performance measure $\prod_{i\in\mathcal{E}} \widetilde{R}_i/\widehat{R}_i$ which is less than or equal to 1.

To get an insight in the relative average performance of our online algorithm compared to the optimal solution, we consider the random, score based and OSB hijacking policy for scenarios 1-3 from Sections 5.1-5.3, and simulate 100 sets of rates for the eMBB and URLLC users for each scenario. Instead of the demand probabilities specified in Sections 5.1-5.3, we will now assume that

$$\mathbb{P}\left(D_{1,t,m} = 0\right) = 1 - p, \qquad \mathbb{P}\left(D_{1,t,m} = 20\right) = p,$$
$$\mathbb{P}\left(D_{2,t,m} = 0\right) = 1 - p, \qquad \mathbb{P}\left(D_{2,t,m} = 25\right) = p$$

for all t, m, where $D_{j,t,m}$ is given in bits. For each set of rates we will generate a set of demands with $p \in \{0, 0.01, 0.02, \ldots, 0.50\}$. For all simulations we assume a time horizon of $T = 3,000$ slots, consisting of $M = 8$ mini-slots, a smoothing parameter $\varepsilon = 10^{-4}$. To generate the rates we will assume that there are 600 slots per second and a maximum Doppler shift of 60 Hz. Results of these simulations can be found in Figure 7.1.

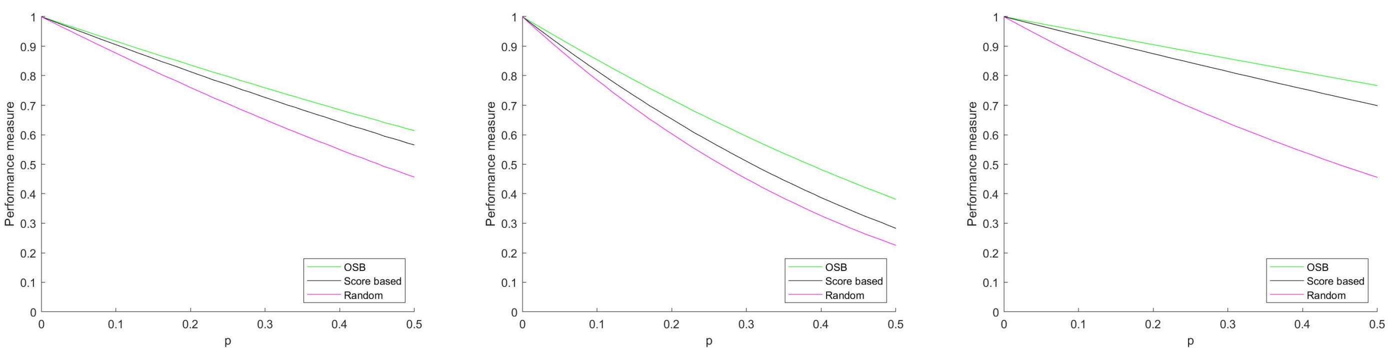

(a) Scenario 1 (b) Scenario 2 (c) Scenario 3

Figure 7.1: Average performance measure $\prod_{i\in\mathcal{E}} \widetilde{R}_i/\widehat{R}_i$ as function of p

When we calculate the sample variances for each scenario, we find that the variance is less than 10^{-4}

for all p in each scenario. This indicates that there is extremely little variation between the performance measures of different runs.

In Figure 7.1 we see that the performance measure decreases when p increases. For all three scenarios we see that the OSB policy has the best performance measure followed by the score based policy, and lastly the random policy. This was to be expected since we have seen that the OSB policy performs best, and the random policy performs worst.

For small values of p the performance measures are close to 1, which indicates that the online algorithm has near optimal performance. However, the performance measures are below 0.7, 0.5 and 0.8 for scenarios 1, 2 and 3 respectively when $p = 0.5$. Even though the performance measures are low, this does not necessarily mean that the online algorithm performs bad compared to the optimal solution in an offline setting. This is because we use the rates corresponding to an upper bound of the utility function (7.1). Because the variance of the performance measures is very small, it seems more logical that the used upper bound was too crude.

For the performance of the online algorithm without hijacking, we only need to consider $p = 0$ for any of the hijacking policies since there is no demand, and thus no hijacking. Because the performance measure is almost 1 for each of the three scenarios, we conclude that the online algorithm performs extremely well in situations without hijacking.

Chapter 8

Conclusions and suggestions for further research

In Chapter 2 we introduced a scheduling model for next-generation wireless networks. In this model we consider two types of users, throughput-oriented and delay-sensitive. Since the demands of the delay-sensitive users are not known at the time of scheduling, we only schedule the throughput-oriented users. Because the demands of delay-sensitive users should be satisfied with high reliability, we assign resources to these users as soon as the demand arrives. However, the the assignment of resources to the delay-sensitive users implies a loss in throughput for the throughput-oriented users.

For our model, we were able to extend the theorems from [6] to our setting. These extended theorems give us more insight in the throughputs of the users in the network over time. Furthermore, these theorems also give us an indication of the optimal performance of the network.

To verify the theorems, we conducted several simulation experiments. The results of these experiments indicated that the performance of the throughputs of the users vary more over time when we choose a larger smoothing parameter. But we have also seen that a higher maximum Doppler shift i.e. a faster moving receiver experiences less variation in throughput over time.

Considering the three hijacking policies we have seen that the OSB policy has best performance. However, as it is too complex to use in practical situations, it gave us an indication how good the algorithm could do. Our simulation experiments showed that the random hijacking policy performed worst. However, the score based policy which could be used in practice performed almost as good as the OSB policy.

To investigate the performance of the hijacking policies, we compared the scheduling decisions of our algorithm against the decisions corresponding to an offline setting. In this comparison, we see that our scheduling algorithm has near-optimal performance when the probability of non-zero demand for the URLLC users is small. However, when the probability of non-zero demand increases, we see that the performance measure decreases, which could imply worse performance, but more likely, it could also mean that the used upper bound was too crude. Therefore a first topic for further research would be to investigate the performance more closely. Either by finding a better upper bound or using a different performance measure.

Another topic for further research would be to consider a more practical situation. For this we could consider the behaviour of the system when a user arrives or leaves the system. For an arrival event, we have no information about the throughput it will receive, so it is not clear what the initial throughput should be in our model. But also how do we treat leaving users that might come back? Do we forget their throughput or stop updating it for some time?

Another practical point would be to determine a suitable smoothing parameter. We have seen that the maximum Doppler shift and the smoothing parameter influence the amount of variation of the throughputs over time. But the smoothing parameter ε also has impact on the convergence time, which we found to be of the order $1/\varepsilon$. Therefore we should choose the smoothing parameter possibly depending on the velocity (and therefore maximum Doppler shifts) of the users in such a way that we balance the convergence time and the amount of variation in throughputs over time. To find a suitable smoothing parameter, it might therefore be useful to investigate the amount of variation as a function of both the maximum Doppler shifts and the smoothing parameter.

Finally, in this report we have considered three hijacking policies, the random, score based and OSB policies. The OSB policy has good performance, but it is too complex to be used in practical applications since we have less than a millisecond to determine the hijacking assignment. The random policy on the other hand does not require many calculations, but it hijacks the frequencies without considering the impact for both the eMBB and URLLC users, and therefore it is not such a good hijacking policy. The score based policy provides reasonably good results and has a fast implementation. However, as the score based policy is not as good as the OSB policy, there could be better policies that can be used in practical situations. So we could also investigate the performance of some other policies, and try to find a policy that can be used in practice and outperforms the policies mentioned in this report.

Bibliography

[1] H. Ji, S. Park, J. Yeo, Y. Kim, J. Lee, and B. Shim. Ultra-reliable and low-latency communications in 5G downlink: Physical layer aspects. *IEEE Wireless Communications*, 25(3):124–130, June 2018.

[2] He Chen, Rana Abbas, Peng Cheng, Mahyar Shirvanimoghaddam, Wibowo Hardjawana, Wei Bao, Yonghui Li, and Branka Vucetic. Ultra-reliable low latency cellular networks: Use cases, challenges and approaches. *IEEE Communications Magazine*, Sep. 2017.

[3] C. Li, J. Jiang, W. Chen, T. Ji, and J. Smee. 5G ultra-reliable and low-latency systems design. In *2017 European Conference on Networks and Communications (EuCNC)*, pages 1–5, June 2017.

[4] Arjun Anand, Gustavo de Veciana, and Sanjay Shakkottai. Joint scheduling of URLLC and eMBB traffic in 5G wireless networks. *IEEE INFOCOM 2018 - IEEE Conference on Computer Communications*, pages 1970–1978, 2018.

[5] K. I. Pedersen, G. Pocovi, J. Steiner, and S. R. Khosravirad. Punctured scheduling for critical low latency data on a shared channel with mobile broadband. In *2017 IEEE 86th Vehicular Technology Conference (VTC-Fall)*, pages 1–6, Sep. 2017.

[6] H. J. Kushner and P. A. Whiting. Convergence of proportional-fair sharing algorithms under general conditions. *IEEE Transactions on Wireless Communications*, 3(4):1250–1259, July 2004.

[7] Alexander L. Stolyar. On the asymptotic optimality of the gradient scheduling algorithm for multiuser throughput allocation. *Operations Research*, 53(1):12–25, 2005.

[8] Vinay Joseph and Gustavo de Veciana. Variability aware network utility maximization. *CoRR*, abs/1111.3728, 2011.

[9] V. Joseph and G. de Veciana. Jointly optimizing multi-user rate adaptation for video transport over wireless systems: Mean-fairness-variability tradeoffs. In *2012 Proceedings IEEE INFOCOM*, pages 567–575, March 2012.

[10] V. Joseph, G. de Veciana, and A. Arapostathis. Resource allocation: Realizing mean-variability-fairness tradeoffs. In *2012 50th Annual Allerton Conference on Communication, Control, and Computing (Allerton)*, pages 831–838, Oct 2012.

[11] H. J. Kushner and G. Yin. *Stochastic Approximation Algorithms and Applications*. Springer New York, 1997.

[12] H. L. Smith. *Monotone Dynamical Systems: An Introduction to Competitive and Cooperative Sys-*

tems, volume 41 of *AMS Math. Surveys and Monographs.* Providence, RI: American Mathematical Society, 1997.

[13] W. C. Jakes. *Microwave mobile communications.* IEEE Press classic reissue. IEEE Press, 1974.

[14] M. Patzold, C. Wang, and B. O. Hogstad. Two new sum-of-sinusoids-based methods for the efficient generation of multiple uncorrelated Rayleigh fading waveforms. *IEEE Transactions on Wireless Communications*, 8(6):3122–3131, June 2009.

[15] S. Boyd and L. Vandenberghe. *Convex Optimization.* Cambridge University Press, 2004.

Appendix A

Formulation in [11]

In [11] the authors consider an algorithm of the form

$$\theta_{n+1}^{\varepsilon} = \theta_n^{\varepsilon} + \varepsilon Y_t^{\varepsilon} + \varepsilon Z_n^{\varepsilon}, \tag{A.1}$$

where $\{Y_n^{\varepsilon}\}$ is the observation sequence, and $\{Z_n^{\varepsilon}\}$ denotes the reflection terms.

Let ξ_n^{ε} be random variables taking values in some separable metric space Ξ. Let $\{F_n^{\varepsilon}\}$ be a sequence of non-decreasing σ-algebras, where F_n^{ε} measures at least $\{\theta_\tau^{\varepsilon}, Y_{\tau-1}^{\varepsilon}, \xi_n^{\varepsilon}, \tau \leq n\}$, and let $\mathbb{E}_n^{\varepsilon}$ denote the expectation conditioned on F_n^{ε}. Let H denote some constraint set.

Now the assumptions are as follows:

A1.1 $\{Y_t^{\varepsilon}, \varepsilon, t\}$ is uniformly integrable.

A1.2 There are functions $g_n^{\varepsilon}(\cdot)$ that are continuous uniformly in n and ε and random variables β_n^{ε} such that

$$\mathbb{E}_n Y_n^{\varepsilon} = g_n^{\varepsilon}(\theta_n^{\varepsilon}) + \beta_n^{\varepsilon}. \tag{A.2}$$

A1.3 There is a continuous function $\bar{g}(\cdot)$ such that for each $\theta \in H$

$$\lim_{m,n,\varepsilon} \frac{1}{m} \sum_{\tau=n}^{n+m-1} [g_\tau^{\varepsilon}(\theta) - \bar{g}(\theta)] = 0. \tag{A.3}$$

A1.4 $\lim\limits_{m,n,\varepsilon} \frac{1}{m} \sum\limits_{\tau=n}^{n+m-1} \mathbb{E}_n^{\varepsilon} \beta_\tau^{\varepsilon} = 0$ in mean.

The $\lim_{m,n,\varepsilon}$ means that the limit is taken as $m \to \infty$, $n \to \infty$, and $\varepsilon \to 0$ simultaneously in any way at all.

A1.5 There are measurable functions $g_n^{\varepsilon}(\cdot)$ and random variables β_n^{ε} such that

$$\mathbb{E}_n Y_n^{\varepsilon} = g_n^{\varepsilon}(\theta_n^{\varepsilon}, \xi_n^{\varepsilon}) + \beta_n^{\varepsilon}. \tag{A.4}$$

A1.6 For each compact set $A \subset \Xi$, $g_n^{\varepsilon}(\cdot, \xi)$ is continuous in θ uniformly in n, ε and in $\xi \in A$.

A1.7 For each $\delta > 0$ there exists a compact $A_\delta \subset \Xi$ such that

$$\inf_{n,\varepsilon} \mathbb{P}\left(\xi_n^\varepsilon \in A_\delta\right) \geq 1 - \delta. \tag{A.5}$$

A1.8 The sequences

$$\{g_n^\varepsilon(\theta_n^\varepsilon, \xi_n^\varepsilon); \varepsilon, n\} \tag{A.6}$$

and

$$\{g_n^\varepsilon(\theta, \xi_n^\varepsilon); \varepsilon, n\},\ \theta \in H, \tag{A.7}$$

are both uniformly integrable.

A1.9 There is a continuous function $\bar{g}(\cdot)$ such that for each $\theta \in H$

$$\lim_{m,n,\varepsilon} \frac{1}{m} \sum_{\tau=n}^{n+m-1} \left[g_\tau^\varepsilon(\theta, \xi_\tau^\varepsilon) - \bar{g}(\theta)\right] = 0. \tag{A.8}$$

in probability.

A1.10 $\{\theta_n^\varepsilon\}$ is bounded with probability one. The limit set L of $\dot{\theta} = \bar{g}(\theta)$ over all initial conditions is bounded and L_H is replaced by L.

Appendix B

Other results Rayleigh fading model

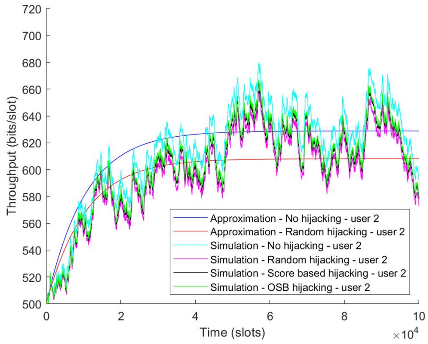

(a) $\varepsilon = 10^{-4}$, $\omega_{\max} = 6$ Hz

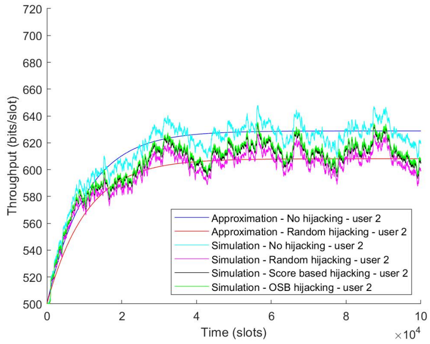

(b) $\varepsilon = 10^{-4}$, $\omega_{\max} = 25$ Hz

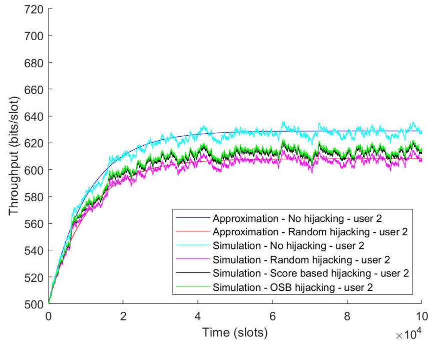

(c) $\varepsilon = 10^{-4}$, $\omega_{\max} = 60$ Hz

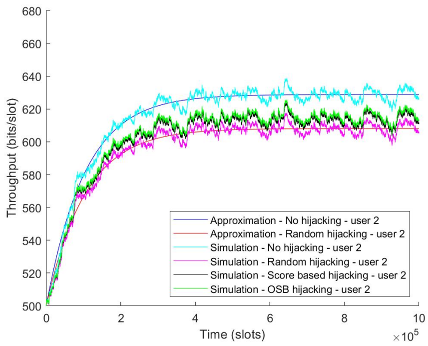

(d) $\varepsilon = 10^{-5}$, $\omega_{\max} = 6$ Hz

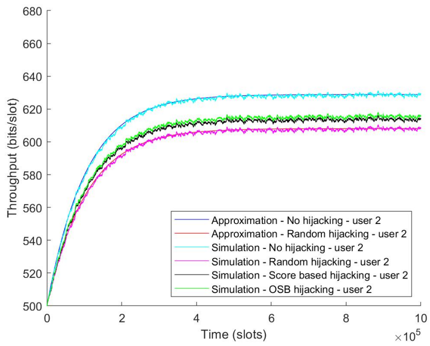

(e) $\varepsilon = 10^{-5}$, $\omega_{\max} = 25$ Hz

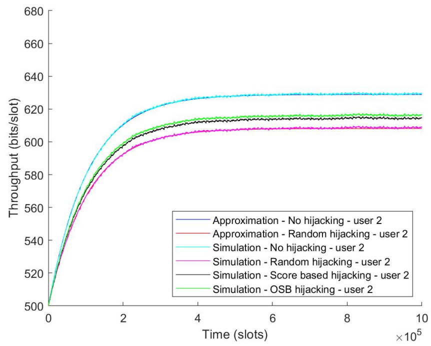

(f) $\varepsilon = 10^{-5}$, $\omega_{\max} = 60$ Hz

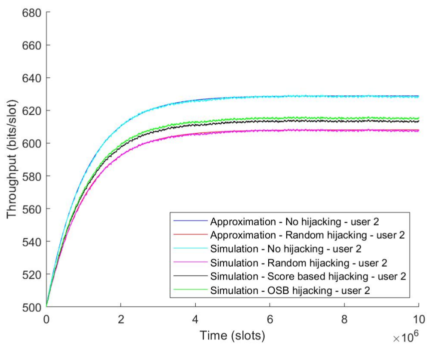

(g) $\varepsilon = 10^{-6}$, $\omega_{\max} = 6$ Hz

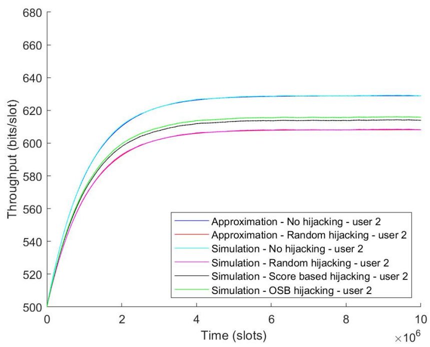

(h) $\varepsilon = 10^{-6}$, $\omega_{\max} = 25$ Hz

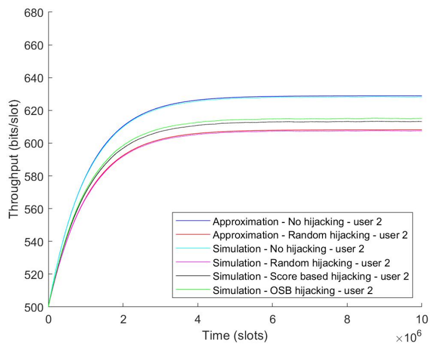

(i) $\varepsilon = 10^{-6}$, $\omega_{\max} = 60$ Hz

Figure B.1: Average throughputs over time for user 2 in scenario 1

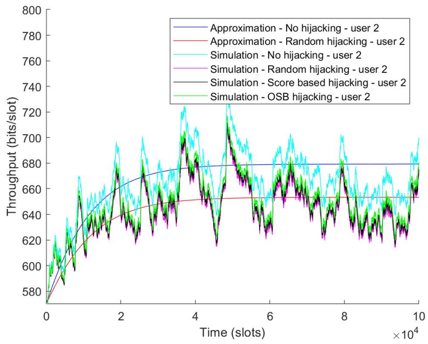

(a) $\varepsilon = 10^{-4}$, $\omega_{\max} = 6$ Hz

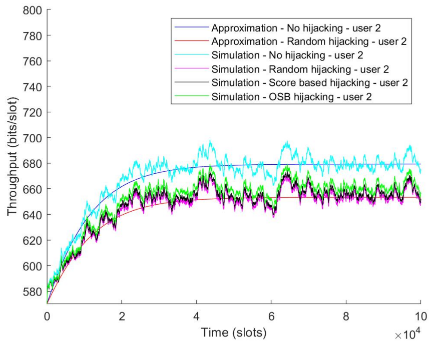

(b) $\varepsilon = 10^{-4}$, $\omega_{\max} = 25$ Hz

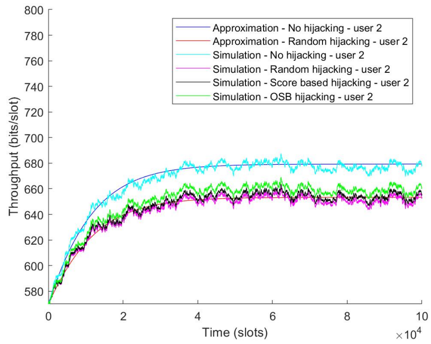

(c) $\varepsilon = 10^{-4}$, $\omega_{\max} = 60$ Hz

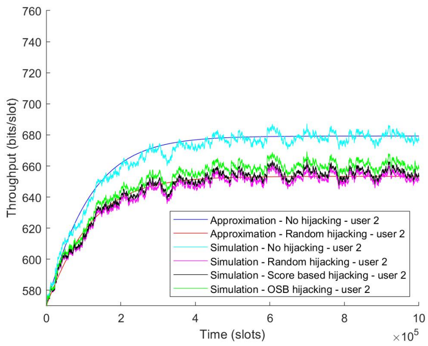

(d) $\varepsilon = 10^{-5}$, $\omega_{\max} = 6$ Hz

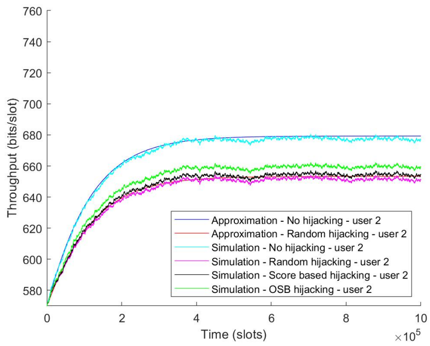

(e) $\varepsilon = 10^{-5}$, $\omega_{\max} = 25$ Hz

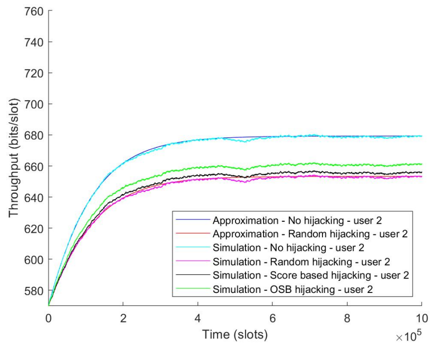

(f) $\varepsilon = 10^{-5}$, $\omega_{\max} = 60$ Hz

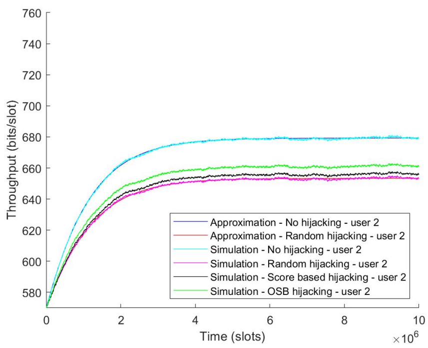

(g) $\varepsilon = 10^{-6}$, $\omega_{\max} = 6$ Hz

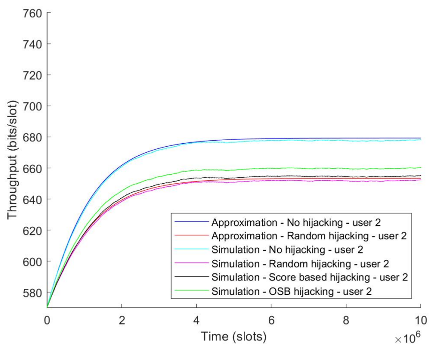

(h) $\varepsilon = 10^{-6}$, $\omega_{\max} = 25$ Hz

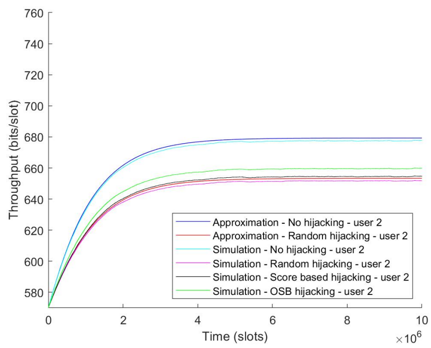

(i) $\varepsilon = 10^{-6}$, $\omega_{\max} = 60$ Hz

Figure B.2: Average throughputs over time for user 2 in scenario 2

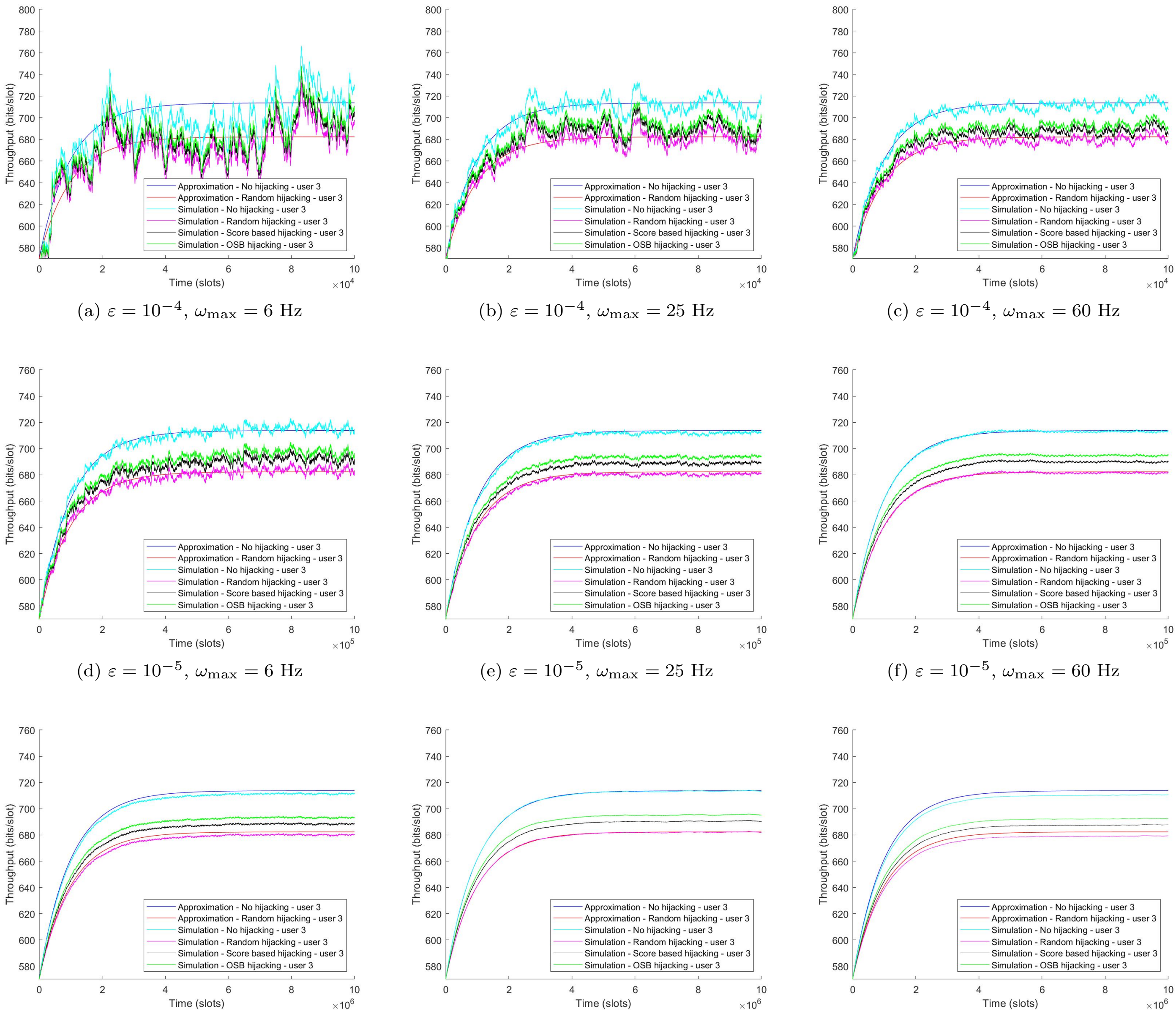

(a) $\varepsilon = 10^{-4}$, $\omega_{\max} = 6$ Hz

(b) $\varepsilon = 10^{-4}$, $\omega_{\max} = 25$ Hz

(c) $\varepsilon = 10^{-4}$, $\omega_{\max} = 60$ Hz

(d) $\varepsilon = 10^{-5}$, $\omega_{\max} = 6$ Hz

(e) $\varepsilon = 10^{-5}$, $\omega_{\max} = 25$ Hz

(f) $\varepsilon = 10^{-5}$, $\omega_{\max} = 60$ Hz

(g) $\varepsilon = 10^{-6}$, $\omega_{\max} = 6$ Hz

(h) $\varepsilon = 10^{-6}$, $\omega_{\max} = 25$ Hz

(i) $\varepsilon = 10^{-6}$, $\omega_{\max} = 60$ Hz

Figure B.3: Average throughputs over time for user 3 in scenario 2

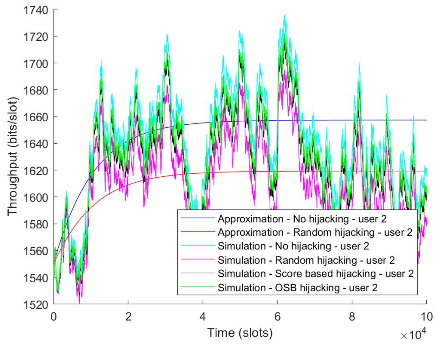

(a) $\varepsilon = 10^{-4}$, $\omega_{\max} = 6$ Hz

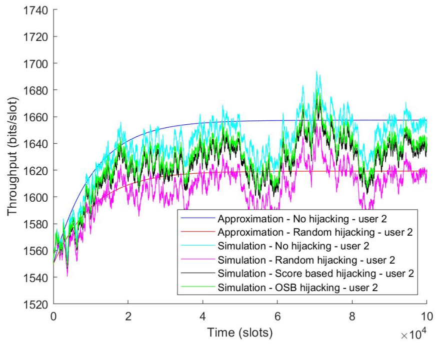

(b) $\varepsilon = 10^{-4}$, $\omega_{\max} = 25$ Hz

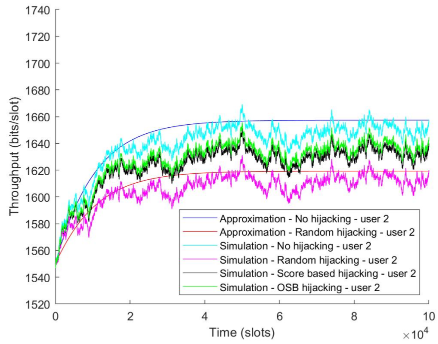

(c) $\varepsilon = 10^{-4}$, $\omega_{\max} = 60$ Hz

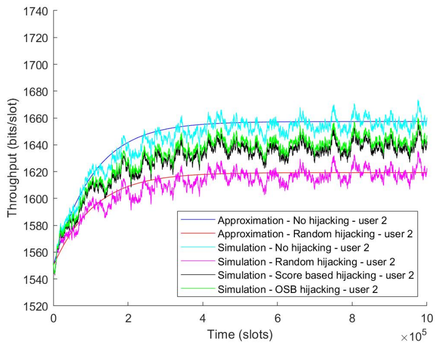

(d) $\varepsilon = 10^{-5}$, $\omega_{\max} = 6$ Hz

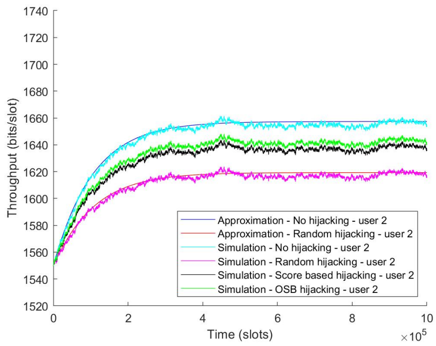

(e) $\varepsilon = 10^{-5}$, $\omega_{\max} = 25$ Hz

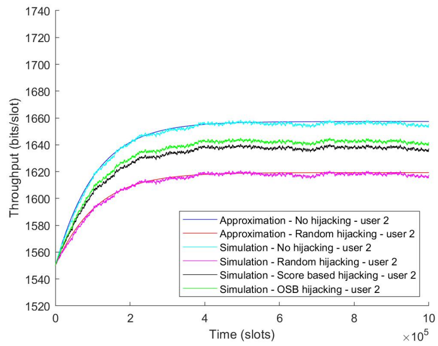

(f) $\varepsilon = 10^{-5}$, $\omega_{\max} = 60$ Hz

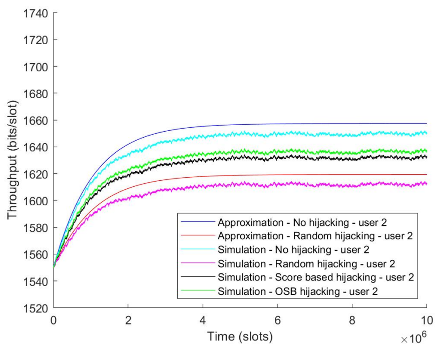

(g) $\varepsilon = 10^{-6}$, $\omega_{\max} = 6$ Hz

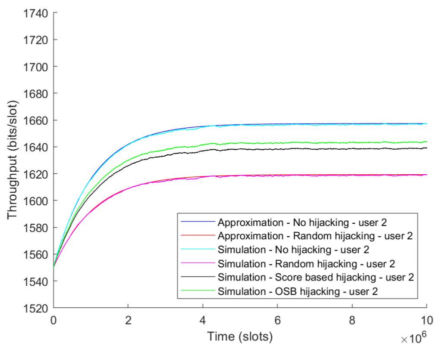

(h) $\varepsilon = 10^{-6}$, $\omega_{\max} = 25$ Hz

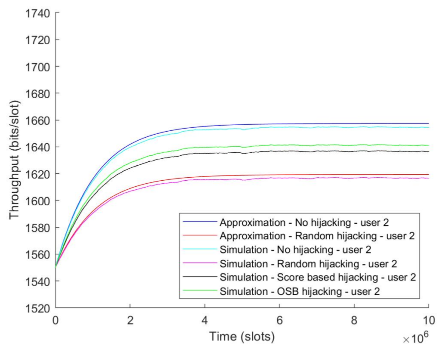

(i) $\varepsilon = 10^{-6}$, $\omega_{\max} = 60$ Hz

Figure B.4: Average throughputs over time for user 2 in scenario 3

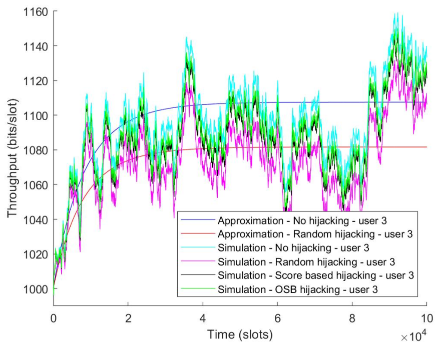

(a) $\varepsilon = 10^{-4}$, $\omega_{\max} = 6$ Hz

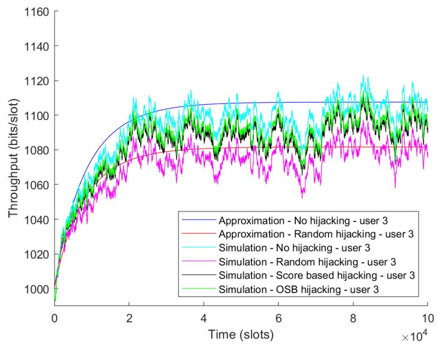

(b) $\varepsilon = 10^{-4}$, $\omega_{\max} = 25$ Hz

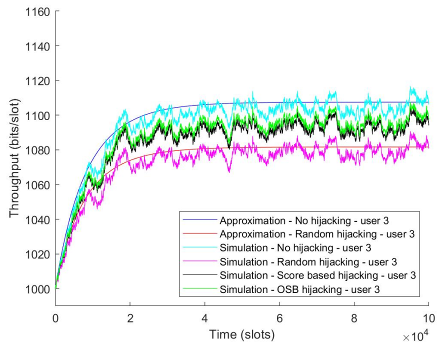

(c) $\varepsilon = 10^{-4}$, $\omega_{\max} = 60$ Hz

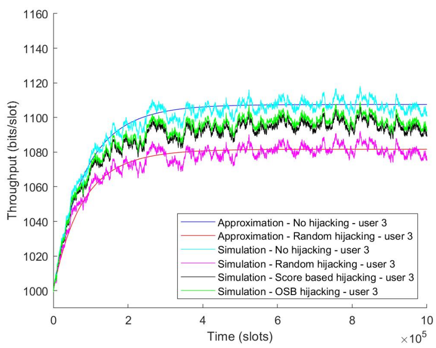

(d) $\varepsilon = 10^{-5}$, $\omega_{\max} = 6$ Hz

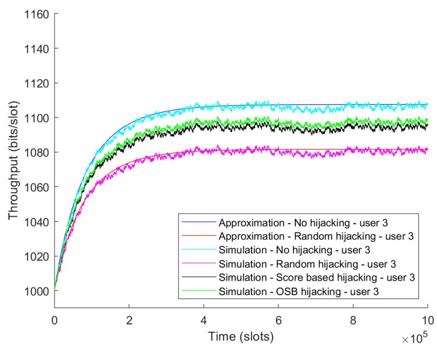

(e) $\varepsilon = 10^{-5}$, $\omega_{\max} = 25$ Hz

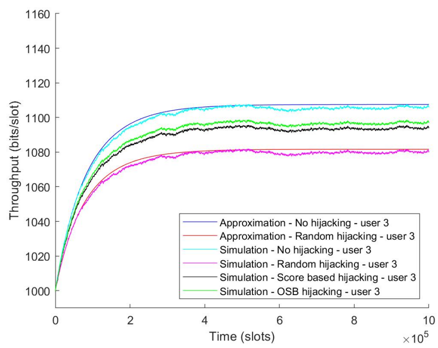

(f) $\varepsilon = 10^{-5}$, $\omega_{\max} = 60$ Hz

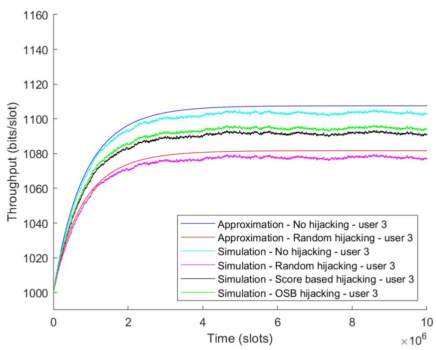

(g) $\varepsilon = 10^{-6}$, $\omega_{\max} = 6$ Hz

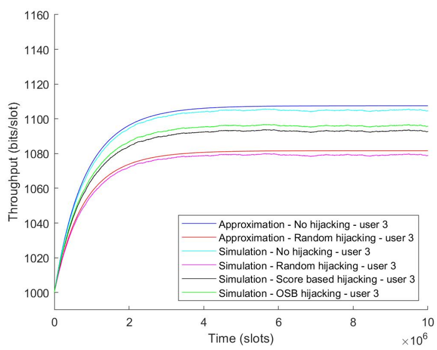

(h) $\varepsilon = 10^{-6}$, $\omega_{\max} = 25$ Hz

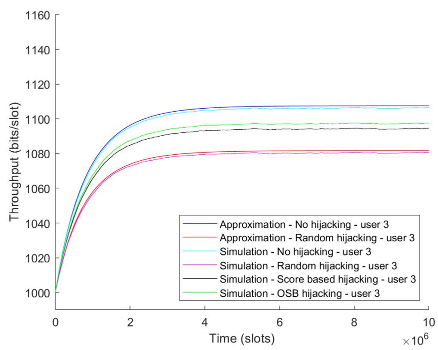

(i) $\varepsilon = 10^{-6}$, $\omega_{\max} = 60$ Hz

Figure B.5: Average throughputs over time for user 3 in scenario 3

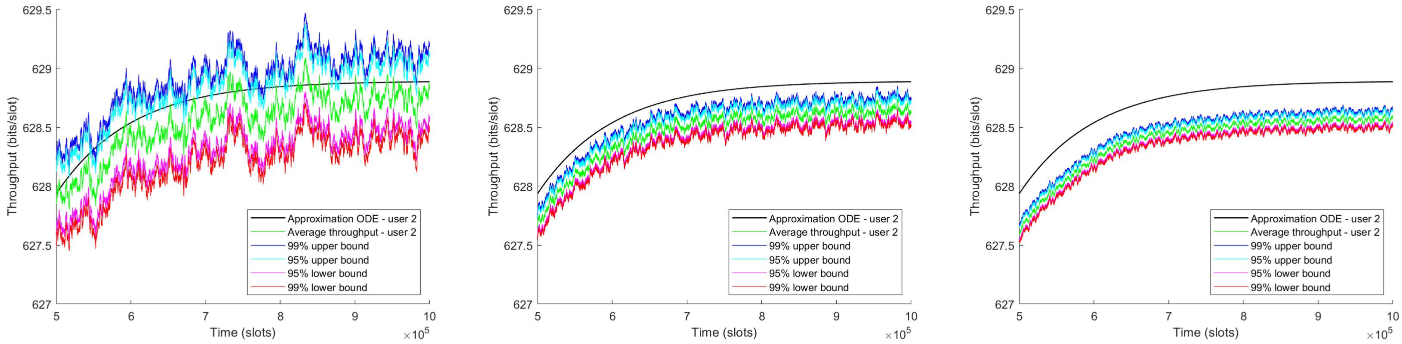

(a) $\omega_{\max} = 6$ Hz (b) $\omega_{\max} = 25$ Hz (c) $\omega_{\max} = 60$ Hz

Figure B.6: Average throughput and confidence bounds over time for user 2 in scenario 1 with Rayleigh fading and $\varepsilon = 10^{-5}$

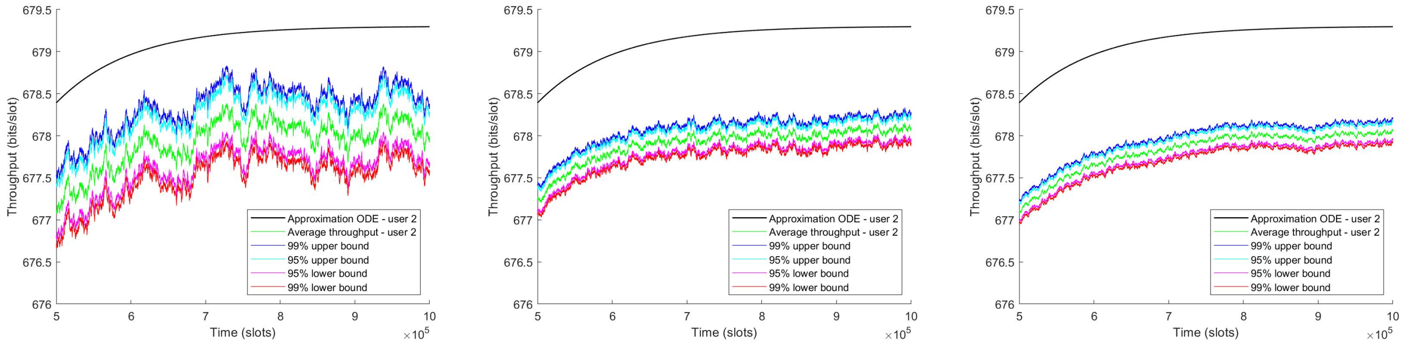

(a) $\omega_{\max} = 6$ Hz (b) $\omega_{\max} = 25$ Hz (c) $\omega_{\max} = 60$ Hz

Figure B.7: Average throughput and confidence bounds over time for user 2 in scenario 2 with Rayleigh fading and $\varepsilon = 10^{-5}$

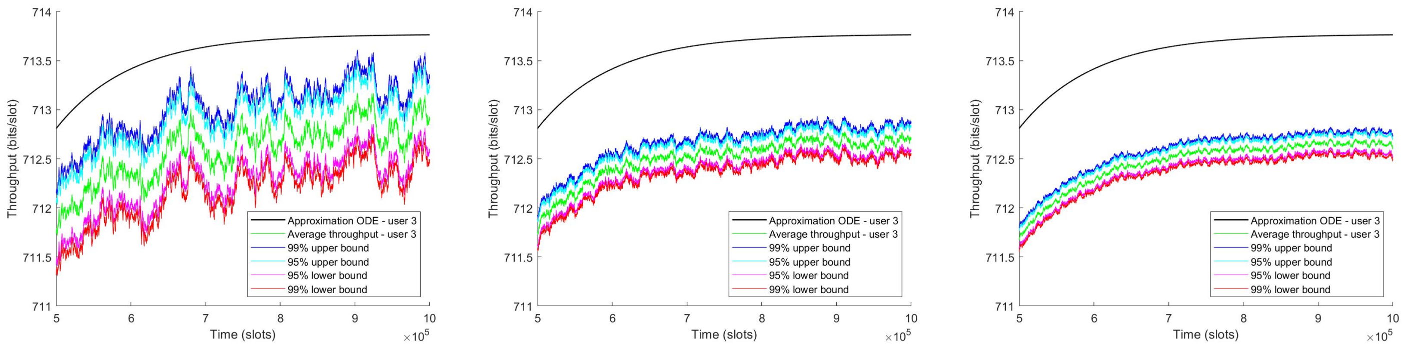

(a) $\omega_{\max} = 6$ Hz (b) $\omega_{\max} = 25$ Hz (c) $\omega_{\max} = 60$ Hz

Figure B.8: Average throughput and confidence bounds over time for user 3 in scenario 2 with Rayleigh fading and $\varepsilon = 10^{-5}$

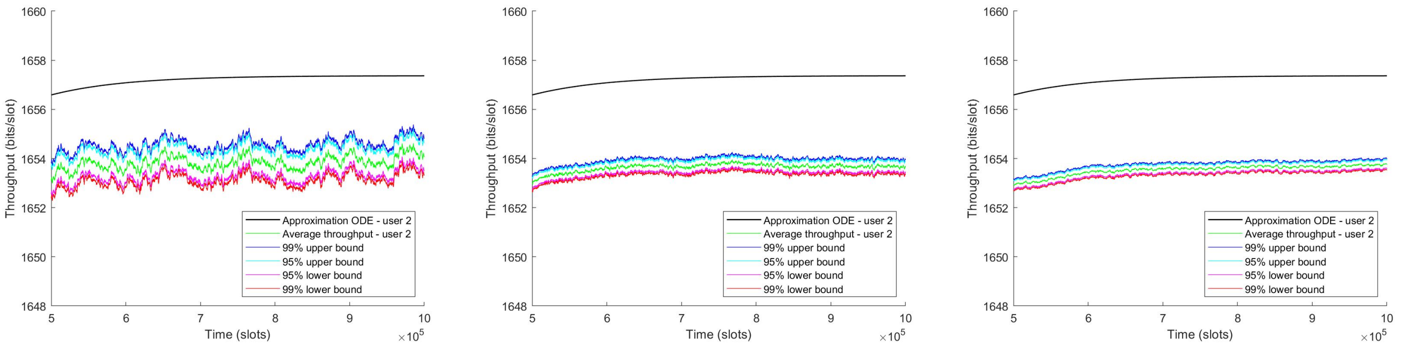

(a) $\omega_{\max} = 6$ Hz (b) $\omega_{\max} = 25$ Hz (c) $\omega_{\max} = 60$ Hz

Figure B.9: Average throughput and confidence bounds over time for user 2 in scenario 3 with Rayleigh fading and $\varepsilon = 10^{-5}$

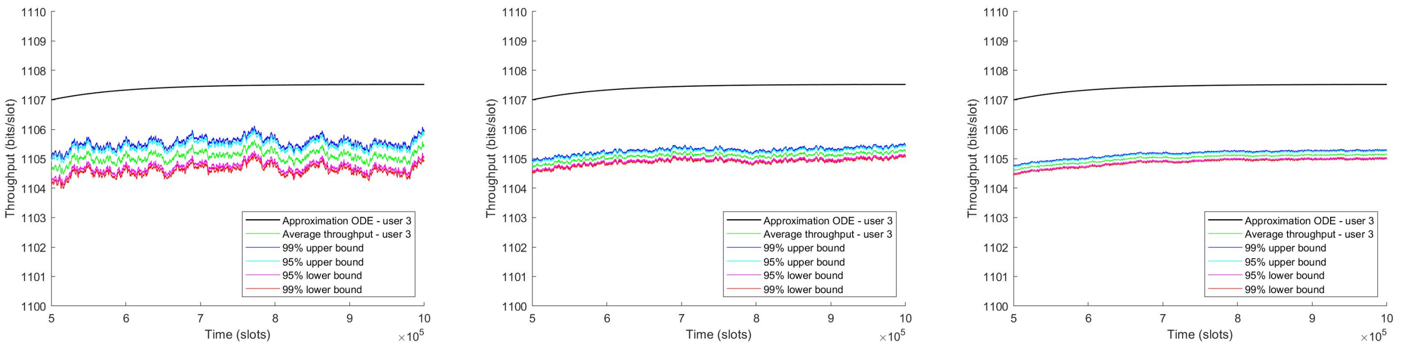

(a) $\omega_{\max} = 6$ Hz (b) $\omega_{\max} = 25$ Hz (c) $\omega_{\max} = 60$ Hz

Figure B.10: Average throughput and confidence bounds over time for user 3 in scenario 3 with Rayleigh fading and $\varepsilon = 10^{-5}$